Available online at www.sciencedirect.com
SCIENCE DIRECT®
Journal of Sound and Vibration 279 (2005) 857–936
JOURNAL OF SOUND AND VIBRATION
www.elsevier.com/locate/jsvi

Uncertainties and dynamic problems of bolted joints and other fasteners

R.A. Ibrahim[a,*], C.L. Pettit[b]

[a] *Wayne State University, Department of Mechanical Engineering Detroit, MI 48202, USA*
[b] *Air Force Research Laboratory AFRL/VASD, Wright-Patterson Air Force Base, OH 45433, USA*

Received 9 January 2003; accepted 18 November 2003

Abstract

This review article provides an overview of the problems pertaining to structural dynamics with bolted joints. These problems are complex in nature because every joint involves different sources of uncertainty and non-smooth non-linear characteristics. For example, the contact forces are not ideally plane due to manufacturing tolerances of contact surfaces. Furthermore, the initial forces will be redistributed non-uniformly in the presence of lateral loads. This is in addition to the prying loading, which is non-linear tension in the bolt and non-linear compression in the joint. Under environmental dynamic loading, the joint preload experiences some relaxation that results in time variation of the structure's dynamic properties. Most of the reported studies focused on the energy dissipation of bolted joints, linear and non-linear identification of the dynamic properties of the joints, parameter uncertainties and relaxation, and active control of the joint preload. Design issues of fully and partially restrained joints, sensitivity analysis to variations of joint parameters, and fatigue prediction for metallic and composite joints will be discussed.

1. Motivation

The design of structural systems involves elements that are connected through bolts, rivets, and pins. Joints and fasteners are used to transfer loads from one structural element to another. In composite structures, there are two types of joints commonly used, namely, mechanically fastened joints and adhesive bonded joints. Fastened joints include bolts, rivets, and pins. The design of adhesive joints depends on the size of the parts to be joined and the amount of overlap required to carry the load. Adhesive joints are often acceptable for secondary structures, but are generally

*Corresponding author. Tel.: +1-313-577-3885; fax: +1-313-577-8789.
E-mail address: raouf_ibrahim@eng.wayne.edu (R.A. Ibrahim).

0022-460X/$ - see front matter © 2003 Elsevier Ltd. All rights reserved.
doi:10.1016/j.jsv.2003.11.064

avoided in primary structures on account of their strength, chemical interaction effects, and reliability. Bolted joints are still the dominant fastening mechanism used in joining of primary structural parts for advanced composites.

The complex behavior of connecting elements plays an important role in the overall dynamic characteristics, such as natural frequencies, mode shapes, and non-linear response characteristics to external excitations. The joint represents a discontinuity in the structure and results in high stresses that often initiate joint failure [1]. The stresses and slip in the vicinity of contact regions determine the static strength, cyclic plasticity, frictional damping, and vibration levels associated with the structure. The need for developing methodologies for constructing predictive models of structures with joints and interfaces has recently been discussed in a white paper by Dohner [2].

Modern mechanical design and analyses are based on deterministic finite element (FE) and multi-body dynamics computer codes. The main objectives of these codes are to estimate the system eigenvalues, system response statistics, and probability of failure. However, these codes do not address the scatter or uncertainty in structural bolted joints. In addition, the system's inherent geometric and material non-linearities will result in difficulties in predicting the response under regular external loading. Deterministic single-point evaluation of the response may result in an over-designed and excessively conservative system without addressing the crucial aspect of parameter uncertainties. There are numerous classes of mechanical problems where the influence of scatter of structural parameters, initial and boundary conditions dictate a stochastic approach [3–5]. In particular, the stochastic finite element method (FEM) is considered a powerful tool for structural mechanics analysis. Recently, fuzzy set theory has been combined with FE algorithms to analyze structural systems with uncertain parameters. Furthermore, some systems are very sensitive to small parameter variations and thus experience significant qualitative dynamic changes known as bifurcation. It is known that bifurcation takes place in certain non-linear systems when the control parameter experiences small and slow variation.

The purpose of this article is to present an assessment of the role of joint uncertainties and relaxation in the design and dynamic behavior of structural systems. In view of joint uncertainties and relaxation, energy dissipation is one of the prime factors in the value of transmitting loads from one structural element to the next connected element. The treatment of joint uncertainties may be described using the theory of fuzzy sets, which will be briefly defined and demonstrated by some examples. The dynamic analysis of non-linear structures with joint relaxation will be presented for random and sinusoidal excitations. The article will address the identification problem of linear and non-linear joints. The reader is encouraged to understand the bolting technology and design aspects that are well documented in several references such as Refs. [6–12]. Basic considerations in the design of joints of composite structures are discussed by Agarwal and Broutman [13]. Some basic terminology and nomenclature are defined in Appendix A.

2. Energy dissipation in bolted joints

The study of energy dissipation in bolted joints deals with sources and mechanisms of the joint slip regimes in addition to the models and governing factors of friction in the joint. Both phenomenological and constitutive models have been studied extensively in the literature.

2.1. Slip regimes

Structural joints are regarded as a source of energy dissipation between contacting surfaces undergoing relative motion. The friction force in a joint arises from shearing and torsional forces between the parts, and is governed by the tension in the bolt and the friction coefficient. As a result, wear and energy losses occur. Ungar [14,15] studied the influence of joint spacing, joint tightness, flange material, and surface finish on the energy dissipation. He found that each mechanism of the energy dissipation rate depends non-linearly on the amplitude of the applied force. The bolt tension generally decreases with time depending on the joint geometry, surface properties, and the induced tensile stress in the bolt. Relaxation of the bolt preload asymptotically reaches 5–6% according to Refs. [16–18]. Chesson and Munse [17] indicated that most of the loss occurs within a day after bolting up. Under these conditions, the coefficient of friction will not be constant because the surface properties change during slip. Since there is a decrease of the clamping pressure with the distance away from the bolt, the frictional stress drops in regions away from the bolt hole. In those regions, microslip develops first. As the tangential load increases, microslip develops closer and closer to the hole. Herrington and Sabbaghian [19,20] studied the factors affecting the friction coefficients between metallic washers and composite surfaces.

In many applications such as vibration of beams, frame structures, gas turbines, and aerospace structures, it is beneficial to increase the structural damping created by joints. Energy dissipation resulting from slip in bolted joints has been the subject of many studies [21–27]. For example, Jezequel [26] proposed an algorithm for calculating the energy loss due to slip in bolted or riveted joints of plates. It was found that the joint friction exhibited viscous-like damping characteristics when the normal force was allowed to vary with the relative slip amplitude [28–35]. However, Beards [36–40] indicated that relative motion between contact surfaces should be avoided because it may result in a reduction of the structure's stiffness and create corrosion of the joint interfaces.

Space structures include complex joints. The influence of joint characteristics on the overall dynamics of the structure is important particularly when the structure becomes "joint-dominated" rather than being simply a perturbation of a linear continuous system. Lee [41] adopted simple modelling of joints represented by flexible connections with linear stiffness and linear damping, which results in a linear system with non-proportional damping. To enhance the inherent passive damping in structures, a number of joints were proposed by Prucz et al. [42] and Prucz [43] using viscoelastic materials. Bowden [44] and Bowden and Dugundji [45] considered linear and non-linear analyses of a simple three-joint beam model to examine the influence of joints on the dynamics of space structures in weightlessness. In the linear analysis, they showed that increasing joint damping would increase resonant frequencies and result in an increase in modal damping up to a point at which the joint became "locked up" by damping. This behavior is different from that predicted by modelling joint damping as proportional damping. Furthermore, the maximum amount of passive modal damping achieved from the joints was found to be greater for low-stiffness joints and for modal vibrations where large numbers of joints were actively participating. In their non-linear analysis, they calculated the forced response of the three-joint model with discrete non-linearities located at the joints and showed the manner in which the non-linearity is spread to all degrees of freedom of the system.

It is reasonable to assume that the clamping pressure decreases with the distance away from the bolt hole, and thus the shearing frictional stress also drops with this distance. Groper and

Hemmye [46,47] indicated that, "the magnitude of slip in regions away from the bolt hole is larger than in regions closer to the hole circumference. If the applied tangential load is not large enough to establish slip in an adjoining annulus to the bolthole, there is some slip in regions of the contact surface, but the joint does not fully slip. As the applied tangential load is increased, the joint might slip completely". Accordingly, two stages of loading can be defined for high strength friction grip bolted joints. These are:

- Microslip, which takes place when the regions away from the hole experience slip while those close to the hole do not slip.
- Macroslip, which occurs for tangential loading that results in slip over the entire contact surface.

Under dynamic loading, bolted joints may slide and produce energy dissipation. The slip cannot be large since the bolt holes are not much larger than the bolt diameter. Thus, some bolts may be sheared at the beginning of the full-slip stage of loading. Groper [48] developed analytical modelling for the friction force and slip in the partial slip and full slip stages of loading. He concluded that if the joint is designed such that the magnitude of slip is at the border between partial slip and full slip, the joint might dissipate a large amount of vibrational energy.

2.2. Friction models and governing factors

The basic models of friction for bolted joints are classified into phenomenological and constitutive [49]. Phenomenological models represent the friction force as a function of the relative displacement. These models include static friction described by signum-friction models, elasto-slip models represented by a set of spring-slider elements in parallel (known as Jenkins- or Masing-element), the LuGre (*Lu*nd–*Gre*noble) model represented by elastic bristles sliding over rigid bristles, and the Vanalis model, which accommodates local microslip and macroslip in one model. Constitutive models establish relationships between stress and displacement fields. They include joint description by contact mechanics with statistical surface roughness description, and fractal characterization of surface roughness in joints. Various aspects of frictional damping in joints have been discussed in previous review articles [49–52].

Structural elements joined with high-strength friction grip bolts are tightened such that a large clamping pressure is realized at the contact surfaces. Thus, the elements transmit the load by friction. Andrew et al. [53] indicated that vibration normal to the joint surfaces is generally undamped. On the other hand, only tangential components of vibrations can be damped out by the high-strength friction grip joint [54]. It was found that the energy loss per cycle in high-strength friction-grip bolted joints depends on surface finish, the magnitude of the cyclic peak load, and the prior load history [55]. In all cases considered in their studies, the energy loss was non-linearly dependent on the tangential load (raised to a power ranging from 2.4 to 3.2). The damping factor estimated from recorded hysteresis loops was found to vary over from 5% to 12%.

The energy dissipation in mechanical joints depends on the clamping pressure. High clamping pressure causes greater penetration of asperities. Dekoninch [56] showed that relative motion due to tangential loads causes plastic deformation of the asperities. Some researchers [15,57–59] reported different mechanisms of energy dissipation that might take place depending on the

clamping pressure. Under high pressure, the slip is small, while under low pressure the shear due to friction is small. Maximum energy dissipation can be achieved somewhere between these two limits. Beards [37] investigated damping of structural vibration by controlling interfacial slip in joints and recognized an optimum joint clamping force exists for maximum energy dissipation due to interfacial slip in the joint. Beards and Williams [60] in their experimental investigation of a frame structure showed that a useful increase in damping could be achieved by fastening joints tightly to prohibit translational slip, but not tightly enough to prohibit rotational slip. Beards and Imam [61] found that the frictional damping of plate-type structures could be enhanced by using laminated plates correctly fastened to allow controlled interfacial slip during vibration. In another study Beards and Woodwat [62] experimentally examined the effect of controlled frictional damping in joints on the frequency response of a frame under harmonic excitation. It was shown that a large increase in damping can be produced by controlling the clamping force in joint and that an optimal clamping force exists under which a joint dissipates maximum vibrational energy.

Dowell [63] and Tang and Dowell [64,65] considered the non-linear response of beams and plates to sinusoidal and random excitations applied at a point close to one end, and with dry friction damping due to slippage at the support boundaries. They studied narrow and wide band random excitations and obtained the response statistics in terms of the normal load at the support joints by using a statistical linearization method, numerical solution, and experimental tests. The results revealed that the stick–slip and stick phenomena take place as the normal load increases. When slip takes place, energy dissipation due to dry friction tends to vanish and the transverse response amplitude becomes larger.

Shin et al. [66] examined the relationship between the bolt preload and system damping. They considered the following three approaches to introduce damping: (1) varying the bolt preload between joint interfaces via bolt torque adjustments; (2) damping associated with the addition of a viscoelastic layer between the contact surfaces at the bolted joints; and (3) a combination of both viscoelastic and varying bolt torque, to obtain an optimum joint damping.

Gaul and Nitsche [49] reviewed different approaches for describing the non-linear transfer behavior of bolted joint connections and their analytical modelling. Segalman [67,68] considered Jenkins-elements in parallel (each composed of a spring and slider) that are capable of reproducing frictional joint properties. In an attempt to circumvent the difficulties of these models he proposed reduced order models based on the original work of Iwan [69].

Esteban et al. [70] and Esteban and Rogers [71] presented an analytical approach to determine the energy dissipation through joints at high frequency and its relation to the localized actuation-sensing region surrounding an integrated piezoceramic (PZT) actuator. The structure consisted of two beams connected with a bolted joint and each having free end boundary conditions. They used a wave propagation approach together with a Timoshenko beam theory to model the inertia and stiffness properties of the system. The energy dissipation in the joint was modelled linearly using mass–spring–dashpot systems and non-linearly with application of friction clearance system with a cubic spring joint. It was found that the wave incident on the joint was consistently larger than the energy transmitted after the joint. This means that significant amount of energy of the incident wave was dissipated after the joint. For example, Fig. 1 shows the amplitude (gain)-frequency of the 19th bending mode, for which the bolted section has maximum deflection. The figure shows analytical and experimental results for both tight and loose bolts. For loose bolts, the amplitude is reduced at resonance due to the larger reduction in amplitude of the propagating

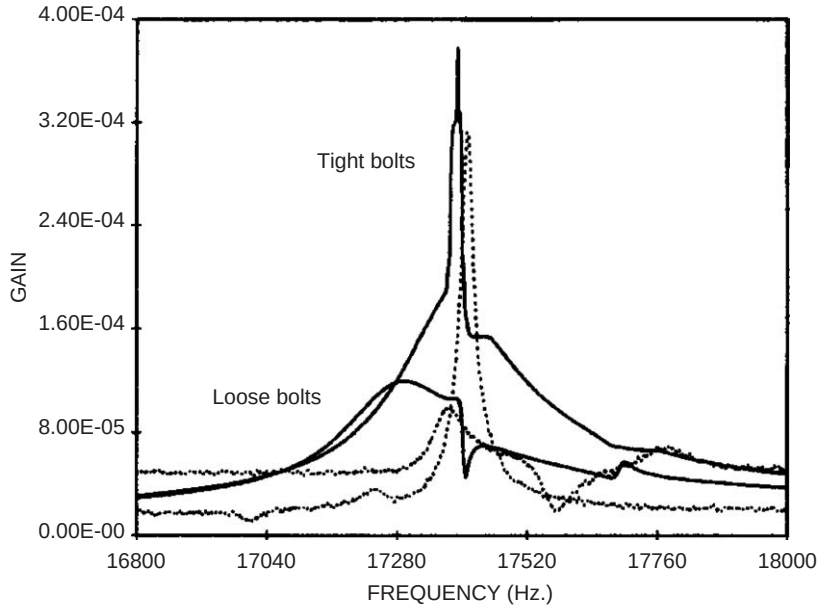

Fig. 1. Amplitude–frequency response of the 19th mode for loose and tight bolts: ----, experimental; ——, analytical [71].

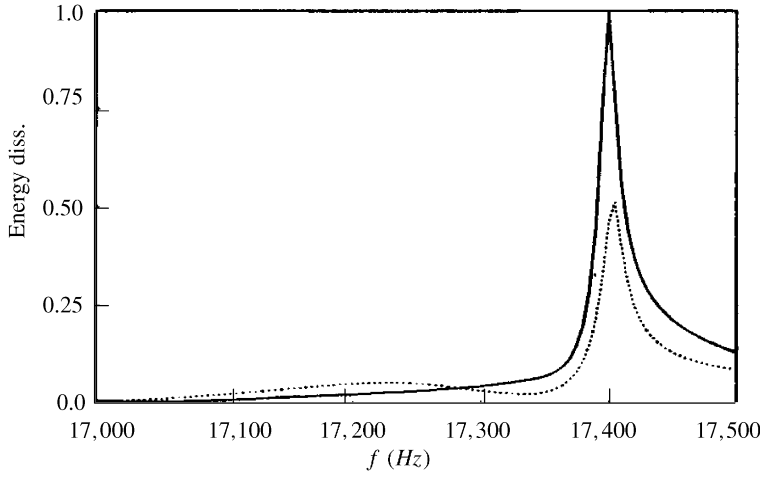

Fig. 2. Energy dissipation of the 19th mode for loose and tight bolts: ----, tight bolts; ——, loose bolts [71].

wave as a result of energy dissipation through the bolted joint. The dependence of the energy dissipation on the excitation frequency at the 19th mode is shown in Fig. 2. The dotted curve represents the energy dissipation for bolts tightened at 25 KN, while the solid curve belongs to loosen bolts at 22 KN, and reveals approximately double the maximum energy dissipation.

Loosely jointed structures are characterized by their bilinear dependence of the lateral displacement on the lateral acting force [72]. Examples of structures with such joints are usually

temporary configurations such as multi-bay, multi-story scaffold with loose tube-in-tube connecting joints.

Song et al. [73,74] determined the contact area of bolted joint interfaces using FEM and experimental tests. Rothert et al. [75] developed a non-linear three-dimensional FE contact analysis of bolted joints in steel frames. Iyer [76,77] found that the contact area, contact pressure and tangential stress distributions in a pinned connection can be modified in a complex manner by the pin-plate friction coefficient, material combination, and plate dimensions. Iyer reported that the magnitude of the friction coefficient also directly reflects the magnitude of the effect of pin-plate material dissimilarity.

3. Joint uncertainties and relaxation

Among the many factors affecting bolted joints and fasteners are friction, hardness, finish, the relative dimensions of all interacting parts, and the creep of gaskets [8]. Each factor will vary from bolt to bolt and joint to joint because of manufacturing or usage tolerances. As a result all joints and jointed structures exhibit parametric uncertainty. The main problems encountered in the analysis and design of bolted joints with parameter uncertainties includes random eigenvalues, response statistics, and probability of failure. Paez et al. [78] studied experimentally and analytically the natural frequency randomness induced by bolted joints of a cantilever beam. The dependence of the natural frequency on the joint stiffness was found to be non-linear and appeared to approach an asymptotic value from below as the stiffness becomes large. Major progress has been achieved within the framework of linear (or linearized) modelling. However, the design of such systems should take into account the influence of joint non-linearities as well as structural geometrical and material non-linearities. The influence of non-linear boundary conditions has been examined by Watanabe [79] and Lee and Yeo [80].

In tightening a bolted joint with a hydraulic tensioner, the most important factor is the ratio of desired clamping force to the initial tension, known as the *effective tensile coefficient*. This coefficient has been estimated using the FEM [81] and spring elements [82]. Fukuoka [83] assumed that the major source of scatter in the effective tensile coefficient is due to interface stiffness in the normal direction, and proposed a numerical procedure to predict the effective tensile coefficient. The inclusion of such uncertainty improves the accuracy of applying hydraulic tensioners.

In real applications, most of the boundary conditions are not ideal since one cannot achieve infinite stiffness for clamped ends. For example, Wang and Chen [84] and Lee and Kim [85] determined the parameters of non-ideal boundary conditions. Wang and Chen represented the unknown boundaries of a slender beam by a boundary stiffness matrix in their FEM. The boundary stiffness matrix was determined from the measured structure modal parameters. Lee and Kim [85] adopted a different approach by representing the non-ideal boundary conditions by frequency-dependent effective boundary transverse and torsional springs. The effective boundary spring constants were determined from the measured frequency response functions (FRFs) in conjunction with the spectral element method. This approach is referred to as the ''spectral element method'', which relates the vector of forces and moments of the boundaries to the displacement vector of the boundaries through the spectral element matrix.

Bolted joints and fasteners have a significant effect on the damping and stiffness of the joint. The damping is created by friction in the screw thread, gas pumping, or impact-induced damping in local microgaps between joint surfaces, material damping in the asperities of contact surfaces, and plastic deformation. The stiffness of the joint is affected by the hardness and roughness of contact surfaces. In most cases, these parameters cannot be accurately modelled due to uncertainties in the production, variability in the material properties, geometry parameters, and the relaxation process. This section considers the uncertainties of bolted joints represented by fuzzy sets or by random variables. Relaxation of bolted joints will be phenomenologically represented based on experimental measurements.

3.1. Uncertainty of bolted joints using fuzzy parameters

3.1.1. Basic definitions of fuzzy arithmetic

Parameter uncertainties of bolted joints can be mathematically represented by fuzzy sets. The theory of fuzzy sets was originally introduced by Zadeh [86] who used this as a basis for the theory of possibility. A possibility distribution is defined as a normal fuzzy set (at least one membership grade equals 1). For example, all fuzzy numbers are possibility distributions. Fuzzy sets convey the idea of "degree of belonging" as described by a membership function. The concept arises in analyzing sets whose boundaries are vaguely defined such that the question of set membership cannot be answered by "yes" or "no". There is a difference between the probability theory and fuzzy logic. Probability measures *the likelihood* that an event will occur, while fuzzy logic deals with the *degree of membership* of an event in a set. With fuzziness, one cannot say unequivocally whether an event occurred, but one tries to model the extent to which an event occurred. When one assigns a normal fuzzy set, this imposes an imprecise constraint on the value of the variable, which is referred to as a *possibility distribution* because it specifies the degree of possibility for the variable to take a certain value. Thus, possibility measures *the degree of ease* for a variable to take a value. Possibility is distinct from probability, but the two concepts converge in the sense that a possibility distribution constitutes a one-point coverage function of a random set. Consequently, a possibility distribution can represent imprecision in a value.

Hanss et al. [87,88] represented the stiffness and damping of bolted joints by fuzzy-valued parameters, which were identified on the basis of measured data. They expressed fuzzy sets by the elements, x, of the set of real numbers, $\Re$, with a certain degree of membership $\mu(x) \in [0, 1]$. The fuzzy sets are distinguished from crisp sets whose elements, x, are characterized by degrees of membership that can only be equal to zero or unity. Accordingly, closed intervals and crisp numbers of the form shown in Fig. 3 are, e.g.,

$$[a, b] = \{x \mid a \leqslant x \leqslant b\}, \quad c = [x \mid x = c], \quad x \in \Re. \tag{1a, b}$$

These can also be expressed by their characteristic function (also known as membership functions):

$$\mu_{[a,b]} = \begin{cases} 1 & \text{for } a \leqslant x \leqslant b, \\ 0 & \text{for other values.} \end{cases} \tag{2a}$$

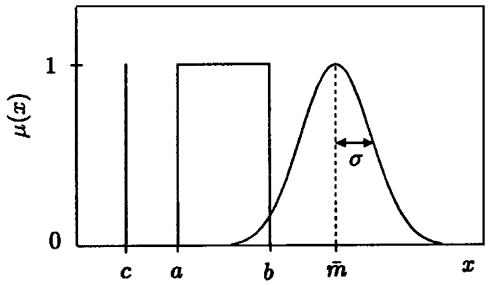

Fig. 3. Crisp number c, closed interval $[a, b]$, and symmetric fuzzy number of quasi-Gaussian shape [88].

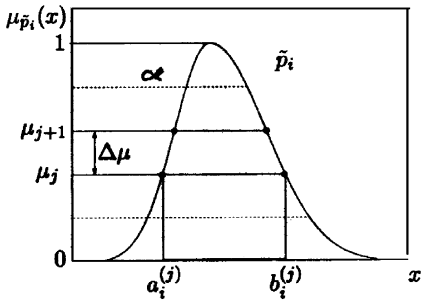

Fig. 4. Membership functions showing the α-cut; the uncertain parameter $\tilde{p}_i$ is decomposed into intervals [88].

$$\mu_c = \begin{cases} 1 & \text{for } x = c, \\ 0 & \text{for other values.} \end{cases} \tag{2b}$$

On the other hand, fuzzy numbers are defined as normal convex fuzzy subsets over the universal set $\Re$ with membership functions $\mu(x) \in [0, 1]$, and where $\mu(x) = 1$ is true only for a single value $x = \bar{m}$. By convex fuzzy sets we mean that as the level of membership increases, the associated interval of membership never increases. The subset A is convex if and only if

$$\mu_A(\lambda a + (1 - \lambda)b) \geqslant \min\{\mu_A(a), \mu_A(b)\} \tag{3}$$

for all $a, b \in \Re$ and $0 \leqslant \lambda \leqslant 1$.

Symmetric fuzzy numbers of a quasi-Gaussian shape may be defined by the membership function

$$\mu(x) = \left\{ \begin{array}{ll} e^{-(x-\bar{m})^2/2\sigma^2} & \text{for } |x - e^{-(x-\bar{m})^2/2\sigma^2}| \leqslant 3\sigma, \\ 0 & \text{for } x > \bar{m} + 3\sigma \text{ or } x > \bar{m} - 3\sigma, \end{array} \right\}, \tag{4}$$

where $\bar{m}$ is the mean value and σ is the standard deviation of the Gaussian distribution.

It is informative before proceeding further to summarize the standard fuzzy arithmetic operations. With reference to Fig. 4, a fuzzy number can be represented by a discrete fuzzy number or decomposed into a number of intervals $[a^{(j)}, b^{(j)}]$ or cuts, $a^{(j)} \leqslant b^{(j)}$, such that, e.g.,

$$\mu_j = \frac{j}{m}, \quad j = 0, 1, \ldots, m. \tag{5}$$

For demonstration sake, consider two fuzzy numbers $\tilde{p}_1$ and $\tilde{p}_2$ decomposed into the sets P_1 and P_2, of $m+1$ intervals, of the form

$$P_1 = \{[a_1^{(0)}, b_1^{(0)}], [a_1^{(1)}, b_1^{(1)}], \ldots, [a_1^{(m)}, b_1^{(m)}]\},$$

$$P_2 = \{[a_2^{(0)}, b_2^{(0)}], [a_2^{(1)}, b_2^{(1)}], \ldots, [a_2^{(m)}, b_2^{(m)}]\}. \tag{6}$$

Note that if μ_j increases the interval of confidence (i.e., the interval of values whose membership is greater than or equal to μ_j) never increases (convexity). An interval of confidence is one way of reducing the uncertainty of using lower and upper bounds. The coupling between the level μ_j and the interval of confidence at level μ_j defines the concept of an uncertain number or a *fuzzy number*. The elementary binary operations $\tilde{p}_1 + \tilde{p}_2$, $\tilde{p}_1 - \tilde{p}_2$, $\tilde{p}_1 \cdot \tilde{p}_2$, and $\tilde{p}_1/\tilde{p}_2$ can be defined in terms of standard interval arithmetic

$$[a_1^{(j)}, b_1^{(j)}] + [a_2^{(j)}, b_2^{(j)}] = [(a_1^{(j)} + a_2^{(j)}), (b_1^{(j)} + b_2^{(j)})], \tag{7}$$

$$[a_1^{(j)}, b_1^{(j)}] - [a_2^{(j)}, b_2^{(j)}] = [(a_1^{(j)} - b_2^{(j)}), (b_1^{(j)} - a_2^{(j)})], \tag{8}$$

$$[a_1^{(j)}, b_1^{(j)}].[a_2^{(j)}, b_2^{(j)}] = [\min(M^{(j)}), \max(M^{(j)})], \tag{9}$$

where $M^{(j)} = \{a_1^{(j)}a_2^{(j)}, a_1^{(j)}b_2^{(j)}, b_1^{(j)}a_2^{(j)}, b_1^{(j)}b_2^{(j)}\}$, and

$$[a_1^{(j)}, b_1^{(j)}]/[a_2^{(j)}, b_2^{(j)}] = [\min(D^{(j)}), \max(D^{(j)})], \tag{10}$$

$$D^{(j)} = \left\{\frac{a_1^{(j)}}{a_2^{(j)}}, \frac{a_1^{(j)}}{b_2^{(j)}}, \frac{b_1^{(j)}}{a_2^{(j)}}, \frac{b_1^{(j)}}{b_2^{(j)}}\right\}, \text{ provided } 0 \notin [a_2^{(j)}, b_2^{(j)}].$$

Hanss and Willner [89] and Hanss [90] showed that the application of standard fuzzy arithmetic [91–93] to the simulation of system uncertainties does not always reflect the real results of the system. For example, the standard fuzzy arithmetic may give different results for the same problem depending on the form of the selected solution procedure. This defect motivated Hanss [90,94] to propose a transformation to implement fuzzy arithmetic to analyze systems with uncertain parameters. The transformation was shown to lead to the proper fuzzy-valued result independent of the selected solution procedure.

3.1.2. Uncertain boundary conditions

Finite element methods (FEMs) have been used to analyze the problem of stochasticity of structural systems. The solution of such problems has been carried out using perturbation techniques and Monte Carlo simulation. The stochastic nature of uncertainty arises from measurements or instrumentation errors involved in experiments as well as random distributions associated with manufacturing errors and natural variability. The uncertainty represented by fuzzy sets, on the other hand, results from the fact that a designer has subjective preference to select estimated data of the system parameters [95]. Generally, FEMs can handle system uncertainties of the two classes, namely, stochastic and fuzzy. Shinozuka and Yamazaki [96] outlined the basic idea of treating structural response variability due to spatial variability of material properties under static deterministic loads. Ghanem and Red-Horse [97] used the spectral

stochastic FEM to solve for the modal properties of a space-frame with localized system uncertainties. The fuzzy FEM has been developed and adopted for static and dynamic response problems of flexible structures [98–105]. Shimizu and Hiroaki [106] developed an algorithm to generate FE meshes using fuzzy sets. Lallemand et al. [107] and Plessis et al. [108] extended fuzzy set theory to a dynamic FEA of structures with uncertainties in material properties.

The ideal assumption of clamped end of structural elements such as beams or rods cannot be realized in practice. In most cases, there are non-zero displacements and slopes that are uncertain in nature. Cherki et al. [109,110] considered the problem of sensitivity to uncertain boundary conditions by representing the uncertainties as fuzzy parameters with assumed membership functions. They considered a structure to be sensitive to uncertainties of prescribed displacements if it propagates these displacements by amplifying them at another location of the structure.

The equilibrium equation for static problems with prescribed displacements may be written in the form [96],

$$\begin{bmatrix} \mathbf{K}_{aa} & \mathbf{K}_{ab} \\ \mathbf{K}_{ba} & \mathbf{K}_{bb} \end{bmatrix} \begin{Bmatrix} \mathbf{U}_a \\ \mathbf{U}_b \end{Bmatrix} = \begin{Bmatrix} \mathbf{F}_a \\ \mathbf{F}_b \end{Bmatrix}, \tag{11}$$

where $\mathbf{U}_a$ represents the unknown displacement vector, $\mathbf{U}_b$ is the imposed (known) vector displacement, which is modelled as fuzzy, $\mathbf{K}_{aa}$ is the stiffness matrix associated with the displacement vector $\mathbf{U}_a$, $\mathbf{F}_a$ is the vector of applied forces corresponding to the unknown displacements, and $\mathbf{F}_b$ is the vector of the unknown reaction forces. Eq. (11) may be divided into two equations:

$$\mathbf{K}_{aa}\mathbf{U}_a = \mathbf{F}_a - \mathbf{K}_{ab}\mathbf{U}_b = \mathbf{G}_a, \tag{12}$$

$$\mathbf{F}_b = \mathbf{K}_{ba}\mathbf{U}_a + \mathbf{K}_{bb}\mathbf{U}_b. \tag{13}$$

Note that the right-hand side of Eq. (12) involves mixed or non-homogeneous terms since one of them, $\mathbf{K}_{ab}\mathbf{U}_b$, is fuzzy and the other is crisp. It is possible to make a fuzzy representation for the crisp part and Eq. (12) may be written in the form

$$\mathbf{K}_{aa}\tilde{\mathbf{U}}_a = \tilde{\mathbf{G}}_a, \tag{14}$$

where tilde denotes the fuzzy representation of Eq. (12).

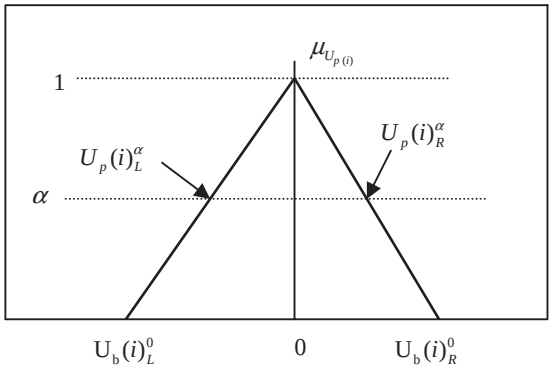

Fig. 5. Membership function for the ith coefficient of prescribed displacement U_p adopted by Cherki et al. [110].

Cherki et al. [110] solved Eq. (14) by discretizing the membership function associated with the fuzzy coefficients in α-cut levels as shown in Fig. 5. The lower and upper bounds of the joint displacement $\tilde{\mathbf{U}}_b(i)$, indicated by $U_b(i)_L^0$ and $U_b(i)_R^0$, respectively, characterize uncertainties on the prescribed displacements for cases in which insufficient information is available to define a probability distribution. For an imperfectly clamped joint, these displacements are not zero in general. The fuzzy linear system is substituted into a set of interval linear systems, which give the interval solution for each α-cut. This is followed by generating the unknown displacements $\tilde{\mathbf{U}}_a$ using this set of intervals. Once the displacement vector $\tilde{\mathbf{U}}_a$ is determined it is then substituted into Eq. (13) to determine the support reactions, $\mathbf{F}_b$.

Cherki et al. [110] considered three cantilevered truss structures and estimated the sensitivity coefficient, which was defined as the ratio of the surface of the fuzzy number of the end point of the structure to the surface fuzzy number of imperfect clamping node. The surface of the fuzzy number represents the area bounded by the membership function. Their numerical results revealed that the three structures could have different behaviors when uncertainty is prescribed for the boundary conditions. Chen and Rao [95] developed a fuzzy FE approach for free vibration analysis of a 3-stepped bar and a 25-bar space truss.

Under fuzzy excitation, Wang and Liou [112] studied the response of a single-degree-of-freedom system with crisp system parameters. Yue et al. [113] outlined the analytical treatment of dynamical systems subjected to fuzzy excitations and systems with variable coefficients. They introduced the general theory of fuzzy stochastic dynamical systems and the basic properties of fuzzy linear systems. Cristea [114] estimated the degree of confidence and sensitivity of the non-linear dynamic response of elasto-plastic frame structure with fuzzy parameters. The dynamic response of machine tool structures with fuzzy parameters and fuzzy excitation was investigated by Fansen and Junyi [115].

In the perturbation-based stochastic FE [96,111] both $\tilde{\mathbf{U}}_a$ and $\tilde{\mathbf{G}}_a$ are represented by their mean values $\bar{\mathbf{U}}_a$, and $\bar{\mathbf{G}}_a$, and deviatoric parts $\Delta\mathbf{U}_a$ and $\Delta\mathbf{G}_a$. In this case, Eq. (14) takes the form

$$\mathbf{K}_{aa}\{\bar{\mathbf{U}}_a + \Delta\mathbf{U}_a\} = \{\bar{\mathbf{G}}_a + \Delta\mathbf{G}_a\}. \tag{15}$$

This equation implies

$$\mathbf{K}_{aa}\bar{\mathbf{U}}_a = \bar{\mathbf{G}}_a, \quad \text{and} \quad \mathbf{K}_{aa}\Delta\mathbf{U}_a = \Delta\mathbf{G}_a. \tag{16a, b}$$

These equations can be solved for $\bar{\mathbf{U}}_a$ and $\Delta\mathbf{U}_a$, i.e.,

$$\bar{\mathbf{U}}_a = \mathbf{K}_{aa}^{-1}\bar{\mathbf{G}}_a, \quad \text{and} \quad \Delta\mathbf{U}_a = \mathbf{K}_{aa}^{-1}\Delta\mathbf{G}_a. \tag{17a, b}$$

3.2. Uncertainty of boundary conditions and material properties

Lindsley et al. [116,117] studied the non-linear aeroelastic flutter of panels with uncertain boundary conditions and spatially variable material properties. The boundary conditions were modelled as pinned, fixed, or rotational spring, with the pinned and fixed boundary conditions being limiting cases of rotational springs on the boundary, which possess zero and infinite stiffness respectively. The boundary value problem was described by coupling the von Karman plate equations for in-plane and out-of-plane deflections with piston theory aerodynamics. The in-plane equations were time independent and linearly coupled in the in-plane displacements, u and v, and

non-linearly coupled with the transverse displacement, w. They could be solved once they have been spatially discretized. The second order transverse equation of motion was written as two first order equations,

$$\frac{\partial s}{\partial t} = -\frac{\mu_s}{M_\infty}\left(s+\frac{\partial w}{\partial x}\right)+\frac{\partial^4 w}{\partial x^4}+r^2\frac{\partial^4 w}{\partial x^2\partial y^2}+r^4\frac{\partial^4 w}{\partial y^4}$$
$$+\left(N_{x0}\frac{\partial^2 w}{\partial x^2}+2rN_{xy0}\frac{\partial^2 w}{\partial x\partial y}+r^2N_{y0}\frac{\partial^2 w}{\partial y^2}\right)+6\left(2\frac{\partial u}{\partial x}+2rv\frac{\partial v}{\partial y}+\frac{\partial w^2}{\partial x}+r^2v\frac{\partial w^2}{\partial y}\right)\frac{\partial^2 w}{\partial x^2}$$
$$+6\left(2r^2v\frac{\partial u}{\partial x}+2r^3\frac{\partial v}{\partial y}+r^2v\frac{\partial w^2}{\partial x}+r^4\frac{\partial w^2}{\partial y}\right)\frac{\partial^2 w}{\partial y^2}+12(1-v)\left(r^2\frac{\partial u}{\partial y}+r\frac{\partial v}{\partial x}+r^2\frac{\partial w}{\partial x}\frac{\partial w}{\partial y}\right)\frac{\partial^2 w}{\partial x\partial y}, \quad (18a)$$

$$\frac{\partial w}{\partial t} = s, \quad (18b)$$

where $w = L_x\bar{w}/h^2$ is non-dimensional transverse plate deflection, $t = L_x\bar{t}/U_\infty$, is non-dimensional time scale, U_∞ is the free stream velocity, $\mu_s = \rho_\infty L_x/(\rho_s h)$ is the air-to-plate mass ratio, M_∞ is the Mach number, h is the plate thickness, ρ_s is the plate density, ρ_∞ is the density of air stream, $r = L_s/L_y$ is the ratio of plate lengths in x, and y respectively, v is the Poisson ratio, $N_{x0} = L_x^2\bar{N}_{x0}/(12D)$, $N_{y0} = L_x^2\bar{N}_{y0}/(12D)$, $N_{xy0} = L_x^2\bar{N}_{xy0}/(12D)$, are scaled in-plane pre-stress forces, and $D = Eh^3/[12(1-v^2)]$. Note all linear elasticity and pre-stress terms were multiplied by λ/μ_s, while non-linear terms were multiplied by $\lambda/(h^2\mu_s)$, where λ is a non-dimensional parameter that reflect the ratio of the dynamic pressure to the stiffness of the panel, i.e., $\lambda = 12\rho_\infty U_\infty^2 L_x^3(1-v^2)/(Eh^3)$.

Consider the boundary conditions for a panel with rotational spring stiffness, K_i, $i = 1, \ldots, 4$. The bending moment and spring reaction moment are specified to be in equilibrium along the selected edge:

$$\frac{\partial^2 w}{\partial x^2} = \frac{K_1}{D}\frac{\partial w}{\partial x}\bigg|_{0,y}, \quad \frac{\partial^2 w}{\partial x^2} = -\frac{K_2}{D}\frac{\partial w}{\partial x}\bigg|_{1,y}, \quad \frac{\partial^2 w}{\partial y^2} = \frac{K_3}{D}\frac{\partial w}{\partial y}\bigg|_{x,0}, \quad \frac{\partial^2 w}{\partial y^2} = -\frac{K_4}{D}\frac{\partial w}{\partial y}\bigg|_{x,1/r}. \quad (19)$$

The spatial discretization of the boundary conditions utilized "ghost" points (x_{-1}, y_n), (x_{M+1}, y_n), (x_{-1}, y_n), and (x_n, y_{-1}) along the edges. Any member (x_m, y_n) of the set of points along the boundary path $[(x_1, y_1), (x_1, y_N), (x_M, y_1), (x_M, y_N)]$ was forced to satisfy the ghost point relations

$$w_{-1,n} = \beta_1 w_{1,n}, \quad w_{M+1,n} = \beta_2 w_{M-1,n}, \quad w_{M,-1} = \beta_3 w_{m,1}, \quad w_{M,N+1} = \beta_4 w_{m,N-1}, \quad (20)$$

where $1 \leqslant m \leqslant M$ and $1 \leqslant n \leqslant N$ are the flow indices for (x) and (y), respectively, $-1 \leqslant \beta \leqslant -1+\delta\beta_P$, $0 \leqslant \beta_P \ll 1$ specify β values in the neighborhood of the pinned condition $(K \to 0)$, and $1-\delta\beta_F \leqslant \beta \leqslant 1$, and $0 \leqslant \beta_F \ll 1$ specify β in the neighborhood of the fixed condition $(K \to \infty)$. β is defined by the expressions:

$$\beta_i = \left[\frac{K_i\Delta x}{2D}-1\right]\Big/\left[\frac{K_i\Delta x}{2D}+1\right], \quad \beta_j = \left[\frac{K_j\Delta y}{2D}-1\right]\Big/\left[\frac{K_j\Delta y}{2D}+1\right], \quad (21)$$

where $i = 1, 2$ along the edges parallel with the y-direction and $j = 3, 4$ along the edges parallel with the x-direction.

Parametric uncertainty was examined by modelling variability in Young's modulus $E(x, y)$ and the boundary condition parameter β. The aeroelastic model described by Eq. (18) was combined with a two-dimensional random field model to simulate the influence of spatially correlated variability in Young's modulus on the occurrence of limit cycle oscillation. The random field was modelled as second order, homogeneous, and isotropic, so that it could be completely represented by a single-variable spatial autocorrelation function or spectral density function. The variability in the boundary conditions was restricted to a single value along the plate boundary edges for each realization. Results were obtained for a square panel, and for the parameters $h/L = 0.003$, $v = 0.3$, $\mu_s/M_\infty = 0.04$ and $M_\infty > 2.0$. The scaled dynamic pressure ratio λ/M_∞ was selected as the bifurcation parameter and was varied between 860 and 980. The panel was discretized with either a 31×31 or 47×47 grid. Young's modulus was specified with a mean value taken as 1.0×10^7 psi and a coefficient of variation of 1% or 10%. The spatial variability was assumed to have an exponential covariance function with correlation length between $0.1L$ and $0.3L$.

The stochastic panel response was estimated using Monte Carlo simulation. Fig. 6 shows the dependence of the response limit cycle amplitude on the dynamic pressure parameter λ/M_∞ for a 47×47 grid. The deterministic backbone curve is bounded by the upper and lower values of the observed limit cycle amplitude along with estimated probability density (pdf). It was reported that for $\lambda = 860$, which is slightly above the deterministic bifurcation point, spatial variability in Young's modulus produced more than 50% of realizations with no significant limit cycle; however, the other realizations produced limit cycle amplitudes that were often much greater than the deterministic value.

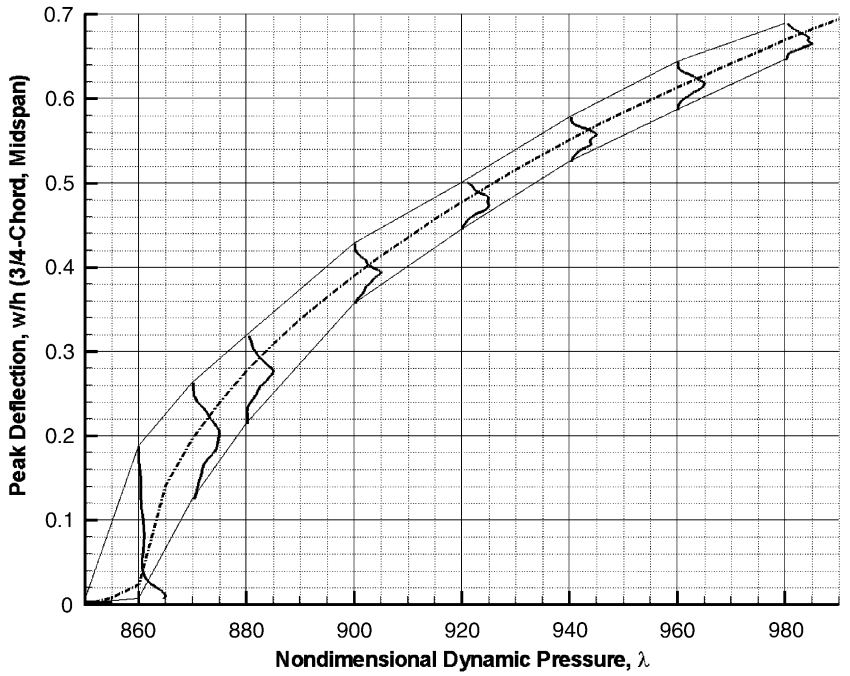

Fig. 6. Stochastic panel response amplitude in the presence of spatial uncertainty of Young's modulus; 47×47 grid [117]; correlation length $CL = 0.10L$.

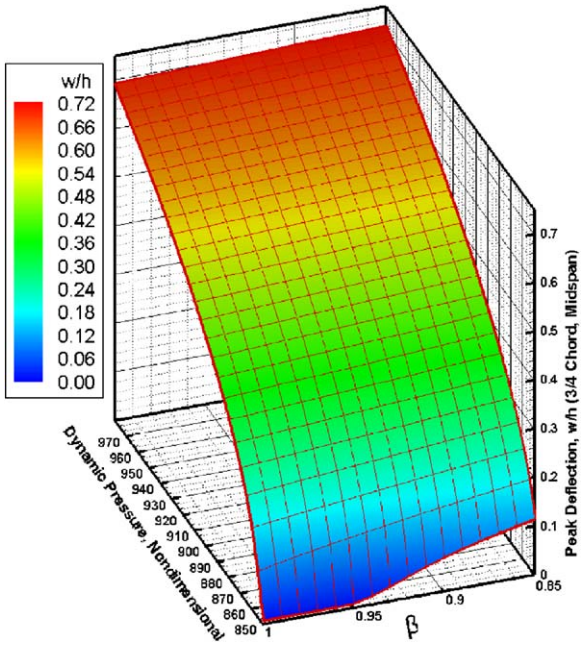

Fig. 7. Response surface to variability in boundary condition parameter $\beta\ -1\leqslant\beta\leqslant -1+\delta\beta_P$, $0\leqslant\beta_P\leqslant 1$, pinned condition; $1+\delta\beta_F\leqslant\beta\leqslant 1$, $0\leqslant\beta_F\ll 1$, clamped condition [116,117].

Fig. 7 shows a three-dimensional plot of the dependence of the plate limit cycle oscillation amplitude, w/h, on the dynamic pressure parameter and the boundary condition rotational spring stiffness parameter, β. It is seen that for values of the dynamic pressure are in the deterministic limit cycle oscillation range, the variability in β affects the plate deflection in an essentially linear manner. However, for values of dynamic pressure in the neighborhood of bifurcation point, the relationship is non-linear. Variation in β results in a softening effect of the clamped panel, and thus induces an increase in the amplitude of plate oscillations. At $\lambda/M_\infty\approx 850$, the global response is sufficiently sensitive to β that small changes in β can induce limit cycle oscillations. Fig. 8 shows a three-dimensional estimated pdf plot as function of the boundary condition variability parameter β, and the amplitude of the limit cycle oscillation. The projection of the pdf on the plane of β-amplitude is shown as contours of equal levels of pdf. Note that the estimated pdf includes the influence of the Young's modulus variability as well; thus, it summarizes the stochastic behavior of the response at a given dynamic pressure.

3.3. Relaxation of bolted joints

3.3.1. Mechanism of relaxation and loosening

Bickford [8] provides an extensive description of several factors that affect joint relaxation. A fastener subjected to vibration will not lose all of its preloads immediately. First there will be a slow loss of preload caused by some of the relaxation mechanisms. Vibration will increase relaxation through wear and hammering. After sufficient preload is lost, friction forces drop below a critical level and the nut actually starts to back off and shake loose. In this case, the joint

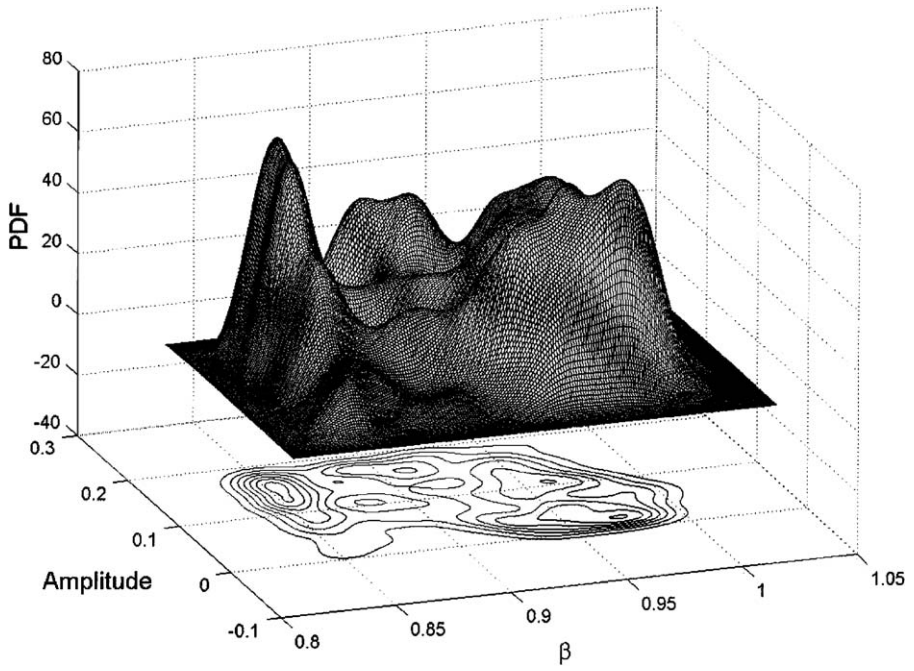

Fig. 8. Three-dimensional pdf plot and its projection on the amplitude. B.C. uncertainty plane showing the contours of equal pdf [116].

will not resemble the ideal boundary conditions but will involve uncertainties. With higher initial preload, longer or more severe vibration is required to reduce preload to the critical point at which back-off occurs. In some circumstances, if the preload is high enough to start with, nut back off will never take place. Usually, safety-wires, coatings and inserts, thread-locking adhesive, and spring-washers are used to prevent loosening [118]. These devices, however, have their limitations and do not necessarily prevent relaxation. Schmitt and Horn [119], and Horn and Schmitt [120] studied the relaxation process in bolted thermoplastic composite joints.

According to Bolt Science [121], the common causes of the relative motion in bolted joint threads are:

1. Component bending that results in forces being induced at the friction surface. If slip occurs, the head and threads will slip, which can lead to loosening.
2. Differential thermal effects caused by either differences in temperature or differences in clamped materials.
3. Applied forces on the joint that can lead to shifting of the joint surfaces and eventually to bolt loosening.

Relaxation effects cause time-dependent boundary conditions and depend on the level of structural vibration. In other words, we have uncertainties in the boundary conditions in addition to a random field due to system parameter uncertainties. Under static loads, the design of such systems is governed by the random field alone while under dynamic loads the designer must take into account the temporal fluctuations of the boundary conditions and the random field. During

an operating period, the non-linear random response can generally change the joint mechanical properties and hence create new self-induced uncertainties. Yost [122] reported a series of random vibration tests on structural blocks with bolted joints to determine whether bolts and studs tightened to various degrees will loosen when subjected to the space shuttle main engine random vibration criteria. Daadbin and Chow [123] modelled the elastic and damping characteristic of the thread interface of a simple bolt model and showed that the contact forces fluctuate because of surface asperities, variations in temperature, and surface chemistry.

The mechanism of vibration-induced loosening of threaded joints is attributed to a reduction in friction, which results in slip at the thread and head interfaces, and a reduction in clamping forces [124–132]. Hess [130] provided a chronological review of the research activities made toward understanding vibration- and shock-induced loosening. Early work [133] was based on static tests in tensile test machines. Sakai [126,127] and Harnchoowong [134] analyzed the static force and torque balance during the relaxation process. Dynamic tests provided the dependence of the tension in the bolt on time or number of cycles. Phenomenological preload plots could be used in developing analytical models of elastic structures [8]. A series of experimental studies were conducted to study the influence of transverse vibration on the self-loosening of fasteners [124,135–140]. Fig. 9, taken from Finkelston [137], shows the dependence of the average vibration life on preload for different values of initial preload, thread pitch, and prevailing torque. In Fig. 9(a) one can see that the initial preload increases the friction forces in the joint and this in turn results in an increase in its vibration resistance. Fine thread nuts endure more vibration cycles than those of coarse thread nuts, as demonstrated in Fig. 9(b). The third plot, Fig. 9(c), shows the effect of the prevailing torque in reducing the rate of loosening.

Recent studies reported experimental observations and measurements of axial harmonic excitation of threaded fasteners [141–145]. They observed that significant relative twisting motion could occur both with and against the weight of the cap screw. Hess and Davis [142] observed that for the frequency range 780–1130 Hz, the nut moved down the screw, and for the range 370–690 Hz it moved up. They attributed the observed behavior to the non-linear dynamic interaction of the vibration and friction, and the resulting patterns of momentary sliding, sticking, and separation between threaded components. Later, Hess and Sudhirkashyap [146,147] and Basava and Hess [148] examined the dynamics of preloaded single-bolt assemblies subjected to axial vibration. Specifically, they studied the effect of vibration level and initial preload on clamping force. They found that the clamping force could remain steady, decrease, or increase depending on preload and vibration levels. As the preload decreases or the vibration level increases, first loosening and then tightening of the assembly took place. They developed an analytical model, which predicted a reduction of 52.9% in the clamping force due to axial vibration. Loosening of threaded fasteners due to dynamic shearing was examined experimentally and numerically by Pai and Hess [149,150]. Kasai et al. [151] and Jiang et al. [152] considered the early stage of self-loosening of bolted joints. Under transverse impact, the thread loosening was examined in references [153–155].

3.3.2. *Structural dynamics involving joint relaxation*

Vibration-induced loosening results in a system with time-dependent boundary conditions. Under stationary excitation one would expect the response to be non-stationary. Qiao et al. [156] developed an analytical model of an elastic beam bolted at both ends. This system is described by

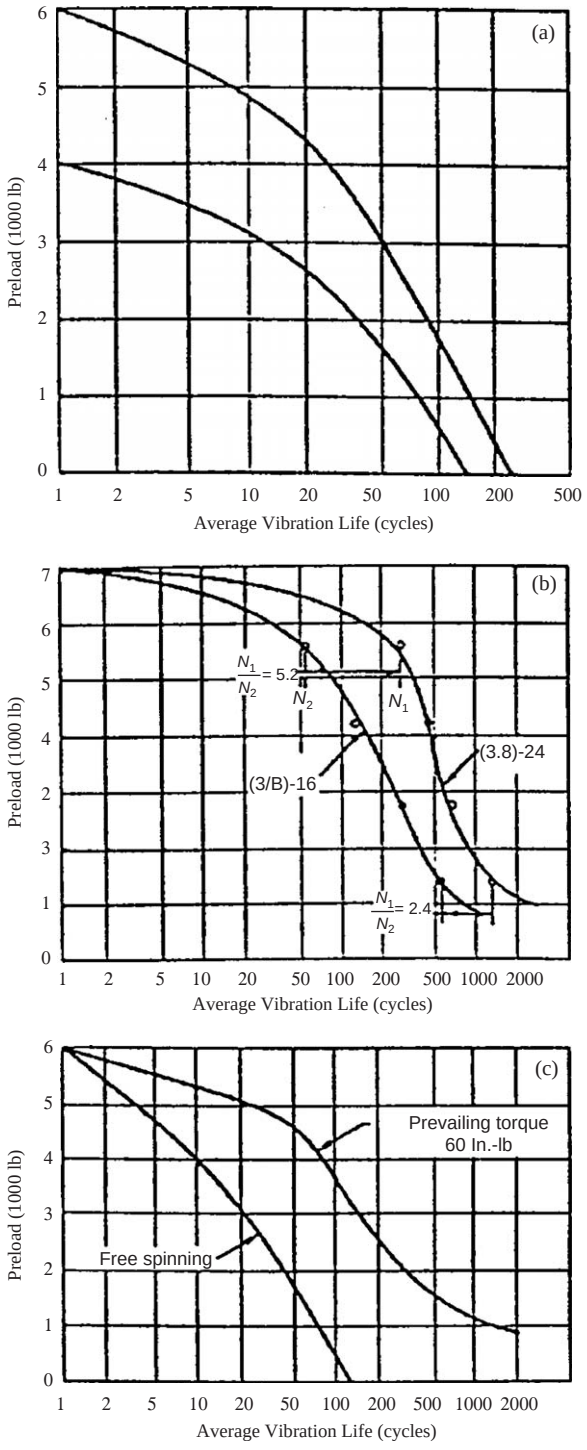

Fig. 9. Dependence of preload relaxation on average vibration life in cycles for different values of (a) initial preload, (b) thread pitch, and (c) prevailing torque level [137].

the partial differential equation

$$\aleph U(x,t) + m(x)\frac{\partial^2 U(x,t)}{\partial t^2} = -m(x)\frac{\partial^2 Y(t)}{\partial t^2} \tag{22}$$

subject to the following boundary conditions at $x = 0$ and $x = L$, respectively:

$$EI\frac{\partial^2 U(0,t)}{\partial x^2} - \alpha_1(t)\frac{\partial U(0,t)}{\partial x} = 0, \quad U(0,t) = 0, \tag{23a, b}$$

$$EI\frac{\partial^2 U(L,t)}{\partial x^2} + \alpha_2(t)\frac{\partial U(L,t)}{\partial x} = 0, \quad U(L,t) = 0, \tag{23c, d}$$

where $U(x,t)$ is the transverse vibration, $Y(t)$ is the transverse support random motion, $\aleph$ is a non-linear integro-differential operator, $m(x)$ is the mass per unit length of the beam, and α_1 and α_2 represent the torsional stiffness of the joints [157], which are considered as random variables in the static case and random processes in the dynamic case. E is Young's modulus, and I is the area moment of inertia about the bending axis. Note that Eqs. (23a–d) are equivalent to Eqs. (19) in the panel limit cycle problem with uncertain boundary stiffness.

Uncertainty in the slope due to the relaxation effect and vibration loosening in joints and fasteners may also be considered. Note that when the end slopes $\partial U(0,t)/\partial x = \partial U(L,t)/\partial x = 0$, or $\alpha_1(t) = \alpha_2(t) = \infty$, one will have the case of a purely clamped–clamped beam. On the other hand, simple supports require $\alpha_1(t) = \alpha_2(t) = 0$. In real situations, both $\alpha_1(t)$ and $\alpha_2(t)$ do not satisfy these ideal conditions: their values are very large for clamped supports, or very small for simple supports. In order to convert these conditions into autonomous form, the following transformation of the response co-ordinate $U(x,t)$ was introduced:

$$U(x,t) = \left[\left(\frac{x}{L}\right)^2 + 2g_1(z_1,z_2)\frac{x}{L} + g_2(z_1,z_2)\right]u(x,t) = \varphi(x;z_1,z_2)u(x,t), \tag{24}$$

where the non-dimensional parameters $z_i(t) = EI/(L\alpha_i(t))$, $i = 1,2$, represent the ratio of the bending rigidity to the torsional stiffness of the joints, and the coefficients g_1 and g_2 are chosen to render the boundary conditions autonomous. This was achieved by substituting transformation (24) into the boundary conditions (23). In this case, the equation of motion takes the form

$$\aleph(\varphi u) + m(x)\frac{\partial}{\partial t}\left(\varphi\frac{\partial u}{\partial t}\right) + m(x)\frac{\partial^2 Y(t)}{\partial t^2} + m(x)\Psi(z_i,\dot{z}_i,\ddot{z}_i)u = 0, \tag{25}$$

where $\Psi(z_i,\dot{z}_i,\ddot{z}_i)$ is a function of the boundary condition uncertainties and their time derivatives. The boundary value problem described by Eq. (25) was transformed into a system of ordinary non-linear differential equations involving uncertain parameters.

3.3.2.1. Joint stiffness as random variables. The uncertain parameters z_1 and z_2 were considered first as random variables independent of time, in which case their time derivatives $\dot{z}_1, \dot{z}_2, \ddot{z}_1$ and $\ddot{z}_2$ vanish. By substituting Eq. (24) into Eq. (25) and applying Galerkin's method by representing the response $u(x,t)$ in terms of the first mode shape,

$$u(x,t) = U_1(t)\sin(\pi x/L), \tag{26}$$

the equation of motion of the first mode was

$$\ddot{U}_1(t) + 2\zeta\omega\dot{U}_1(t) + b_1(z)\omega^2 U_1(t) + b_3(z)\beta[U_1(t)]^3 = b_0(z)\xi(t), \tag{27}$$

where $\omega = \sqrt{(EI/L^4m)}\pi^2$, and $\beta = EA/L^4m$. Eq. (27) is a Duffing oscillator subjected to the random external excitation $\xi(t)$, with coefficients, $b_0(z)$, $b_1(z)$, and $b_3(z)$ that depend on the uncertainty parameter z. Klosner et al. [158] obtained an exact solution of the response probability density function of the special Duffing oscillator with zero linear stiffness and with uncertain non-linear coefficient. Alternatively, the random excitation $\xi(t)$ can be numerically generated such that it has a zero-mean and a constant spectral density over a wide frequency band that exceeds the system natural frequency. The dependence of the response center frequency on the uncertain parameter $z = z_1 = z_2$ is shown in Fig. 10. The limiting values of the beam's natural frequency with zero uncertainty (i.e., clamped) and simply supported case are indicated by the values 3.5607 and 1.5708 respectively. Fig. 11 shows the dependence of the mean square response on z.

3.3.2.2. Joint stiffness as time-dependent. A fastener subjected to vibration will experience a slow loss of preload caused by relaxation mechanisms. Based on this trend the torsional stiffness parameters α_1 and α_2 must be functions of time, i.e., $\alpha_i = \alpha_i(t)$. Consider the torsional stiffness parameters to be function of the number of vibration cycles $n = n(t)$,

$$\bar{\alpha}_i(n) = \frac{\alpha_i(n)L}{EI} = \frac{1}{z_i(n)}, \tag{28}$$

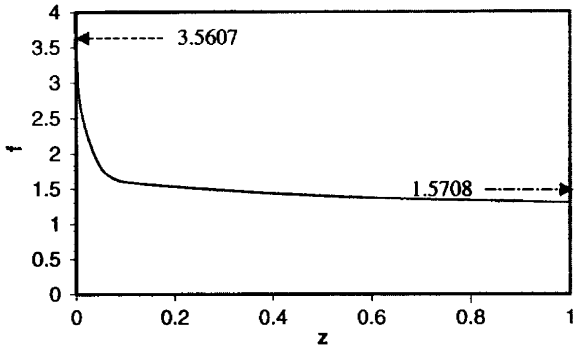

Fig. 10. Dependence of the response central frequency on the boundary condition uncertainty [156].

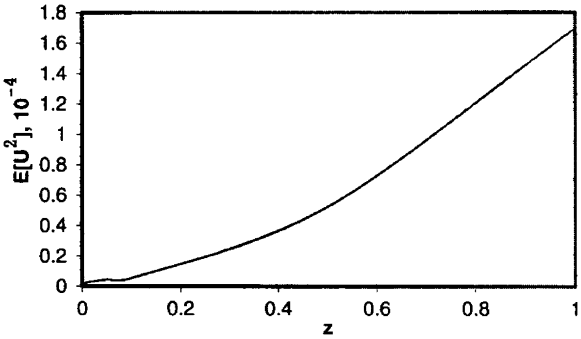

Fig. 11. Response mean squares on the boundary condition uncertainty [156].

where the over-bar denotes that the parameter is dimensionless. An explicit expression for the parameters $\bar{\alpha}_i(n)$ can be obtained based on experimental curves, similar to those shown in Fig. 9. An appropriate elementary function that describes this type of behavior may be selected in the form

$$\bar{\alpha}(n) = A + B\tanh[-k(n - n_c)], \tag{29}$$

where the subscript i has been dropped, and n_c is a critical number of cycles, indicating the center location of the step with respect to the origin, $n = 0$. The parameter k is associated with the slope of the curve at $n = n_c$. The constants A and B are given in terms of the initial and final values of the stiffness parameter, $\bar{\alpha}(0)$ and $\bar{\alpha}(\infty)$. The explicit dependence of $n = n(t)$ is based on the average number of cycles of the random vibration process and can be estimated as $n = n(t) = \langle\omega\rangle t/2\pi$, where $\langle\omega\rangle$ is the mean value of the response frequency and can be taken as the center frequency.

Taking into account expressions (28) and (29), one can write the explicit expression

$$z(t) = Z_0 Z_\infty \left[Z_0 - (Z_0 - Z_\infty)\frac{1 + \tanh(-\lambda(t - t_c))}{1 + \tanh(\lambda t_c)} \right]^{-1}, \tag{30}$$

where $\lambda = (\langle\omega\rangle/2\pi)k$, $Z_0 = z(0)$, and $Z_\infty = z(\infty)$.

Under random excitation of the first mode, the resulting non-linear differential equation (27) was solved using Monte Carlo simulation for three values of the relaxation slope parameter, $\lambda = 0.05, 0.1$, and 0.15. Each response was found to display temporal variation of the torsional stiffness parameter $\alpha(t)$. The response mean square revealed two levels corresponding to the two extreme values of the torsion stiffness parameter. As the relaxation slope parameter increases, the mean square response switches to a higher level at an earlier time. The corresponding correlation function resembles the case of modulated narrow band random process possessing two frequency components as reflected in the response spectra. The evolution of the response spectral density with time was obtained by dividing the response time history record into 30-s small segments, as shown in Fig. 12. The influence of the relaxation process is reflected in moving the response central frequency to the left as the time increases. Obviously the response process is non-stationary even though the excitation is stationary. The source of the non-stationarity is the relaxation in the joint.

In order to explore the influence of the excitation level, the Monte Carlo simulation is carried out for relatively large excitation levels. Figs. 13 and 14 are obtained for excitation spectra $S_\xi = 200$ and 2000, respectively. It is interesting to observe occasional spikes in the time history records indicating that the kurtosis is greater than 3 and the response becomes non-Gaussian. The second important observation is that the bandwidth of the response spectra increases as the excitation level increases. This observation is reflected in both the correlation and power spectral density functions. The third observation is that the response tends to be more stationary in the mean-square as the excitation level increases.

Ibrahim et al. [159] extended the work reported in reference [160] and Qiao et al. [156] to examine the influence of relaxation of boundary conditions on the modal natural frequencies and limit cycle amplitudes of aeroelastic panels subjected to supersonic air flow. The dependence of the real and imaginary parts of the modal eigenvalues on the dynamic pressure λ and relaxation parameter z is shown in Figs. 15(a) and (b) by three-dimensional diagrams for a damping

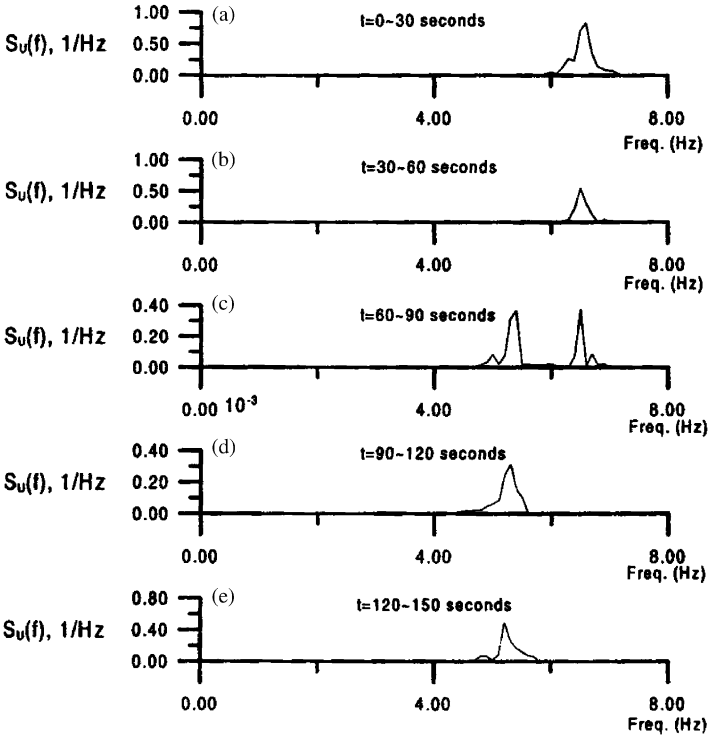

Fig. 12. Response spectra estimated over short interval of time history record of duration 30 s each: (a) $t = 0$–30 s, (b) $t = 30$–60 s, (c) $t = 60$–90 s, (d) $t = 90$–120 s, (e) $t = 120$–150 s [156].

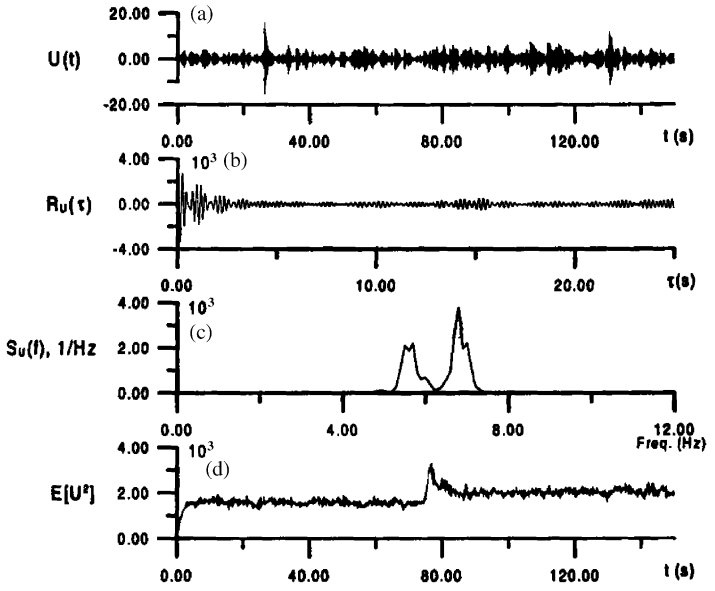

Fig. 13. Time history response and response statistics for slope parameter $\lambda = 0.1$ under excitation spectral density $S_{\xi} = 200$: (a) response time history record, (b) response autocorrelation function, (c) response power spectral density function, (d) response mean square [156].

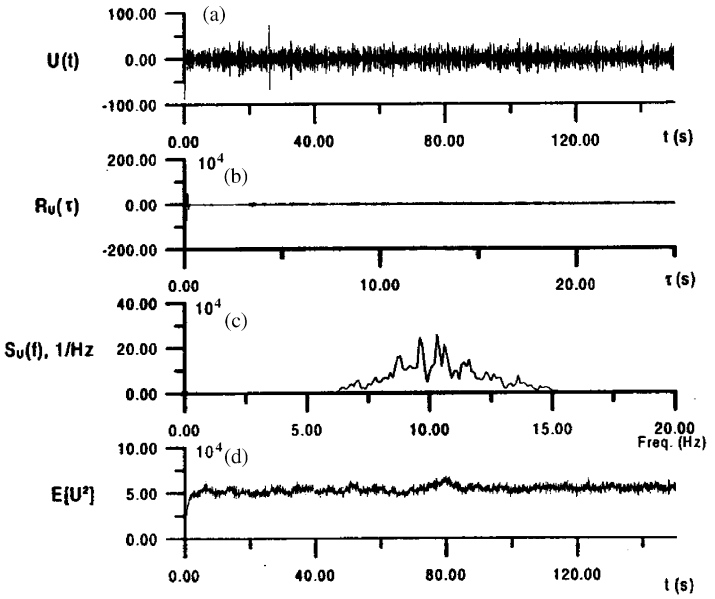

Fig. 14. Time history response and response statistics for slope parameter $\lambda = 0.1$ under excitation spectral density $S_\xi = 2000$, (a) response time history record, (b) response autocorrelation function, (c) response power spectral density function, (d) response mean square [156].

parameter $\zeta = 0.01$, and a mass parameter $\zeta = 0.1$. It is seen that the real parts are always negative up to a critical value of the dynamic pressure, depending on the value of the relaxation parameter z, above which one real part crosses to the positive zone indicating the occurrence of panel flutter. Note that the value $z = 0$ corresponds to clamped–clamped panel and the corresponding critical dynamic pressure is greater than any case with $z \neq 0$. For equal modal viscous damping coefficients, damping is known to stabilize the panel [160].

The panel experiences flutter above those critical values of dynamic pressure and relaxation parameter. The inclusion of non-linearities in the panel equations of motion causes the flutter to achieve a limit cycle. However, due to relaxation the panel response experiences non-stationary limit cycle oscillations as shown in Figs. 16(b, c). The FFT shown in Fig. 16(d) reveals that the frequency content of the first mode includes one spike at zero frequency, due to the static in-plane load, and another band limited response covering a frequency band ranging from nearly 5.8 to 6.8 (dimensionless frequency). This frequency band reflects the time variation of the panel frequency with time. This is demonstrated by using the spectrogram technique. The time evolution of the frequency content represented by the spectrogram in Fig. 16(e) demonstrates the correlation between the variation of the frequency with the relaxation process given in Fig. 16(a). It is seen that the response frequency increases as the joint passes through relaxation. This perhaps surprising result can be explained as follows: on the one hand, the relaxation causes a decrease in the frequency. On the other hand, the non-linearity of the panel has hard spring characteristics. It appears that the non-linearity overcomes the softening effect of relaxation. Figs. 17(a) and (b) show the dependence of the limit cycle amplitudes on the dynamic pressure for different discrete

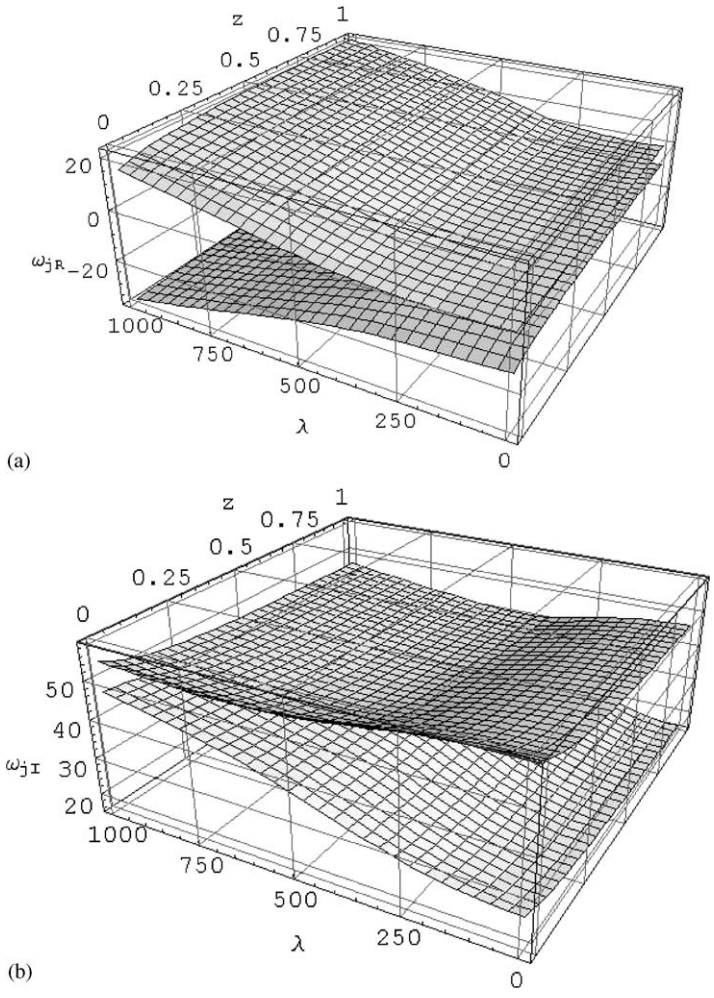

Fig. 15. Dependence of the panel eigenvalues on the dynamic pressure λ and relaxation parameter z for damping ratio $\zeta = 0.01$ and air to panel mass ratio 0.1: (a) real part, (b) imaginary part [159].

values of the relaxation parameter z. The two ideal cases of purely simple–simple and clamped–clamped boundary conditions are plotted by solid curves. The limit cycles occur as supercritical Hopf bifurcations. Note that the relaxation results in moving the bifurcation point to lower values of dynamic pressure and the limit cycle amplitude is very sensitive to the boundary stiffness.

Fig. 16. (a) Relaxation parameter, (b) first mode time history response, (c) second mode time history response, (d) first mode FFT, and (e) spectrogram of the first mode [159].

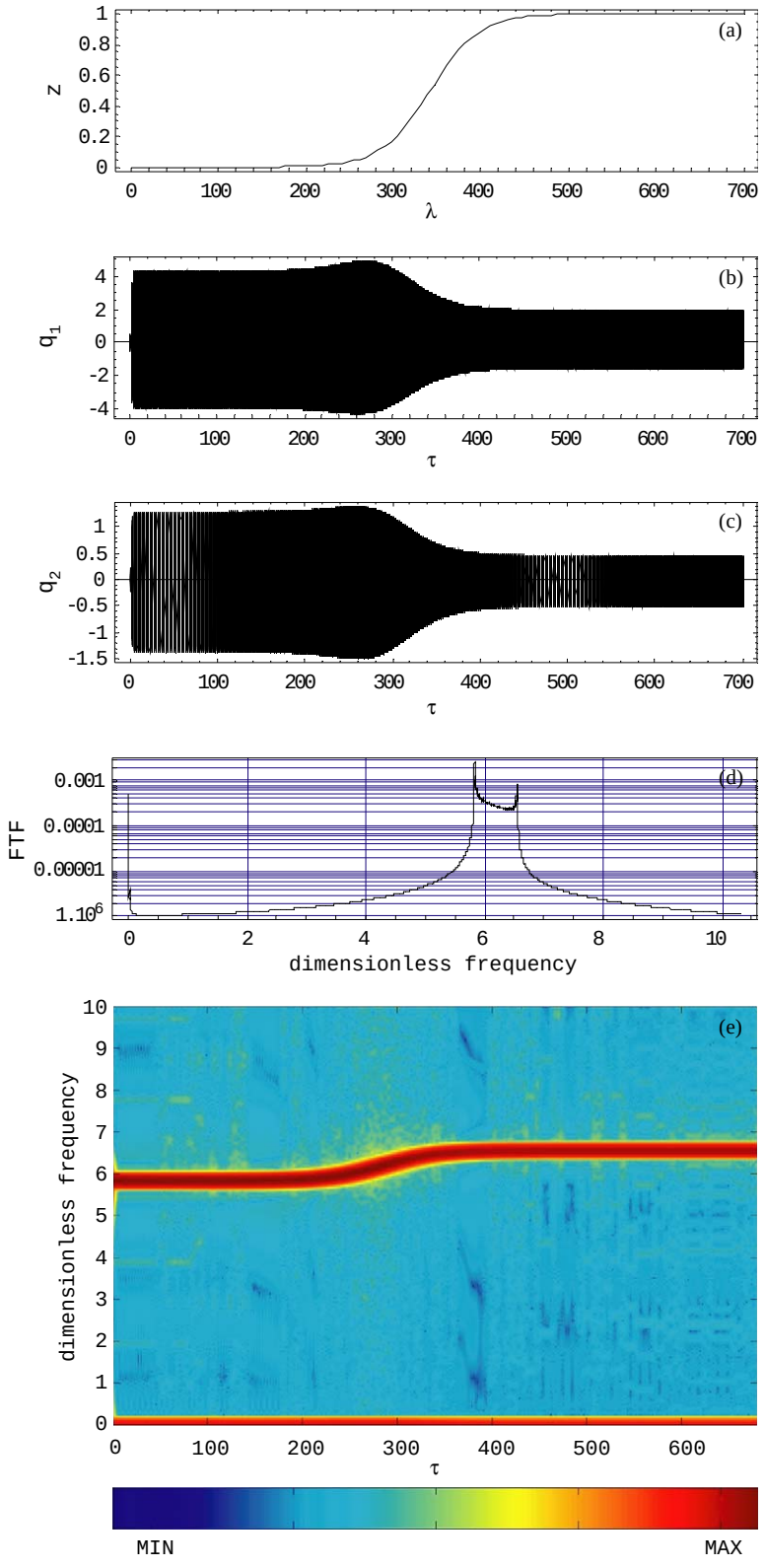
(a)
z
λ
(b)
q1
τ
(c)
q2
τ
(d)
FTF
dimensionless frequency
(e)
dimensionless frequency
τ
MIN
MAX

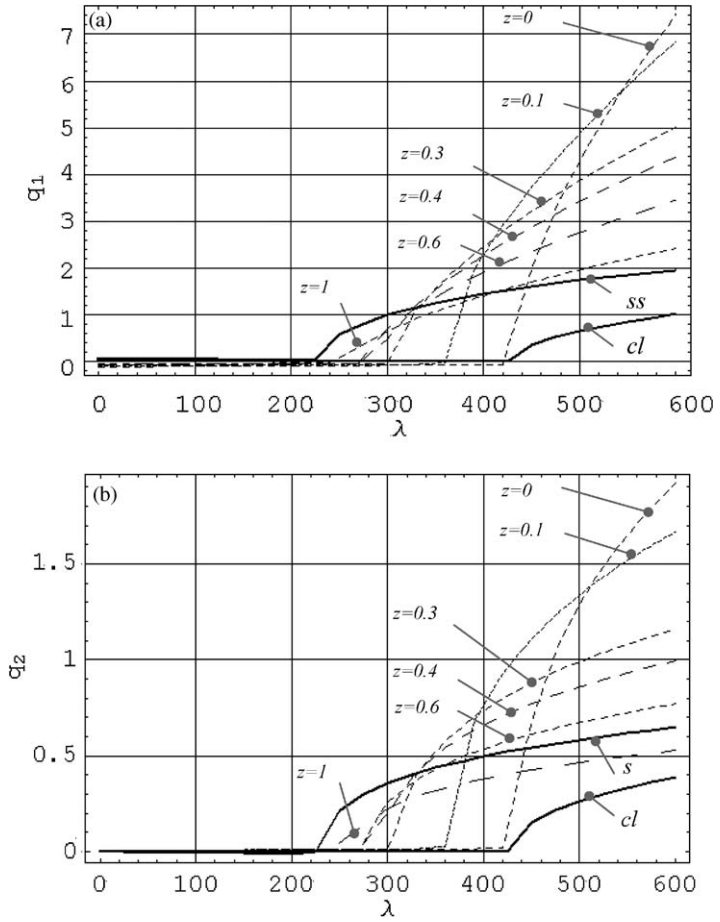

Fig. 17. Bifurcation diagrams for different values of relaxation parameter: (a) first mode, (b) second mode [159].

4. Identification of joint properties

4.1. The need for joint identification

The main purpose of joint identification is to estimate the joint parameters that minimize the difference between the measured assembly response characteristics, such as frequency response functions (FRFs), and those predicted analytically or numerically. Identification of joint properties is an important task in predicting the dynamic characteristics of mechanical systems such as machine tool dynamics [161–163], aerospace structures [164–167], and many other structural systems.

The numerical techniques used for structural dynamic problems, such as FEM, often give different results from those measured experimentally. For a converged mesh, discrepancy is believed to be due in large part to the uncertainty of FE models such as unmodelled variability in joint properties and boundary conditions, and also unmodelled non-linearities. In an attempt to

improve the numerical results, various techniques have been proposed in which experimental data are integrated with a corresponding FEM [168–170]. Bolted joints are considered as a source of parameter uncertainties, which result in mismatch between finite element analysis (FEA) and experimental measurements. The main parameters considered in structural dynamics are stiffness and damping properties of a joint. Several studies have been conducted to extract joint properties from measured data.

4.2. Joint identification approaches and difficulties

There are several approaches that have been utilized to identify joint parameters. These approaches rely on the experimental measurements of FRFs. Yoshimura [171,172] conducted a series of experimental investigations to measure dynamic characteristics and quantitative values of the stiffness and damping of a bolted joint, welded joint, and representative joints in machine tool structures. Measured modal parameters have been used in several studies to identify joint structural parameters [173,174]. For example, Inamura and Sata [175] proposed a joint structural parameter identification approach based on the use of the complete mode shapes and eigenvalues. Yuan and Wu [176] and Kim et al. [163] used a condensed FE model and incomplete mode shapes to identify joint stiffness and damping properties. These methods require accurate modal parameters, which are difficult to extract especially in cases of closely coupled or heavily damped modes.

In order to overcome the difficulties encountered in extracting accurate modal parameters, some methods based on FRFs for determining joint properties have been proposed in the literature [177–180]. Mottershead and Stanway [180] proposed an algorithm for obtaining structural parameters from FRF measurements. In theory, it can be applied to the identification of joint parameters; however, it may not be practical for cases where measurements are not possible for certain locations. Other attempts were made to identify joint properties from the substructure FRFs and the joint-dependent FRFs of the whole structure [177,181,182]. This method also has some difficulties when the FRF measurement at a joint is not possible. Yang and Park [183] combined the incomplete measured FRFs with the substructure FE model, which excludes undetermined joint properties. The unmeasured FRFs were estimated by solving an over-determined set of linear equations derived from measured FRFs and the substructure FE model. By assuming a model of the joint, the joint structural parameters were extracted from measured and estimated FRFs by an iterative output error algorithm.

Arruda and Santos [184,185] treated the problem of FE model updating of structures that consist of substructures connected through mechanical joints whose stiffness and damping properties are unknown. The model was updated by estimating the mechanical joint parameters via curve fitting of measured FRFs using a non-linear least-squares scheme. Joint parameters can be experimentally determined from the FRFs measured with and without the joints [112,177,182,186,187]. Hwang [187] employed the FRFs for each discrete frequency so that the connection properties could be estimated for each frequency and averaged using statistical methods. This approach may not be convenient when some joints are not accessible for instrumentation.

Alternatively, model-based techniques that involve a hybrid of experimental data and FE model results have been widely used in the literature. For example, one class of the model-based

techniques is referred to as *direct methods* in which the joint parameters are determined by solving a set of characteristic or dynamic (impedance) equations [84,165,176,178,181,188]. These equations consist of the stiffness and mass matrices generated from a FE model and the measured frequency response data. Theoretically, joint stiffnesses can be determined from the characteristic equation by using only one set of complete modal data (natural frequency and modal vector). Another class is known as *penalty techniques*, which are based on minimizing errors or residuals that are used to assess the discrepancies between the FEMs and experimental measurements. The corrections to the model parameters can be related to the prediction errors of the FEMs through a sensitivity (Jacobian) matrix. The sensitivity matrix typically involves the derivatives of the stiffness, damping, and mass matrices with respect to each of the model parameters to be updated. The bolted joint may simply be treated as a lumped element in the model [183,185,189–191]. Li [192] reported that the penalty techniques are usually more flexible and versatile than the direct methods in that various constraints are readily imposed on the model parameters. Li [192] introduced a so-called reduced order characteristic polynomial defined in terms of the measured natural frequencies. This polynomial was then used for updating or identifying joint stiffnesses. Ahmadian et al. [193] proposed a generic element approach to model some quite complicated joints. Various other computer models have been developed for metal and composite fasteners [194–196].

The dynamic properties of a joint are difficult to model analytically. An alternative approach for establishing a theoretical model for a joint is to use an experimental approach. For example, Burdekin et al. [197,198] established a mathematical joint model by measuring the response and force at a joint. Unfortunately, in many cases the response or force at the joint is not measurable, so one must use one of the joint identification techniques, such as those proposed in references [112,177,179,199–203]. Ren and Beards [188] outlined an alternative approach for establishing a theoretical model of a joint by extracting the model parameters from experimental data using joint identification techniques. Their work was based on the identification of linear joints using FRF data. The basic strategy of most FRF joint identification methods is to measure the properties of the structure without joints (referred to as the substructure system) and the structure with joints (referred to as the assembled system). The difference between the dynamic properties of the two cases is caused by the joints. In real applications, this difference cannot be attributed to the joint properties alone because it may include measurement errors and parameter uncertainties in the two systems. Furthermore, many of the identification procedures assume that the identified parameters are deterministic. Therefore, updating a model based on measurements from one structure may still leads to apparent discrepancies when the model is used to simulate a different but nominally similar structure.

4.3. Identification of linear joints

4.3.1. Identification of joint damping and stiffness

In many procedures, the joint properties are extracted from the measured receptances of structures without introducing mathematical models of the mass, damping, and stiffness matrices. Tsai and Chou [177] proposed an identification method for bolt joint properties based on a synthesis method originally developed by Bishop [204]. In Bishop's formulation, the interface serves to enforce kinematic consistency between the substructures. Consider two substructures I,

and II joined at interface, b. Substructure I consists of regions a, and b, while substructure II consists of regions c, and b. The relationship between the displacement vectors and force vectors for the two substructures are given in terms of the receptance as

$$\begin{Bmatrix} \mathbf{X}_a^{(1)} \\ \mathbf{X}_b^{(1)} \end{Bmatrix} = \begin{bmatrix} \mathbf{H}_{aa}^{(1)} & \mathbf{H}_{ab}^{(1)} \\ \mathbf{H}_{ba}^{(1)} & \mathbf{H}_{bb}^{(1)} \end{bmatrix} \begin{Bmatrix} \mathbf{f}_a^{(1)} \\ \mathbf{f}_b^{(1)} \end{Bmatrix}, \quad \begin{Bmatrix} \mathbf{X}_c^{(2)} \\ \mathbf{X}_b^{(2)} \end{Bmatrix} = \begin{bmatrix} \mathbf{H}_{cc}^{(2)} & \mathbf{H}_{cb}^{(2)} \\ \mathbf{H}_{bc}^{(2)} & \mathbf{H}_{bb}^{(2)} \end{bmatrix} \begin{Bmatrix} \mathbf{f}_c^{(2)} \\ \mathbf{f}_b^{(2)} \end{Bmatrix}, \tag{31a, b}$$

where $\mathbf{X}_j^{(i)}$ is the displacement vector on region j for substructure i, $\mathbf{H}_{jk}^{(i)}$ is the receptance matrix between regions j and k for substructure i, and $\mathbf{f}_j^{(i)}$ is the force vector on region j for substructure i. Using Eqs. (31) and the equilibrium state at the joint, $\mathbf{f}_b^{(1)} + \mathbf{f}_b^{(2)} = 0$, in the compatibility condition, $\mathbf{X}_b^{(1)} = \mathbf{X}_b^{(2)}$, gives

$$\mathbf{f}_b^{(1)} = \mathbf{H}_B^{-1}\{\mathbf{H}_{bc}^{(2)}\mathbf{f}_c^{(2)} - \mathbf{H}_{ba}^{(1)}\mathbf{f}_a^{(1)}\}, \tag{32}$$

where $\mathbf{H}_B = \mathbf{H}_{bb}^{(1)} + \mathbf{H}_{bb}^{(2)}$. Using Eq. (32) in Eqs. (31) gives

$$\mathbf{X}_a^{(1)} = [\mathbf{H}_{aa}^{(1)} - \mathbf{H}_{ab}^{(1)}\mathbf{H}_B^{-1}\mathbf{H}_{ba}^{(1)}]\mathbf{f}_a^{(1)} + \mathbf{H}_{ab}^{(1)}\mathbf{H}_B^{-1}\mathbf{H}_{bc}^{(2)}\mathbf{f}_c^{(2)}, \tag{33}$$

$$\mathbf{X}_c^{(2)} = [\mathbf{H}_{cc}^{(2)} - \mathbf{H}_{cb}^{(2)}\mathbf{H}_B^{-1}\mathbf{H}_{bc}^{(2)}]\mathbf{f}_c^{(2)} + \mathbf{H}_{cb}^{(2)}\mathbf{H}_B^{-1}\mathbf{H}_{ba}^{(1)}\mathbf{f}_a^{(1)}. \tag{34}$$

For a single bolted joint, Tsai and Chou [177] assumed that its mass is very small compared with the neighboring structure, and its dynamic properties are dominated by the stiffness and damping. The interface force vectors $\mathbf{f}_b^{(1)}$ and $\mathbf{f}_b^{(2)}$ acting on substructures I and II are assumed equal in magnitude and opposite in direction. However, the interface displacement vectors $\mathbf{X}_b^{(1)}$ and $\mathbf{X}_b^{(2)}$ are not equal but are related to the interface forces through the compatibility condition

$$\mathbf{X}_b^{(2)} - \mathbf{X}_b^{(1)} = \mathbf{H}_{jt}\mathbf{f}_b^{(1)}, \tag{35}$$

where subscript jt stand for joint. Substituting Eqs. (31) into Eq. (35) gives

$$\mathbf{H}_{bc}^{(2)}\mathbf{f}_c^{(2)} + \mathbf{H}_{bb}^{(2)}\mathbf{f}_b^{(2)} - \mathbf{H}_{ba}^{(1)}\mathbf{f}_a^{(1)} - \mathbf{H}_{bb}^{(1)}\mathbf{f}_b^{(1)} = \mathbf{H}_{jt}\mathbf{f}_b^{(1)}. \tag{36}$$

In view of the equilibrium condition, $\mathbf{f}_b^{(1)} + \mathbf{f}_b^{(2)} = 0$, Eq. (36) may be written in the form

$$\mathbf{f}_b^{(1)} = [\mathbf{H}_B + \mathbf{H}_{jt}]^{-1}\{\mathbf{H}_{bc}^{(2)}\mathbf{f}_c^{(2)} - \mathbf{H}_{ba}^{(1)}\mathbf{f}_a^{(1)}\}. \tag{37}$$

Now the relationship between the displacement and force vectors of the assembled structure is written in the form

$$\mathbf{X}^{(3)} = \mathbf{H}^{(3)}\mathbf{f}^{(3)}, \tag{38}$$

where

$$\mathbf{X}^{(3)} = \begin{Bmatrix} \mathbf{X}_a^{(1)} \\ \mathbf{X}_c^{(2)} \end{Bmatrix}, \quad \mathbf{f}^{(3)} = \begin{Bmatrix} \mathbf{f}_a^{(1)} \\ \mathbf{f}_c^{(2)} \end{Bmatrix}, \tag{39a, b}$$

$$\mathbf{H}^{(3)} = \begin{bmatrix} \mathbf{H}_{aa}^{(1)} - \mathbf{H}_{ab}^{(1)}[\mathbf{H}_B + \mathbf{H}_{jt}]^{-1}\mathbf{H}_{ba}^{(1)} & \mathbf{H}_{ab}^{(1)}[\mathbf{H}_B + \mathbf{H}_{jt}]^{-1}\mathbf{H}_{bc}^{(2)} \\ \mathbf{H}_{cb}^{(2)}[\mathbf{H}_B + \mathbf{H}_{jt}]^{-1}\mathbf{H}_{ba}^{(1)} & \mathbf{H}_{cc}^{(2)} - \mathbf{H}_{cb}^{(2)}[\mathbf{H}_B + \mathbf{H}_{jt}]^{-1}\mathbf{H}_{bc}^{(2)} \end{bmatrix}. \tag{39c}$$

Eqs. (38) and (39) of the assembly are exactly the same form as Eqs. (33) and (34) of the substructures, except that Eqs. (38) and (39) include the receptance of the joint.

Alternatively, Eq. (39c) can be written in the form

$$\mathbf{H}^{(\gamma)} = \mathbf{H}^{(\alpha)}[\mathbf{H}_B + \mathbf{H}_{jt}]^{-1}\mathbf{H}^{(\beta)}, \tag{40}$$

where

$$\mathbf{H}^{(\gamma)} = \mathbf{H}^{(3)} - \begin{bmatrix} \mathbf{H}_{aa}^{(1)} & \mathbf{0} \\ \mathbf{0} & \mathbf{H}_{cc}^{(2)} \end{bmatrix}, \quad \mathbf{H}^{(\alpha)} = \begin{bmatrix} -\mathbf{H}_{ab}^{(1)} \\ \mathbf{H}_{cb}^{(2)} \end{bmatrix}, \quad \mathbf{H}^{(\beta)} = [\,\mathbf{H}_{ba}^{(1)} \quad -\mathbf{H}_{bc}^{(2)}\,].$$

By measuring the receptance of the substructures and the assembled structure, one can extract the dynamic properties of the joint, $\mathbf{H}_{jt}$, from Eq. (40). By neglecting the mass of the joint, the joint can be represented by linear damping, $\mathbf{C}$, and stiffness, $\mathbf{K}$, matrices. Under harmonic excitation of frequency Ω, the joint model can be written in the form

$$[\mathrm{i}\Omega\mathbf{C} + \mathbf{K}][\mathbf{X}_b^{(2)} - \mathbf{X}_b^{(1)}] = \mathbf{f}_b^{(1)}, \tag{41}$$

where $\mathrm{i} = \sqrt{-1}$. Comparing Eq. (35) with Eq. (41) one can write the joint receptance as

$$\mathbf{H}_{jt} = [\mathbf{K} + \mathrm{i}\Omega\mathbf{C}]^{-1}. \tag{42}$$

Note that the number of unknowns, $\mathbf{C}$, and $\mathbf{K}$, in Eq. (46) are $2 \times n^2$, where n is the number of degrees of freedom on the substructure interface. All other quantities in Eq. (40) can be measured. By taking inverses on both sides of Eq. (40), one writes

$$\mathbf{H}^{(c)} = \mathbf{H}^{(\alpha)}[\mathbf{K} + \mathrm{i}\Omega\mathbf{C}]\mathbf{H}^{(\beta)}, \tag{43}$$

where $\mathbf{H}^{(c)} = [\mathbf{H}^{(\gamma)^{-1}} - \mathbf{H}^{(\beta)^{-1}}\mathbf{H}_B\mathbf{H}^{(\alpha)^{-1}}]^{-1}$.

If the measured FRFs are inertances instead of receptances, the joint properties should be identified from

$$\mathbf{H}^{(c)} = -\frac{1}{\Omega^2}\mathbf{H}^{(\alpha)}[\mathbf{K} + \mathrm{i}\Omega\mathbf{C}]\mathbf{H}^{(\beta)}. \tag{44}$$

For each Ω Eq. (43) or Eq. (44) constitutes $2 \times n^2$ unknowns, and if there are m frequencies the total number of equations is $2 \times m \times n^2$; therefore the number of equations exceeds the number of unknowns and the least-squares method may be used to solve for the unknowns. Eq. (44) was used to identify the joint properties for different frequency ranges. Tsai and Chou [177] found that the identified values vary with the selected frequency range. Accordingly, it was recommended to use the identified properties only for the frequency range that is applied on the system in practice.

Hanss [90] also applied fuzzy arithmetic to simulate and analyze the friction interface between the sliding surfaces of a bolted joint. The friction interface was represented as a contact between bristles involving seven uncertain parameters described by symmetric fuzzy number of quasi-Gaussian shape. The frictional moment was expressed in terms of the relative angular sliding velocity at the friction interface and an internal variable. The seven parameters were coefficients in the governing equation of the model but Hanss [90] commented that their exact definition could not be extracted. It was shown that the influence of three of seven parameters was significant.

4.3.2. Identification of joint mass and stiffness

In some cases, when the joints are rigidly connected and slip cannot take place, one may ignore the joint's damping and consider only its inertia and stiffness parameters. Ren and Beards [201,205,206] generalized the FRF joint identification technique for systems involving rigid and

flexible joints. In their formulation, the co-ordinates on the assembly are divided into joint and non-joint regions with subscripts, j, and n respectively. For the substructure systems the co-ordinates are also divided into joint and non-joint regions with subscripts a and b respectively. The joint system is represented by subscript c. The relationships between the displacement vectors and the force vectors for the assembly is

$$\begin{Bmatrix} \mathbf{X}_n \\ \mathbf{X}_j \end{Bmatrix} = \begin{bmatrix} \mathbf{H}_{nn} & \mathbf{H}_{nj} \\ \mathbf{H}_{jn} & \mathbf{H}_{jj} \end{bmatrix} \begin{Bmatrix} \mathbf{f}_n \\ \mathbf{f}_j \end{Bmatrix}. \tag{45}$$

The relationship for the substructures is

$$\begin{Bmatrix} \mathbf{X}_a \\ \mathbf{X}_b \end{Bmatrix} = \begin{bmatrix} \mathbf{H}_{aa} & \mathbf{H}_{ab} \\ \mathbf{H}_{ba} & \mathbf{H}_{bb} \end{bmatrix} \begin{Bmatrix} \mathbf{f}_a \\ \mathbf{f}_b \end{Bmatrix}. \tag{46}$$

The characteristics of the joint are described by the dynamic stiffness matrix $\mathbf{Z}_j$,

$$\mathbf{Z}_j \mathbf{X}_c = \mathbf{f}_c. \tag{47}$$

Compatibility conditions require that the non-joint displacements on the substructure system and the assembly to be identical, i.e.,

$$\mathbf{f}_b = \mathbf{f}_n, \quad \mathbf{X}_b = \mathbf{X}_n. \tag{48a, b}$$

Compatibility and equilibrium conditions at the joint co-ordinates are

$$\mathbf{f}_b + \mathbf{f}_c = \mathbf{f}_j, \quad \mathbf{X}_j = \mathbf{X}_b = \mathbf{X}_c. \tag{49a, b}$$

Multiplying both sides of the equation for $\mathbf{X}_b$, formed by the second row of Eq. (46), by $\mathbf{Z}_j$, and using the identity (49b) gives

$$\mathbf{Z}_j \mathbf{X}_c = \mathbf{f}_c = \{\mathbf{f}_j - \mathbf{f}_b\} = \mathbf{Z}_j \mathbf{H}_{ba} \mathbf{f}_a + \mathbf{Z}_j \mathbf{H}_{bb} \mathbf{f}_b. \tag{50}$$

Rearranging, Eq. (50) can be written in the form

$$\mathbf{f}_b = [\mathbf{I} + \mathbf{Z}_j \mathbf{H}_{bb}]^{-1} \{\mathbf{f}_j - \mathbf{Z}_j \mathbf{H}_{ba} \mathbf{f}_a\}. \tag{51}$$

Substituting Eq. (51) into Eq. (46) and using the identities (48) and (49b) gives

$$\begin{Bmatrix} \mathbf{X}_n \\ \mathbf{X}_j \end{Bmatrix} = \begin{bmatrix} [\mathbf{H}_{aa} - \mathbf{H}_{ab}[\mathbf{I} + \mathbf{Z}_j \mathbf{H}_{bb}]^{-1} \mathbf{Z}_j \mathbf{H}_{ba}] & \mathbf{H}_{ab}[\mathbf{I} + \mathbf{Z}_j \mathbf{H}_{bb}]^{-1} \\ [\mathbf{H}_{ba} - \mathbf{H}_{bb}[\mathbf{I} + \mathbf{Z}_j \mathbf{H}_{bb}]^{-1} \mathbf{Z}_j \mathbf{H}_{ba}] & \mathbf{H}_{bb}[\mathbf{I} + \mathbf{Z}_j \mathbf{H}_{bb}]^{-1} \end{bmatrix} \begin{Bmatrix} \mathbf{f}_n \\ \mathbf{f}_j \end{Bmatrix}. \tag{52}$$

Comparing Eq. (52) with Eq. (45) gives

$$\mathbf{H}_{aa} - \mathbf{H}_{nn} = \mathbf{H}_{nj} \mathbf{Z}_j \mathbf{H}_{ba}, \quad \mathbf{H}_{ba} - \mathbf{H}_{jn} = \mathbf{H}_{jj} \mathbf{Z}_j \mathbf{H}_{ba}, \tag{53a, b}$$

$$\mathbf{H}_{bb} - \mathbf{H}_{jj} = \mathbf{H}_{jj} \mathbf{Z}_j \mathbf{H}_{bb}, \quad \mathbf{H}_{ab} - \mathbf{H}_{nj} = \mathbf{H}_{nj} \mathbf{Z}_j \mathbf{H}_{bb}. \tag{53c, d}$$

Eqs. (53) are used to identify the joint impedance matrix $\mathbf{Z}_j$ $(N \times N)$ and they have the general form $\mathbf{C} = \mathbf{A}\mathbf{Z}_j\mathbf{B}$ and can be written as a set of linear equations $[\mathbf{E}]\{\mathbf{z}\} = \{\mathbf{g}\}$, where $\{\mathbf{z}\}$ is a frequency-dependent $N^2 \times 1$ vector whose elements are constructed from $\mathbf{Z}_j$, $[\mathbf{E}]$ is the coefficient matrix constructed from $\mathbf{A}$ and $\mathbf{B}$ matrices, and $\{\mathbf{g}\}$ is a coefficient vector constructed from matrix $\mathbf{C}$. Ren and Beards [201] introduced a linear transformation to convert $\{\mathbf{z}\}$ into a frequency independent vector. If the joint is stiff, the matrix $\mathbf{A}$ becomes ill-conditioned and the linear transformation is not be applicable.

In practice, it is not always possible to measure $\mathbf{H}_{nj}$. However, it can be calculated from the relationship

$$\mathbf{H}_{nj} = \mathbf{H}_{ab} - [\mathbf{H}_{aa} - \mathbf{H}_{nn}]\mathbf{H}_{ba}^{+}\mathbf{H}_{bb}, \tag{54}$$

where $\mathbf{H}_{ba}^{+} = [\mathbf{H}_{ba}^{\mathrm{T}}\mathbf{H}_{ba}]^{-1}\mathbf{H}_{ba}^{\mathrm{T}}$ is the pseudo-inverse of matrix $\mathbf{H}_{ba}$.

The properties of an assembly can be predicted from the properties of its components through coupling techniques [177,205,207]. The coupling process involves the coupling of two joint co-ordinates. For example, if the ith and jth co-ordinates in the substructure matrix $\mathbf{H}_s$ are coupled, the following relationship gives the receptance of the assembly matrix $\mathbf{H}_A$ in terms of $\mathbf{H}_s$ [205],

$$\mathbf{H}_A = \mathbf{H}_s - \frac{1}{h_{ii} + h_{ji} - 2h_{ij}}\{\{h_{sj}\} - \{h_{si}\}\}\{\{h_{sj}\} - \{h_{si}\}\}^{\mathrm{T}}, \tag{55}$$

where h_{ii}, h_{ij}, h_{ji} are elements at ith and jth columns in the substructure matrix $\mathbf{H}_s$; the $\{h_{si}\}$ and $\{h_{sj}\}$ represent the ith and jth columns in the matrix $\mathbf{H}_s$. Since the effects of measurement errors can be significantly magnified at resonance frequencies of substructures in the coupling process, the FRFs at resonance frequencies of the substructures should not be used in the identification process. Ren and Beards [187] indicated that the accuracy of joint identification could be improved by using the coupling-identification approach outlined in Ren and Beards [205].

Wang and Liou [112,182] tried to identify the joint damping and stiffness from the noise contaminated FRFs of the whole structure and the substructures. They suggested a noise insensitive algorithm to calculate joint parameters by taking only the diagonal elements of FRF matrices instead of taking the time consuming inverse of FRF matrices. Ratcliffe and Lieven [208] showed that a joint identification procedure that calculates system matrix terms individually results in a joint that has an incorrect connectivity, although it may reproduce the experimental data successfully. They proposed some improvements to Ren and Beards [188] method that yield significantly improved lower order modal properties. They also used generic element matrices in conjunction with an optimization scheme to make adjustments to the system matrices that yield correct connectivity. This approach does not include damping which is very important in bolted joints.

Hanss et al. [88] estimated the stiffness and damping coefficient as an inverse fuzzy arithmetic problem for the joint of two longitudinal rods (Fig. 18). The joint was modelled as a two-parameter model Kelvin–Voigt element. The measured data involved the natural frequency, f, and damping ratio, ζ. Fuzzy numbers $\tilde{f}$ and $\tilde{\zeta}$ were defined according to Eq. (4) to represent the uncertainty in the measured data. From the analytical model, the damping coefficient, c, and stiffness, k, are given by

$$c = \frac{1}{\mathrm{Im}(s)}\mathrm{Im}\left\{-\frac{s(A_1\sqrt{E_1\rho_1})(A_2\sqrt{E_2\rho_2})}{A_1\sqrt{E_1\rho_1}\coth(sl_2\sqrt{\rho_2/E_2}) + A_2\sqrt{E_2\rho_2}\coth(sl_1\sqrt{\rho_1/E_1})}\right\}, \tag{56a}$$

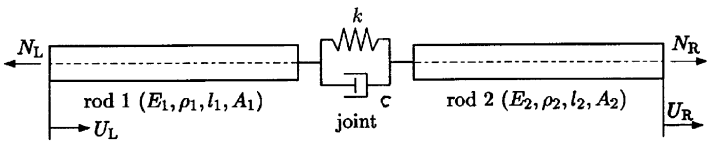

Fig. 18. Two-parameter joint model of two rods [88].

$$k = \mathrm{Re}\left\{ - \frac{s(A_1\sqrt{E_1\rho_1})(A_2\sqrt{E_2\rho_2})}{A_1\sqrt{E_1\rho_1}\coth(sl_2\sqrt{\rho_2/E_2}) + A_2\sqrt{E_2\rho_2}\coth(sl_1\sqrt{\rho_1/E_1})} \right\} - c\,\mathrm{Re}(s), \quad (56b)$$

where $s = -\zeta/\sqrt{1-\zeta^2}\omega + \mathrm{i}\omega$, A_i, $i = 1, 2$, are the cross-sectional areas of the two bars. E_i, ρ_i, and l_i are the Young's modulus, densities, and lengths of the two bars, respectively. Fig. 19 shows the membership functions of the fuzzy-valued model parameters $\tilde{k}$ and $\tilde{c}$. It is seen that the damping coefficient exhibits asymmetry implying non-linear behavior of the model.

4.4. Identification of non-linear joints

4.4.1. Sources of non-linearities

Structural joints are regarded as a potential source of non-linear behavior. An example of this can be found in frame structures constructed from individual truss elements with pin joint in which small play or looseness in the joints represents non-linear departures from ideal pin jointed structures [164,165,209–214]. It is important to understand how the non-linear system parameters change with amplitude and frequency when designing an active control system. Small amounts of play in the joints could lead to chaotic dynamics in the response of the structure under periodic excitation. Chaotic dynamics in space structures may impose some difficulties in the design of active control systems to damp out transient dynamics [209]. Bolted joints also are non-linear due to clearance and non-linear contact stiffness of the joint.

Another source of non-linearity in bolted joints is the prying load [8]. Usually it is assumed that the resultant external load in bolted joints under tension load acts at some point along the axis of the bolt. In reality, the tensile load is applied off to one side of the bolt as shown in Fig. 20, and thus is called a prying load. Such load can drastically increase the amount of tensile and bending stress produced in the bolt. A bolt subjected to prying must ultimately resist the full external load F_e plus the full prying load Q, i.e., $F_B \geqslant F_e + Q$, where F_B is the bolt force. Note that $F_B \geqslant F_e + Q$ does not include preload, since it defines that the bolt must "ultimately" resist. The bolt will not carry the full external load plus prying load at low values of external load any more than it would fully have a small axial tension load. Accordingly, it is always desirable for the stiffness ratio between bolt and joint, K_B/K_J, to be small. The small stiffness ratio will reduce the percentage of external load transmitted by the bolt (at least until joint separation). Thus, it improves the static load capability and fatigue life of the joint. Fig. 21(a) shows that under purely axial load, when the

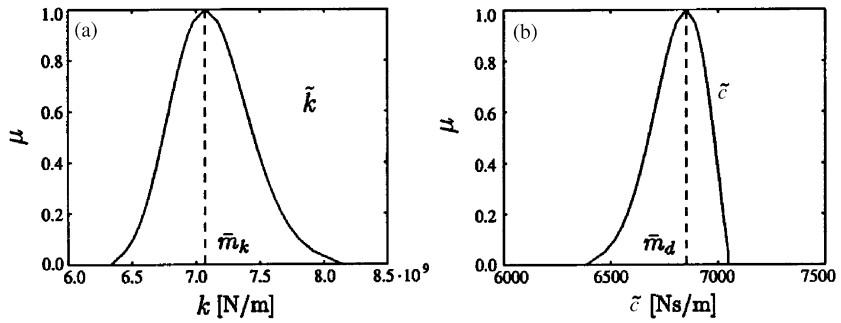

Fig. 19. Uncertain (a) stiffness and (b) damping parameters of the joint model shown in Fig. 18 [88].

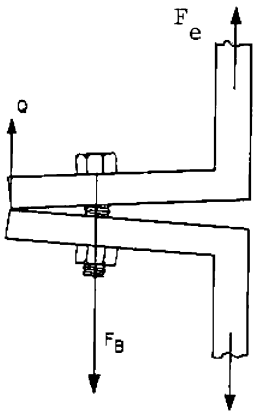

Fig. 20. A schematic diagram showing a bolt subjected to prying [8].

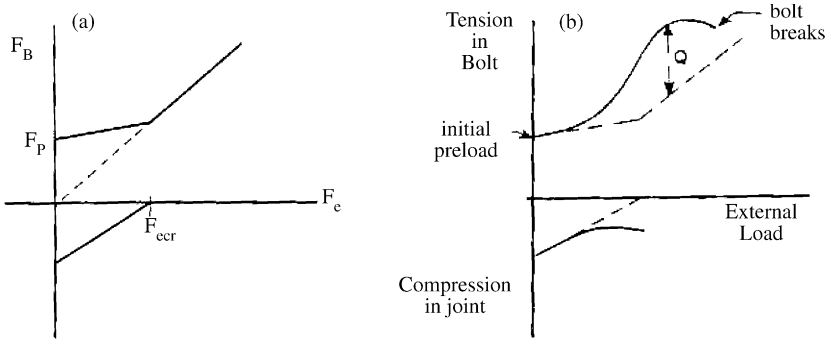

Fig. 21. Dependence of the bolt force on the external force under (a) axial tension load; (b) prying load [8].

external load starts to build up, there is only a small change in the bolt force, since most of the newly applied external load will be absorbed by the flange. Once the external load reaches a critical value, the bolt absorbs all additional external load. Fig. 21(b) illustrates the modification of Fig. 21(a) for offset loading, as shown in Fig. 20. When the flanges are very thick, the prying load will be created if the flanges are flexible enough. It starts along the same line it followed when the flange was rigid, as demonstrated in Fig. 21(a). However, once the external load becomes large enough to deform the flange and create prying action, the force within the bolt becomes greater than that which would be produced by the same external load applied axially.

In Fig. 21(a), the bolt and joint behave linearly until joint separation. After separation, the bolt follows a second, but still linear, path. In contrast, Fig. 21(b), the bolt load is a roughly S-shaped function of the external load, not because the bolt itself has become a non-linear spring, but becomes the mechanism by which the bolt is loaded in the system is non-linear. Note that upon removing the external load, the bolt tension will return to the original preload along the original curve. This means the system behavior is purely elastic and strongly non-linear [8]. The influence of prying and shear in end-plate connections was studied in Refs. [215–217].

4.4.2. Non-linear identification

In view of the inherent non-linearities of bolted joints, non-linear identification algorithms and models should more accurately reflect the behavior of bolted joints than linear approaches do. Masri and Caughey [218] and Masri et al. [219–221] proposed a non-parametric method to identify non-linear joint properties. Their approach is based on the restoring-force method, which fits a non-linear function to the restoring force, $f(x, \dot{x})$, in the joint. They constructed a joint model with the Chebyshev polynomials to take advantage of their orthogonality characteristics and fitted the model with the time domain states of the joint co-ordinate (displacement, velocity, and acceleration). The Chebyshev polynomials can, however, lose odd or even behavior and require interpretation of data over a uniform grid as pointed out by Al-Hadid and Wright [222].

In the presence of locally strong non-linearities such as joints, simple load stroke or force–displacement testing has been used by Soni and Agrawal [223]. As pointed by Crawley and O'Donnell [167], such force–displacement testing yields only a partial state space representation of the joint characteristics. This gives the force transmitted by the joint as a function of its displacement, but the dependence of the force on the velocity or on the true memory effect in the joint is not explicitly displayed. O'Donnell and Crawley [166], Crawley and Aubert [224], and Crawley and O'Donnell [167] developed the "force-state mapping technique" for identifying strongly non-linear properties of joints by expressing the force transmitted by the member as a function of its mechanical state co-ordinates. This technique is very simple and effective if the joint can be separated or isolated easily from the whole structure; however, this generally is not the case. The method requires a large amount of data since it is based on the signal processing of the time domain state to extract joint properties.

Kim and Park [225] extended the conventional force-state mapping technique for identifying the non-linear properties of joints that connect linear substructures. Their approach is based on estimating the entire substructure FRFs using the FEM or by using experimental modal analysis techniques. This is followed by measuring the response signal at the joint degrees of freedom when the whole structure is sinusoidally excited at an arbitrary point. The last step is to set up a non-linear joint force model and fit the model using the joint degree responses and the substructure FRFs. Lee and Park [226] proposed an efficient method to identify the position and type of non-linear elements. They introduced a local identification method to identify joint properties using the non-linear elements' position information.

Tzou [227] studied the non-linear structural dynamics of jointed flexible structures with initial joint clearance and subjected to external excitations. Tzou proposed a method of using viscoelastic and active vibration control technologies (joint actuators) to reduce dynamic contact force and to stabilize the systems. Dynamic contacts in an elastic joint were simulated by a non-linear joint model comprised of a non-linear spring and damper. Space frame structures with pin joints involve non-linearities due to very small gaps in the pin-joints. Such non-linearities can lead to chaotic-like vibrations under sinusoidal excitation [209,228].

By controlling the normal force in the joint interface, one can improve the damping performance in large structures. Ferri and Heck [229] proposed passively and actively controlled joints. In each case, the normal force was allowed to vary yielding a connecting joint with increased damping performance. Their results suggested that joints with amplitude or rate-dependent frictional forces could offer substantial improvements. Gaul et al. [230] and Gaul and Nitsche [231] studied the use of active control to vary the normal contact force in a joint by means

of a piezoelectric element. Their model consisted of two elastic beams connected by a single active joint as shown in Fig. 22. A friction model with velocity-dependent dynamics was used to describe the friction phenomena. Control of the normal force is accomplished by placing a piezoelectric stack disc between the bolt nut and beam surface such that any applied voltage at the stack disc will result in thickening the piezoelectric material. This in turn causes an increase of the normal force.

Cameron and Griffin [232] and Ren and Beards [206] developed different techniques for predicting the steady state response of structures containing non-linear joints. Ren et al. [233] proposed an identification method to extract dynamic properties of non-linear joints using dynamic test data. The non-linear force at the joint was treated as an external force and the principle of multi-harmonic balance was employed. This approach enables one to obtain the force–response relationship of a non-linear joint. Ma et al. [234] treated the joint as a local force operator in the structure's equations of motion and used a Green's function to solve for the response by considering the joint as a pseudo-force. In one case, their model consists of clamped–clamped beam, and in the other case, the beam was replaced by two half beams joined at their free ends by a bolt. They considered the local dynamic effect of the joint to be the only difference between a joint structure and non-joint structure. Experimentally, their approach is valid as long as the supports of the two ends of the two structures are identical. If the ends are not identical then their uncertainty and relaxation should be considered.

Several models were developed to describe the dynamic transfer behavior of an isolated joint by Coulomb friction elements. These models can only describe the states of global stick or slip (macroslip in the whole interface). Gaul and Bohlen [235,236] measured the dependence of the reaction force of a bolted joint on the relative displacement of the joint and the results revealed the dependence of hysteresis on the amplitude of the excitation force and the mean contact pressure. Based on experimental measurements, it was concluded that the influence of gaps and viscous damping can be neglected in the microslip regime. The joint stiffness and slip force of the elastic Coulomb element were evaluated by minimizing the squared difference between the measured and calculated dissipation work done per cycle. While there was no significant shift in the natural frequencies, damping ratios were found to be significantly increased at higher excitation levels.

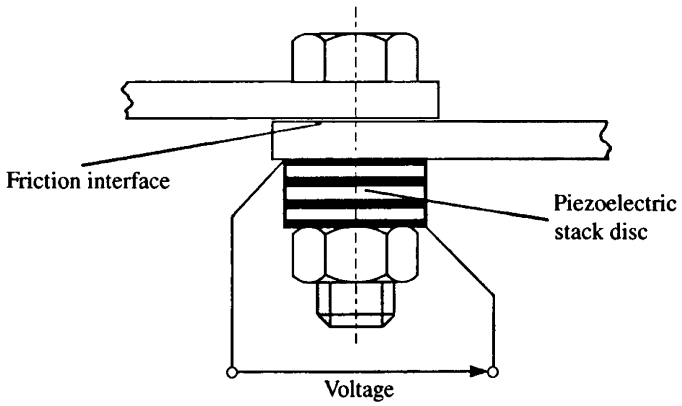

Fig. 22. Active control to vary the normal contact force in a joint by means of a piezoelectric element [230].

Gaul et al. [237] found that the actual normal contact pressure distribution in a dynamically loaded lap joint is not constant in time on the interface. Depending on the transmitted load, the interface may be divided into stick and slip zones. Lenz and Gaul [238] and Gaul and Lenz [239] developed a three-parameter joint model that can describe the presence of stick and macroslip condition. They designed two resonators to isolate bolted joints and measure their dynamical transfer behavior in longitudinal and torsional motion. The dependence of the dissipated energy per cycle of joint hysteresis on the relative displacements or rotations provided the means to distinguish between microslip and macroslip regimes. A detailed FE model was developed to estimate the dynamic response of assembled structures incorporating the influence of micro- and macroslip of several bolted joints.

4.4.3. Force-state mapping technique

Crawley and O'Donnell [167] outlined the force-state mapping technique for a single-degree-of-freedom non-linear damped oscillator. With reference to the transfer of the axial load through a space truss joint, the spring and damper are properties of the joint, and the mass is the mass of the adjacent truss element. Thus, the state of the joint is completely described in terms of the displacement, x, and velocity, $\dot{x}$, across the joint. The model can be described by the non-linear differential equation

$$M\ddot{x} + C(x,\dot{x})\dot{x} + K(x,\dot{x})x = F(t), \tag{57}$$

where M is the mass of the substructure, and $C(x,\dot{x})$ and $K(x,\dot{x})$ are the generalized damping and stiffness of the joint, respectively, both of which are functions of the state. Note that the force transmitted by the joint, F_T, is given by the expression

$$F_T = C(x,\dot{x})\dot{x} + K(x,\dot{x})x = F(t) - M\ddot{x}. \tag{58}$$

The transmitted force depends on the state of the joint, x and $\dot{x}$, and can be plotted for a memoryless single-degree-of-freedom model in a three-dimensional diagram, which is referred to as the force-state map. A typical force-state map of a general linear spring mass damper system is shown in Fig. 23, which depicts an inclined plane whose slopes with respect to displacement and velocity give the spring stiffness, K, and damping coefficient, C respectively. If the surface of the force-state map is not planar, the joint is non-linear. In this case, the force-state mapping will display superposable non-linearities in which the transmitted force is a combination of linear and non-linear force components. Crawley and O'Donnell proposed an expression describing the transmitted force as

$$F_T = F_0 + K_1 x + K_n x^n + C_1\dot{x} + C_n\dot{x}^n + K_{DB} + C_{DB} + F_f\,\mathrm{sign}(\dot{x}) + g|x|\,\mathrm{sign}(\dot{x}), \tag{59}$$

where

$$K_{DB} = \begin{cases} k_{DB}(x - x_{DB}), & x_{DB} \leqslant x, \\ 0, & -x_{DB} \leqslant x \leqslant x_{DB}, \\ k_{DB}(x + x_{DB}), & x \leqslant -x_{DB}, \end{cases}$$

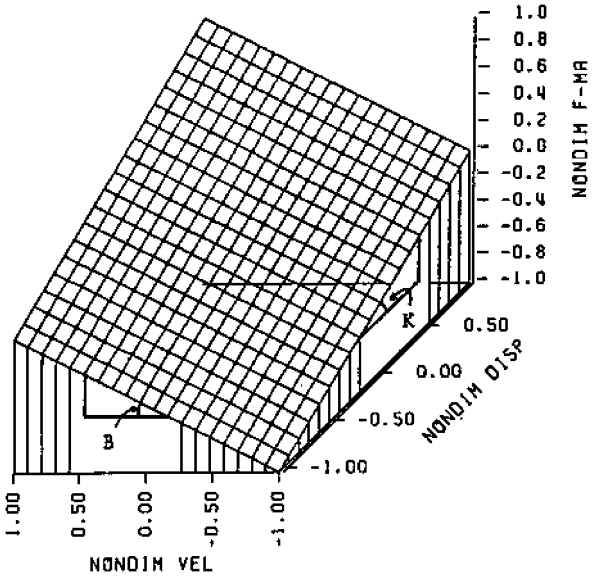

Fig. 23. Force-state map of an ideal linear spring dashpot joint model [167].

$$\text{and} \quad C_{DB} = \begin{cases} c_{DB}(\dot{x}), & x_{DB} \leqslant x, \\ 0, & -x_{DB} \leqslant x \leqslant x_{DB}, \\ c_{DB}(\dot{x}), & x \leqslant -x_{DB}. \end{cases}$$

F_0 is a constant preload, $K_1 x$, and $C_1 \dot{x}$ are linear spring and damping forces respectively. $K_n x^n$ and $C_n \dot{x}^n$ are non-linear spring and damping forces, respectively, K_{DB} and C_{DB} are dead-band springs and dampers, respectively, and the last two expressions represent classical Coulomb friction and material hysteresis damping. Fig. 24 shows the force-state map of a typical non-linear joint that includes a dead-band due to play in the joint and classical Coulomb friction between moving surfaces.

For a small class of non-linearities that exhibit true memory effects, a higher order force-state map can be created for memory effects linearly related to the state. For memory effects that are not linearly related, system parameters can be obtained by testing at appropriate frequencies and amplitudes. Curve fitting can be used to fit a surface to the force-state map and the system parameters can be retrieved from the entire surface or a small operating region.

Kim and Park [225] extended the force-state mapping for multi-degree-of-freedom systems by estimating the FRFs of substructures with the FEM or experimental modal analysis. Their approach is based on measuring the response signal at the joint degrees of freedom and setting up a non-linear joint force model to fit the model using the joint responses and the substructure FRFs. The equation of motion of the kth substructure connected to m non-linear joints may be written in the matrix form

$$\mathbf{M}\ddot{\mathbf{X}} + \mathbf{C}\dot{\mathbf{X}} + \mathbf{K}\mathbf{X} = \mathbf{f}(t) + \mathbf{g}(t), \tag{60}$$

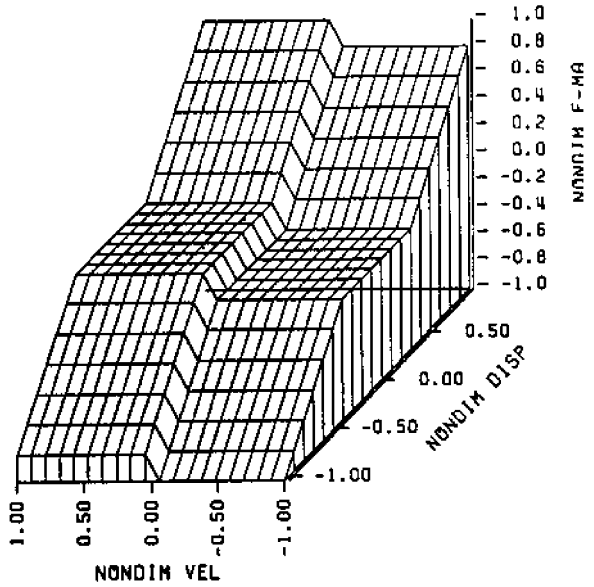

Fig. 24. Force-state map of an ideal dead-band spring with Coulomb friction [167].

where $\mathbf{M}$, $\mathbf{C}$, $\mathbf{K}$ are the mass, damping and stiffness matrices of the kth substructure, $\mathbf{f}(t)$ is the external force vector and $\mathbf{g}(t)$ is the joint force vector. The joint force vector has m joint forces and zero values at other points, i.e.,

$$\mathbf{g}^{\mathrm{T}}(t) = \{0, 0, \ldots, 0, g_1(t), g_2(t), \ldots, g_l(t), g_{l+1}(t), \ldots, g_m(t)\}. \tag{61}$$

The non-linear joint forces can be Fourier transformed by assuming a specific type of non-linear joint force and adopting the idea of the harmonic balance. In this case, the Fourier transform of Eq. (60) takes the form

$$[\mathbf{K} - \omega^2\mathbf{M} + \mathrm{i}\omega\mathbf{C}]\mathbf{X}(\omega) = \{\mathbf{F}(\omega) + \mathbf{G}(\omega)\}. \tag{62}$$

The FRF matrix of the kth linear substructure is

$$\mathbf{H}_k(\omega) = [\mathbf{K} - \omega^2\mathbf{M} + \mathrm{i}\omega\mathbf{C}]^{-1}. \tag{63}$$

The response amplitude may be written in the form

$$\mathbf{X}_k(\omega) = \mathbf{H}_k(\omega)\{\mathbf{F}(\omega) + \mathbf{G}(\omega)\}. \tag{64}$$

The FRF matrix in Eq. (64) can be divided into two parts according to the joint and non-joint states,

$$\begin{Bmatrix} \mathbf{X}(\omega) \\ \mathbf{X}_j(\omega) \end{Bmatrix} = \begin{bmatrix} \mathbf{H}_{11} & \mathbf{H}_{12} \\ \mathbf{H}_{21} & \mathbf{H}_{22} \end{bmatrix}_k \begin{Bmatrix} \mathbf{F}_1(\omega) \\ \mathbf{F}_2(\omega) + \mathbf{G}(\omega) \end{Bmatrix}, \tag{65}$$

where $\{\mathbf{F}(\omega)\}^{\mathrm{T}} = \{\{\mathbf{F}_1(\omega)\}^{\mathrm{T}}\{\mathbf{F}_2(\omega)\}^{\mathrm{T}}\}$, $\{\mathbf{G}(\omega)\}^{\mathrm{T}} = \{\{0\}^{\mathrm{T}}\{\mathbf{G}(\omega)\}^{\mathrm{T}}\}$.

The joint force vector $\mathbf{G}(\omega)$ can be determined from the equation that is generated from the second row of Eq. (65), i.e.,

$$\mathbf{H}_{22}\mathbf{G}(\omega) = \mathbf{X}_j(\omega) - \mathbf{H}_{21}\mathbf{F}_1(\omega) - \mathbf{H}_{22}\mathbf{F}_2(\omega). \tag{66}$$

The joint force models connecting the joint forces with the joint states can be constructed by first writing the joint force vector in the form

$$\mathbf{g}(t) = \left\{ \begin{array}{c} g_{11}(t)\theta_{11} + g_{12}(t)\theta_{12} + \cdots + g_{1n_1}(t)\theta_{1n_1} \\ g_{21}(t)\theta_{21} + g_{22}(t)\theta_{22} + \cdots + g_{2n_2}(t)\theta_{2n_2} \\ \cdots\cdots \\ g_{m1}(t)\theta_{m1} + g_{m2}(t)\theta_{m2} + \cdots + g_{mn_m}(t)\theta_{mn_m} \end{array} \right\}, \tag{67}$$

where $g_{rs}(t)$ are the components of the assumed joint force model and θ_{rs} are unknown parameters. The parameters θ_{rs} are determined from the measured frequency domain joint degree responses, i.e.,

$$g_r(t) = \sum_{k=1}^{n_r} \sum_{p=0}^{P} \sum_{q=0}^{Q} \theta_{rk}^{pq} y_{rk}^{p} \dot{y}_{rk}^{q}, \tag{68}$$

where $y_{rk} = (x_r - x_k)$ and $\dot{y}_{rk} = (\dot{x}_r - \dot{x}_k)$, if $r \neq k$, or $y_{rk} = x_r$ and $\dot{y}_{rk} = \dot{x}_r$ if $r = k$. n_r is the number of non-linear joints connected to the rth co-ordinate. The Fourier transform of the joint force vector may be written in the form

$$\mathbf{G}(t) = \left\{ \begin{array}{c} G_{11}(\omega)\theta_{11} + G_{12}(\omega)\theta_{12} + \cdots + G_{1n_1}(\omega)\theta_{1n_1} \\ G_{21}(\omega)\theta_{21} + G_{22}(\omega)\theta_{22} + \cdots + G_{2n_2}(\omega)\theta_{2n_2} \\ \cdots\cdots \\ G_{m1}(\omega)\theta_{m1} + G_{m2}(\omega)\theta_{m2} + \cdots + G_{mn_m}(\omega)\theta_{mn_m} \end{array} \right\}. \tag{69}$$

Substituting Eq. (69) into Eq. (66) results in $2m$ equations (m equations from the real parts and m from the imaginary parts). The resulting algebraic equations are then solved for the point force coefficients θ_{rs}. If the joint properties are frequency dependent, the model set of joint forces should be solved uniquely at a given frequency and thus the number of equations required to obtain force coefficients can be increased by selecting as many frequencies as needed.

This method is effective only for cases in which the joint properties are stationary with time. However, due to preload relaxation and external environmental conditions the joint properties will experience non-stationarity. In this case the FFT should be applied for discrete intervals to observe how the joint properties are changing with time. More powerful techniques do exist such as the spectrogram and wavelet transfer to reflect the non-stationarity in the time history records.

5. Design considerations

5.1. Fully and partially restrained joints

Conventional design and analysis of structural systems are based on the well-known two extreme idealizations of joints; perfectly rigid (or fully restrained) and ideally pinned. However, they are impractical, difficult to produce, and do not represent the real structural behavior as reflected experimentally [8,240]. Rigid joints typically exhibit flexibility and sometimes are referred to as semi-rigid. The importance of frame structures with partially restrained connections (e.g.,

riveted joints) was recognized by Wilson and Moore [241] and the concept was introduced to the American Institute of Steel Construction in 1946. The flexibility of joints has been the subject of several studies [242–248]. Bjorhovde et al. [249] indicated that structural connections exhibit semi-rigid non-linear response characteristics even when the applied loads are very small.

Most structural connections exhibit non-linear moment–rotation ($M-\phi$) characteristics, where M (in N m) is the applied moment, and ϕ (in radian) is the relative rotation on the two sides of the joint. The stiffness of a connection decreases as the load applied to the connection increases. When the connection is unloaded, the ($M-\phi$) curve normally follows an unloading path parallel to the initial slope of the loading curve and therefore exhibits hysteresis. Several experimental and numerical studies have been conducted to establish linear and non-linear moment–rotation relationships that can be used for predicting the actual behavior of flexible joints [243,245,250–253]. These studies have focused exclusively on joints in steel-frame structures. Monforton and Wu [243] derived the stiffness matrix of a member with elastic restraints by multiplying the stiffness matrix of a member with rigid connection by a correction matrix. The elements of the correction matrix were given in terms of two-dimensional parameters, referred to as *fixity factors*. Alternatively, another parameter, referred to as *connection rigidity*, has been used to define the ratio of the moment the connection would have to carry according to the beam linear theory and the fixed end moment of the girder.

Romstad and Subramanian [254] and Frye and Morris [245] presented other forms of modified stiffness matrix. Wong et al. [255] modelled the bolted connection by a linear spring element, which comprises both rotational and shear springs. Experimental results were used to identify the stiffness of the connections. It was found that the rigidity of the connections obtained from static load was lower than that obtained from the vibration impact test in a frame-type structure; however, the value was very close to that in a cantilever beam. It was concluded that the rotational stiffness estimated from static tests to determine the dynamic characteristics of a steel-framed structure could not yield satisfactory results, particularly for higher modes. Rodrigues et al. [256] modelled the semi-rigid joint by three fictitious springs that allow rotation, horizontal, and vertical displacements. They used an iterative algorithm to predict the non-linear behavior of the joint.

Under dynamic and cyclic loading, a tri-linear ($M-\phi$) model was used by Moncarz and Gerstle [257] whereas a bilinear model was employed by Sivakumaran [258]. However, these models do not accurately represent the connection behavior since they do not reflect the abrupt changes in connection stiffness as it moves from the elastic to plastic regime. In references [259,260] a bounding-line model was proposed for the hysteretic moment–rotation ($M-\phi$) response that provides a smooth transition between the elastic and plastic regimes. Furthermore, cyclic performance tests of 10 beam-column moment connections conducted by Tsai et al. [261] indicated that the plastic moment capacities were somewhat erratic. Recently, Chan and Chui [262] documented non-linear static and cyclic behavior of steel frames with semi-rigid connections.

Non-linear behavior of joints under static loads has been accounted for by using iterative analytical procedures. Chen and Lui [263,264] considered the flexibility of the connected frames and included the non-linear behavior of the joint and the possible formation of plastic hinges in the members. Pui et al. [265] obtained the following non-linear moment–rotation relationship for

welded and bolted steel joints:

$$M = \frac{(S - S_p)\phi}{[1 + |(S - S_p)\phi/M_0|^n]^{1/n}} + S_p\phi, \tag{70}$$

where S is the initial slope of moment versus rotation curve, S_p is the slope of the asymptote for large rotation, and M_0 is a reference moment, and n is a power that defines the sharpness of the curve. Liew et al. [266,267] showed that the power law given by relation (70) is accurate in predicting the connection behavior. Pui et al. [265] adopted the values $S = 21,248$ N m/rad, $S_p = 300.68$ N m/rad, $M_0 = 88,680$ N m, and $n = 3$ for the tested welded joint; and $S = 20,058$ N m/rad, $S_p = 258.37$ N m/rad, $M_0 = 89,660$ N m, and $n = 1$ for the tested bolted joint. Sekulovic and Salatic [268] found that the influence of geometric non-linearity increases with the applied load; furthermore, the influence is higher for semi-rigid type joints than for fully rigid connections. It was found that the critical load and buckling capacity of the frame structure significantly decrease as the flexibility of joints increases.

The static behavior of semi-rigid connected composite frames was studied in Refs. [269–274] to determine the rotations of composite joints and their moment capacity. Li et al. [273,275] predicted and measured the response of composite connections in frames. Li et al. [276] presented the analysis treatment and design of composite frames involving semi-rigid and partial strength connections. Their study revealed that the quasi-plastic approach originally proposed by Nethercot [277] provides close estimation of actual behavior and was recommended for the design of semi-rigid non-sway frames. Their measured connection moment capacities and stiffnesses were found to be lower in the frame test than in isolated joint tests. This was largely due to the inevitable unbalanced loads in the frame test, which implies that the connections in frames are more prone to buckling.

Reliability analysis of two-dimensional William toggles, with non-linear flexible connections, was studied by Haldar and Zhou [278] using stochastic FEM and Monte Carlo simulation. They found that the flexibility of connections has a significant influence on the reliability of the structure.

The design analysis of steel frames with semi-rigid joints has received extensive study (see, e.g., Refs. [279–284]). The purpose of these studies was to achieve an optimum design of frame structures with semi-rigid joints. Optimum design studies involved the computation of design sensitivities to constraints and the influence of inherent geometric non-linearities on the structure response [285,286]. Given the significant influence of connection flexibility on structural reliability, it is reasonable to suggest that optimum design of frame structures should explicitly recognize variability in the connection properties.

Dynamic response analyses of steel frames with semi-rigid joints in the time and frequency domains were reported in Refs. [287–292]. Deformations of the joints introduce additional degrees of freedom. Suarez et al. [291] considered this by enforcing kinematic relationships between the displacement co-ordinates of the joint and beam end. It was found that joint flexibility has the most effect on the lowest natural frequency of the structure. Hsu and Fafitis [293] and Xu and Zhang [294] considered the case of viscoelastic connections and connection dampers, while Shi and Atluri [295] and Al-Bermani et al. [260] considered the case of non-linear flexible connections. These studies showed that the connection characteristics greatly modify the dynamic properties of the structure such as the eigenvalues and eigenvectors. The stiffness and damping characteristics

of the connection can be tuned in a fairly large range; however, due to the inherent uncertainty in the evaluation of the effective behavior of the joints, the design can lead to high-risk conditions. This is particularly true when stiffness and damping coefficients are chosen in a range where a small variation in the joint parameters produces a large variation in the response. The non-linear dynamic response of steel frames with fully restrained and partially restrained connections was studied in the time domain using FEM by Gao and Halder [296]. Reyes-Salazar and Haldar [297] determined the non-linear seismic response of steel frames with fully restrained and partially restrained connections.

5.2. Sensitivity analysis to joint parameter variations

The sensitivity of a jointed structure to parametric variations is among the most basic aspects of structural design. Sensitivity theory is a mathematical field that investigates the change in the system behavior due to parameter variations. The basic concepts of sensitivity theory are well documented in several books (see, e.g., Ref. [298]). Sensitivity of a physical property of a dynamical system to variations of different parameters can be determined by estimating the corresponding partial derivatives at some fixed combination of the parameters. In many cases, however, such a fixed combination of parameters cannot be selected since they vary according to the system working regimes. Therefore, one may need a global investigation of the derivative fields, which complicates visualization. In the case of two independent parameters, a geometrical meaning of the level curves can be used for such a visualization of the sensitivity analysis. The evaluation of the derivatives of the structural response with respect to the joint parameters such as stiffness, mass, and damping is very useful for evaluating the parameter ranges over which the system response is reduced and the parametric uncertainty thereby results in a low risk level due to a small sensitivity of the response.

5.2.1. Sensitivity function

The sensitivity problem can be stated by defining the actual system parameters represented by the vector, $\boldsymbol{\alpha} = \{\alpha_1, \ldots, \alpha_n\}^{\mathrm{T}}$, which differs from the nominal value $\boldsymbol{\alpha}_0$ by a deviation $\Delta\boldsymbol{\alpha}$. These parameters are related to a certain vector $\mathbf{x}$, which can be taken as the system response vector

$$\dot{\mathbf{x}} = \mathbf{A}\mathbf{x}. \tag{71}$$

Let $\mathbf{v}_i$ be the eigenvector associated with the eigenvalues λ_i, it follows that

$$\mathbf{A}\mathbf{v}_i = \lambda_i \mathbf{v}_i. \tag{72}$$

Similarly, for the eigenvector $\mathbf{w}_j$ of the transposed system $\mathbf{w}_k^{\mathrm{T}}$ one can write

$$\mathbf{w}_j^{\mathrm{T}} = \lambda_j \mathbf{w}_k^{\mathrm{T}}. \tag{73}$$

The eigenvectors $\mathbf{v}_i$ and the adjoint eigenvectors $\mathbf{w}_j$ are orthonormal, i.e.,

$$\mathbf{v}_i^{\mathrm{T}}\mathbf{w}_j = \mathbf{w}_j^{\mathrm{T}}\mathbf{v}_i = \delta_{ij}, \tag{74}$$

where δ_{ij} stands for Kronecker delta. Taking partial derivatives of Eq. (72) with respect to a parameter α gives

$$\frac{\partial \mathbf{A}}{\partial \alpha}\mathbf{v}_i + \mathbf{A}\frac{\partial \mathbf{v}_i}{\partial \alpha} = \frac{\partial \lambda_i}{\partial \alpha}\mathbf{v}_i + \lambda_i \frac{\partial \mathbf{v}_i}{\partial \alpha}. \tag{75}$$

Pre-multiplying Eq. (75) by the transpose adjoint vector $\mathbf{w}_i^{\mathrm{T}}$ gives

$$\mathbf{w}_i^{\mathrm{T}}\frac{\partial \mathbf{A}}{\partial \alpha}\mathbf{v}_i + \mathbf{w}_i^{\mathrm{T}}\mathbf{A}\frac{\partial \mathbf{v}_i}{\partial \alpha} = \mathbf{w}_i^{\mathrm{T}}\frac{\partial \lambda_i}{\partial \alpha}\mathbf{v}_i + \mathbf{w}_i^{\mathrm{T}}\lambda_i \frac{\partial \mathbf{v}_i}{\partial \alpha}. \tag{76}$$

Using Eq. (73) and $i = j$, the sensitivity of the eigenvalue λ_i with respect to a parameter α is expressed in the form

$$S_{\alpha}^{\lambda_i} = \frac{\partial \lambda_i}{\partial \alpha} = \frac{\mathbf{w}_i^{\mathrm{T}}(\partial \mathbf{A}/\partial \alpha)\mathbf{v}_i}{\mathbf{w}_i^{\mathrm{T}}\mathbf{v}_i}, \quad i = 1, 2, \ldots, n. \tag{77}$$

Generally, a unique relationship between the parameter vector and the response vector is assumed. However, this is not possible in real problems because they cannot be identified exactly. It is a common practice in sensitivity theory to define a *sensitivity function*, $\mathbf{S}$, which relates the elements of the set of the parameter deviation $\Delta\boldsymbol{\alpha}$, $\Delta\boldsymbol{\alpha} = \boldsymbol{\alpha} - \boldsymbol{\alpha}_0$, where $\boldsymbol{\alpha}_0$ is the vector of the nominal values of the parameters, to the elements of the set of the parameter-induced variations of the system function, $\Delta\mathbf{x}$, by the linear relationship

$$\Delta\mathbf{x} \approx \mathbf{S}(\boldsymbol{\alpha}_0)\Delta\boldsymbol{\alpha}. \tag{78}$$

This relation is valid only for small parameter variation, i.e., $\|\Delta\boldsymbol{\alpha}\| \ll \|\boldsymbol{\alpha}_0\| \cdot \mathbf{S}$. $\mathbf{S}$ is a matrix function known as the trajectory sensitivity matrix, which can be established either by a Taylor series expansion or by a partial differentiation of the state equation with respect to the system nominal parameters. The sensitivity of eigenvalues to small changes in the system parameters is given by the expression

$$S_{\alpha_j}^{\lambda_i} = \left.\frac{\partial \lambda_i}{\partial \alpha_j}\right|_{\alpha_0}. \tag{79}$$

This is known as the eigenvalues sensitivity parameter. Derivatives of the eigenvalues are very useful in design optimization of structures under dynamic response restrictions. They have been extensively used in studying vibratory systems with symmetric (i.e., self-adjoint) mass, damping, and stiffness properties (see, e.g., Refs. [299–302]) and non-self-adjoint systems (see, e.g., Refs. [303–305]). Baniotpolos and Abdalla [306] studied the sensitivity of joint properties of bolted steel column-to-column connections.

5.2.2. *Stochastic sensitivity*

Under random excitation, one must deal with stochastic sensitivity. The stochastic sensitivity of structures subjected to Gaussian random excitation was the subject of several studies [307–309]. Huang and Soong [310] and Huang et al. [311] extended the stochastic sensitivity analysis to composite primary–secondary structural systems with the purpose of reducing the response of the primary structure. Socha [307] considered stochastic sensitivity by studying the derivatives of the response of the structure with respect to the system parameters such as stiffness, mass, and

damping. Sensitivity analyses reported by Der Kiureghian and Ke [312] and Mahadevan and Haldar [313] were used to reduce the number of basic random variables in structural joints.

Cacciola et al. [314] evaluated deterministic and stochastic sensitivity to characterize connection parameters of dynamic response of multistory steel frames with viscoelastic semi-rigid connections. They employed a FE consisting of an elastic beam having two Kelvin–Voigt elements at its nodes and consistent mass, stiffness and damping matrices based on the work of Xu and Zhang [294]. In order to allow the evaluation of the response sensitivity for large structural systems, they adopted the same procedure formulated by Benfratello et al. [315], and Muscolino [316] in conjunction with modal expansion of the response. Cacciola et al. [314] modelled the joints in steel frames as rotational discontinuities between connected members as shown in Fig. 25. The joint is represented by a torsional spring of stiffness k_{ci} $(i = 1, 2)$ with a rotational dashpot of damping coefficient c_i. The stiffness, mass, and damping matrices were written in terms of the rigidity factor v_i defined by the expression

$$v_i = \frac{1}{1 + (3EI/k_{ci}L)}, \tag{80}$$

where L is a characteristic length. This factor relates the rotational stiffness of the ith joint to the flexural rigidity of the beam. Its value ranges from zero (pinned joint) to one (rigid joint). Deterministic sensitivity analysis was extended to structures subjected to zero-mean white noise excitations. The equation of motion of the structure in state vector form was written as

$$\dot{\mathbf{x}}(t, \boldsymbol{\alpha}) = \mathbf{A}(\boldsymbol{\alpha})\mathbf{x}(t, \boldsymbol{\alpha}) + \mathbf{G}(\boldsymbol{\alpha})W(t), \tag{81}$$

where $W(t)$ is the ground acceleration, which is assumed to be a zero-mean white noise, and $\mathbf{G}(\boldsymbol{\alpha})$ is a matrix of system parameters.

Applying the Itô stochastic calculus (see, e.g., Ref. [317]) to determine the evolution of second order moments in the modal space gives the second order stochastic sensitivity vector

$$\begin{aligned}\mathbf{S}^{(2)}_{x,i}(t, \boldsymbol{\alpha}_0) &= \frac{\partial}{\partial \alpha_i}\mathbf{m}^{(2)}_x(t, \boldsymbol{\alpha}_0)|_{\boldsymbol{\alpha}_0} \\ &= E[\{\mathbf{S}_{x,i}(t, \boldsymbol{\alpha}_0)\} \otimes \{\mathbf{x}(t, \boldsymbol{\alpha}_0)\}] + E[\{\mathbf{x}(t, \boldsymbol{\alpha}_0)\} \otimes \{\mathbf{S}_{x,i}(t, \boldsymbol{\alpha}_0)\}],\end{aligned} \tag{82}$$

where $\mathbf{m}^{(2)}_x(t, \boldsymbol{\alpha}_0)$ is the second moment vector of the response state vector $\mathbf{x}$ which is function of time and the nominal value of the parameter vector $\boldsymbol{\alpha}_0$, $E[..]$ denotes expectation, $\otimes$ is the Kronecker product, which implies that every element of $\mathbf{S}^{(2)}_{x,i}(t, \boldsymbol{\alpha}_0)$ is multiplied by $\mathbf{x}(t, \boldsymbol{\alpha}_0)$, and $\mathbf{S}^{(2)}_{x,i}(t, \boldsymbol{\alpha}_0)$ is the second order stochastic sensitivity. The evolution of the stochastic sensitivity of the modal response in the state variables is given by the set of differential equations,

$$\dot{\mathbf{S}}^{(2)}_{x,i}(t, \boldsymbol{\alpha}_0) = \mathbf{A}_2(\boldsymbol{\alpha}_0)\mathbf{S}^{(2)}_{x,i}(t, \boldsymbol{\alpha}_0) + \mathbf{A}_{2i}(\boldsymbol{\alpha}_0)\mathbf{m}^{(2)}_x(t, \boldsymbol{\alpha}_0) + 2\pi\mathbf{B}_{2i}(\boldsymbol{\alpha}_0)S_0, \tag{83}$$

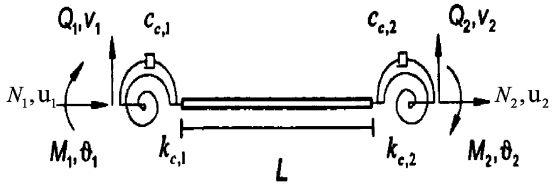

Fig. 25. Beam element with torsional spring–dashpot joint modelling [314].

where

$$\mathbf{A}_2(\boldsymbol{\alpha}_0) = \mathbf{A}(\boldsymbol{\alpha}_0)\otimes\mathbf{I} + \mathbf{I}\otimes\mathbf{A}(\boldsymbol{\alpha}_0),$$

$$\mathbf{A}_{2i}(\boldsymbol{\alpha}_0) = \left.\frac{\partial\mathbf{A}(\alpha)}{\partial\alpha_i}\right|_{\alpha_0}\otimes\mathbf{I} + \mathbf{I}\otimes\left.\frac{\partial\mathbf{A}(\alpha)}{\partial\alpha_i}\right|_{\alpha_0},$$

$$\mathbf{B}_{2i}(\boldsymbol{\alpha}_0) = \left.\frac{\partial\mathbf{G}(\alpha)}{\partial\alpha_i}\right|_{\alpha_0}\otimes\mathbf{G}(\boldsymbol{\alpha}_0) + \mathbf{G}(\boldsymbol{\alpha}_0)\otimes\left.\frac{\partial\mathbf{G}(\alpha)}{\partial\alpha_i}\right|_{\alpha_0},$$

$$\mathbf{m}_x^{(2)}(t,\boldsymbol{\alpha}_0) = -2\pi S_0[\mathbf{A}_2(\boldsymbol{\alpha}_0)]^{-1}\mathbf{G}^{(2)}(\boldsymbol{\alpha}_0),$$

$$\mathbf{S}_{x,i}^{(2)}(t,\boldsymbol{\alpha}_0) = -[\mathbf{A}_2(\boldsymbol{\alpha}_0)]^{-1}[\mathbf{A}_{2i}(\boldsymbol{\alpha}_0)\mathbf{m}_x^{(2)}(\boldsymbol{\alpha}_0) + 2\pi S_0\mathbf{B}_{2i}(\boldsymbol{\alpha}_0)].$$

$\mathbf{I}$ is the identity matrix and S_0 is the spectral density level of the white noise.

Fig. 26(a) shows the dependence of the second order moment response of the top story displacement of an eight-story two-bay semi-rigid frame on the rigidity parameter v for undamped and damped cases. Fig. 26(b) shows the dependence of the mean square response on the damping value for three different values of the rigidity parameter $v = 0, 0.47$, and 1. Derivatives of the mean square response with respect to the damping and rigidity parameters are shown in Figs. 27(a) and (b). It is seen from Fig. 27(a) that for the damping coefficient $c_c = 9\times10^6$ N s m and values of v less than 0.7 the response mean square is very sensitive to the variation of the joint damping coefficients of the first two stories only. For values of v close to 0.9 there is a significant sensitivity to c_{ci} for every story, which results in large increment of the response. Fig. 27(b) reveals that for c_c greater than 5×10^5 N s m the response is not sensitive to any variation of the stiffness.

5.3. Metallic joints

In the design of bolted flanged joints, it is necessary to examine the contact stress distribution, which governs the clamping effect on the sealing performance and the load factor. The load factor is defined as the ratio of an increment in axial bolt force to the external force. When an external load is applied to a joint, the contact stress distribution is changed and the axial bolt force is also changed. Thus, it is important to know the relationship between the changes in the contact stress distribution and the axial bolt force when an external load is applied to the joint.

Petersen [318] conducted an experimental investigation to study the effect of geometrical imperfections of the contact surface in pre-stressed flange connections. He found that fatigue life is not substantially affected by imperfections. However, another independent study by Schmidt et al. [319], based on deterministic imperfection shapes, showed that geometrical imperfection results in a significant increase in fatigue-relevant stress amplitudes. Bucher and Ebert [320] used a stochastic FEM combined with Monte Carlo simulation to estimate the statistical properties of the random ultimate load of bolted joints. They showed that the effect of imperfect contact can considerably deteriorate structural performance.

Sawa et al. [321] addressed the problem of estimating the load factor for the external bending moments in bolted circular flanged joints. The characteristics of circular bolted flanged joints subjected to external bending moments (torque) were examined analytically and experimentally.

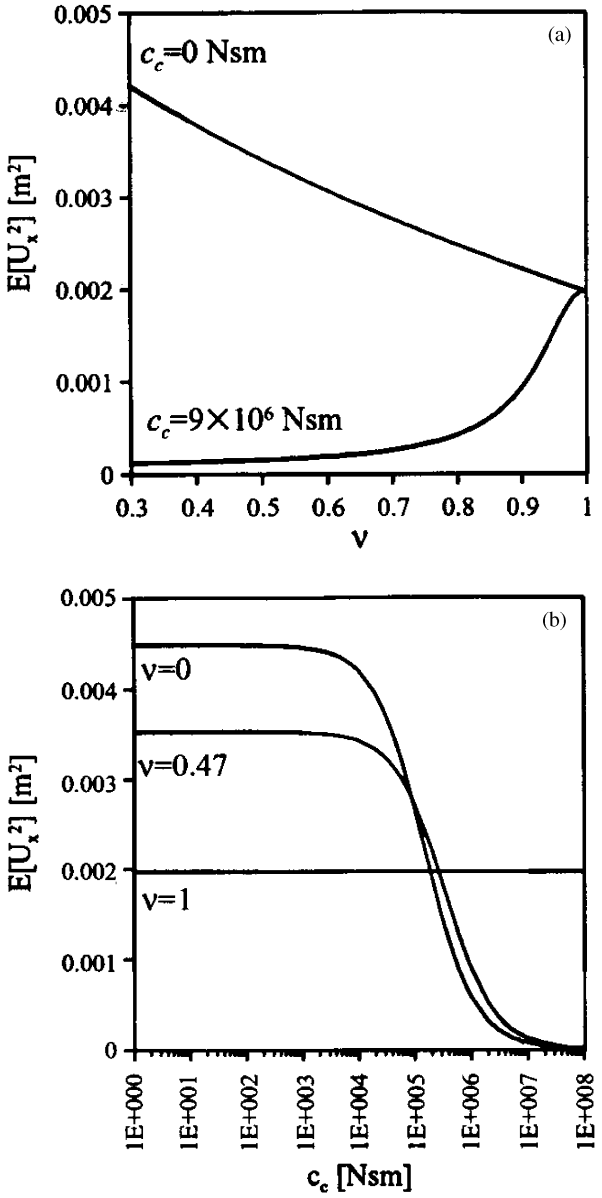

Fig. 26. Dependence of the mean square response of the top floor on (a) the fixity parameter, and (b) the damping ratio [314].

By replacing a circular bolted flanged joint with a finite solid bar, the contact stress distribution of the joint was determined using the three-dimensional theory of elasticity.

Zhao [322] analyzed the load distribution in a bolt–nut connector. Taniguchi et al. [323] conducted experimental tests and argued that the well-known Ostrovskii's equation of interface stiffness holds up to a certain critical pressure p_c. In this case, the displacement of interface z is

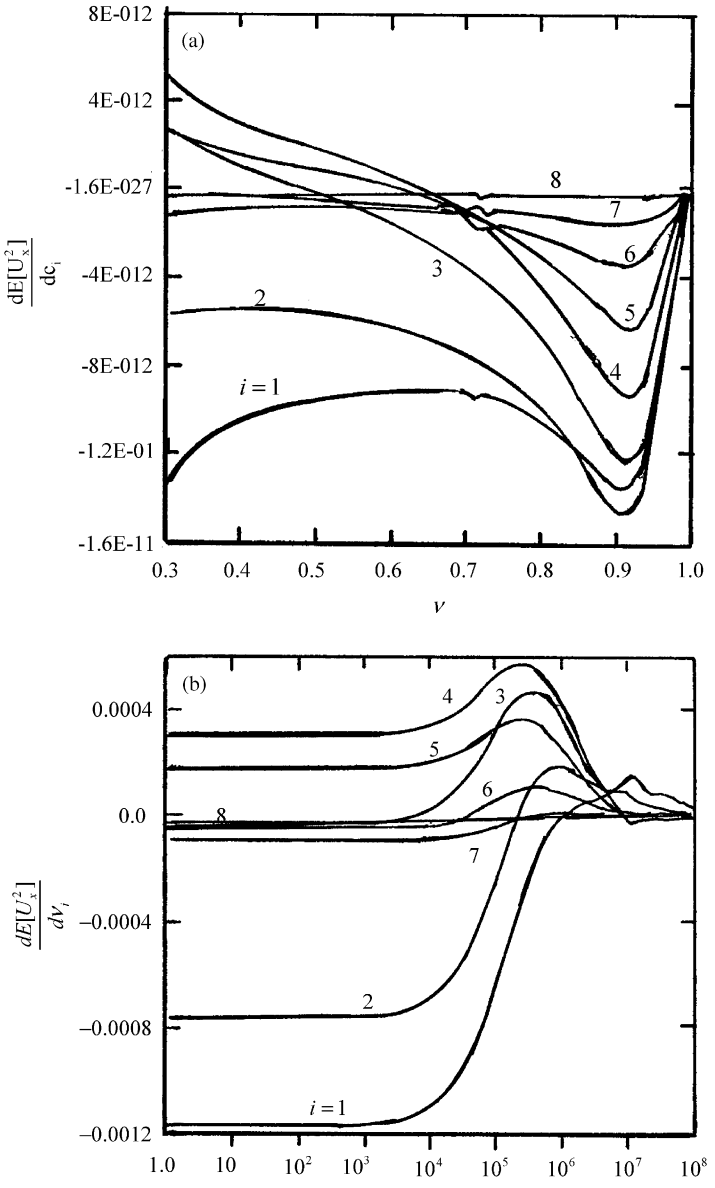

Fig. 27. Sensitivity curves showing the derivative of the second order moment of the top story displacement with respect to (a) the damping coefficient of the connections of the ith story versus fixity factor v for $c_c = 9 \times 10^6$ N s m, (b) the fixity factor of each story versus damping coefficient for $v = 0.47$ [314].

related to the contact pressure by the simple equation

$$z = cp^m, \quad p \leqslant p_c, \tag{84}$$

which is based on experimental data.

The relationship between the maximum approach z_{max} and the sum of surface roughness is

$$z_{max} = 0.25R_{mt}. \tag{85}$$

One of the design objectives in bolted joints is to reduce the portion of the external load carried by the bolt such that the joint members carry a large portion of the external load. The calculation of bolt and member stiffness has been considered in several FEM-based studies [324–330]. By designing the bolted joint such that the joint members carry a large portion of the external load, the joint strength can be much stronger than if the bolt were carrying the entire load. Norton [331] concluded that this could be done by selecting a bolt that is stiffer than the members. Lehnoff and Wistehuff [329] conducted FEA on different joint models and found that the bolt stiffness decreased and the member stiffness increased for all models as the magnitude of the external load was increased. This only takes place due to bending of the threads and the decrease in cross-sectional area of the bolt when the threads are included in the FEA. Later, Lenhoff and Bunyard [330] found significant differences in both bolt and member stiffness when the thread geometry is included. The observed decrease in the bolt stiffness was explained by both the increased flexibility of the bolt due to bending of the threads and the decrease in cross-sectional area of the bolt when the threads are included. When the bolt preload is applied, the member stiffness increases due to the resulting decrease in the initial member deflection.

The effects of surface roughness, compressional moment, and torsional angle on the torsional moment were studied by Karamis and Selcuk [332] and Niisato et al. [333]. It was found that the surface roughness plays a major role in the joint reliability. Higher values of surface roughness resulted in loosening of the joint. As the surface roughness increases the critical sliding load, above which the sliding stops, increases. The effect of thread pitch and friction coefficient on the stress concentration in nut–bolt connections was studied by Dragoni [334]. The optimum position of bolts in structures was the subject of many studies (see, e.g., Refs. [335–339]). Simulation of non-linear dynamics of bolted assemblies revealed that fastener placement could be optimized to reduce vibration-induced loosening [340].

The design of screw threads involves several geometric features and dimension characteristics [341]. The mechanical performance of threaded components depends on material properties, thread geometry, and environment conditions. The effect of thread dimensional conformance on vibration-induced loosening was studied by Dong and Hess [342]. It was found that, when compared with fastener combinations within conformance, resistance to vibration was significantly degraded for the fasteners combinations with undersized pitch and major bolt diameters or oversized pitch and minor nut diameter. Leon et al. [341] found that variations in bolt pitch diameter would affect the yield and tensile strength by about an order of magnitude more than variations in bolt major diameter or nut pitch and minor diameters.

5.4. Composite joints

Although this review focuses primarily on bolted joints, some basic issues in bonded composites are provided here for comparison with bolted composite joints. There are many parameters involved in the design of composite bonded joints. Some of these are the bond length, bond thickness, and adhesive curing temperature. The design of mechanical fastening of plastics is described in a book by Lincoln et al. [343], while the mechanical behavior of adhesive joints is well

documented in Verchery [344]. Vinson [345] outlined some design factors of composite fasteners. The modelling of bolted pretension in composite structures was developed by Stallings and Hwang [346]. Rastogi et al. [347–349] studied the effect of these parameters on the failure loads of a double-lap adhesively bonded joint. They found that a smaller bond length results in higher magnitude of stresses in the joint along the bond length. Apalak and Davies [350] discussed a number of design aspects of adhesively bonded corner joints. Lee and McCarthy [351] presented an overview of composite-to-metal joints. Ogunjimi et al. [352], Bailey et al. [353,354] and Hermann et al. [355] studied the role of critical thermal/structural parameters on the design of a metal/composite joint. Wang et al. [356] presented an assessment of different design approaches for bolted joints in laminated components.

The load distribution in single- and double-lap composite joints and multi-fastener joints was determined in Refs. [357–367]. Highly loaded bonded joints for aircraft thin skins were analyzed by Elsly et al. [368]. The stress distribution and load resistance in composite joints were estimated by Prasad et al. [369] and Prabhakaran et al. [370]. Hamada et al. [371,372] estimated the strength of quasi-isotropic carbon/epoxy joints and considered effects of stacking sequences. Ireman [373] developed three-dimensional stress analysis of bolted single-lap composite joints.

Although utilized quite extensively, bolted joints in laminated composites are not well understood. Experimental and statistically based investigations of ultimate strengths of bolted joints for laminated composites were reported in Refs. [374–376]. Stress concentrations at hole-edges in advanced composites can be as high as nine [377] and joint efficiencies are often as low as 50% [378]. Ankara and Dara [379,380] and Arnold et al. [381] applied optimization techniques for composite bolted joints design. Ireman et al. [382] reported a number of design methods for bolted joints in composite aircraft structures. Snyder et al. [383] and Shih [384] presented different numerical approaches for the analysis of composite bolted joints. The behavior of joints under central and eccentrically loaded bolted and welded joints was determined by Skalerud [385] and Gattesco [386]. The design of composite fasteners subjected to transverse loads was considered by Running et al. [387]. Rosner and Rizkalla [388,389] experimentally and analytically examined the behavior of bolted connections in composite materials used for civil engineering applications. A design procedure was introduced to account for material orthotropy, pseudo-yielding capability, and other factors that influence bolted-connection behavior.

Different design approaches of multiple-row bolted composite joints under general in-plane loading were considered in Refs. [390–394]. Chutima and Blackie [395] studied the effect of pitch distance, row spacing, end distance, and bolt diameter on multi-fastened composite joints.

Camanho and Matthews [396] presented an overview on the strength analysis of mechanically fastened joints made from fiber-reinforced plastic (FRP). It was remarked that there is no universally accepted strength design method for mechanically fastened composite joints [381,397–399]. However, analytical and numerical methods have been widely used to determine the stress and failure occurrence for an optimal joint design [400]. The case of multi-bolted joints was considered by Hassan et al. [401–403]. Analytical and experimental studies pertaining to the tensile response and failure of joints made from carbon fiber-reinforced plastic (CFRP) were reported in Refs. [404–406]. They observed that the dynamic behavior of composite joints is much more complicated than quasi-static behavior because of the involvement of strain rate and inertia effects. The effect of clamping on the tensile strength of composite plates with a bolt-filled hole

was studied in Refs. [407–412]. Erki et al. [413] addressed the factors affecting the design of glass-fiber reinforced plastic (GRFP) bolted connections.

6. Failure and fatigue of structural joints

6.1. Metallic joints

In Section 3, the mechanisms of relaxation and vibration-induced loosening of joint structures were discussed and assessed. The behavior of a bolted joint under dynamic loading is affected by the type of load transfer in the connection. As mentioned earlier, depending on clamping pressure, the applied load can be transmitted either by friction between contact surfaces, or by shear and bearing of the bolts. Dynamic loading can cause fatigue and failure of the joint structure. In general, the likelihood of a particular failure mechanism in the joint depends on the load and the structural properties. The principal modes of failure of mechanically fastened joints are (1) bearing failure of the material, (2) tension failure of the material, (3) shear-out failure of the material, and (4) shear failure of the bolt.

Lazzarin et al. [414] and Atzori et al. [415] studied the fatigue modes of aluminum alloy bolted joints. Their statistical analysis revealed that the clamping forces are not high enough to prevent slipping into bearing and shear. With a high number of cycles of repeated loads, the friction-type joints were slip resistant and fatigue cracks started in the gross section, in front of the first boltholes. Fatigue cracks initiated outside the zone weakened by the holes near the external diameter or at the interface of the contact surfaces. The dependence of the stress amplitude on the number of cycles was found to be scattered within a band that is limited at the top by the yielding properties of the materials.

In road vehicles subjected to impact loading, the structural collapse is controlled such that it offers protection to the occupants. Birch and Alves [416] conducted a series of experimental tests to study the dynamic failure of spot welded lap joints and bolted joints in thin sheet materials that are used in road vehicles. Under pulling in-plane shear load, failure of the bolted joints first began as rotation of the bolt and local out-of-plane buckling of the joint material, which were followed by tearing and extension of the hole in the jointed plates. Final failure occurred either by a pull out of the bolt, head or nut. Fig. 28 shows the dependence of the pulling load on the displacement of 3- and 5-mm bolted joints under different values of pull velocity.

High-temperature turbine cylinders and valve covers are joined using studs or bolts. High-temperature bolts are tightened either by thermal or mechanical means to an initial displacement or stretch [417]. The initially high stress relaxes with time as the bolt creeps at the operating temperature. Mantelli and Yovanovich [418] and Fukuoka et al. [419] analytically and numerically studied the influence of thermal loading on the behavior of bolted joints. Ellis et al. [420] developed and validated an analytical life prediction method for high-temperature turbine and valve bolts. The failure criterion was an accumulated inelastic or creep strain limit of 1%. Life assessment was based on the measured bolt length to calculate the accumulated creep strain. The conversion of elastic strain by stress reduction into creep strain was given by the relationship

$$-\frac{1}{E}\frac{\mathrm{d}\sigma}{\mathrm{d}t}=\frac{\mathrm{d}\varepsilon_c}{\mathrm{d}t}, \tag{86}$$

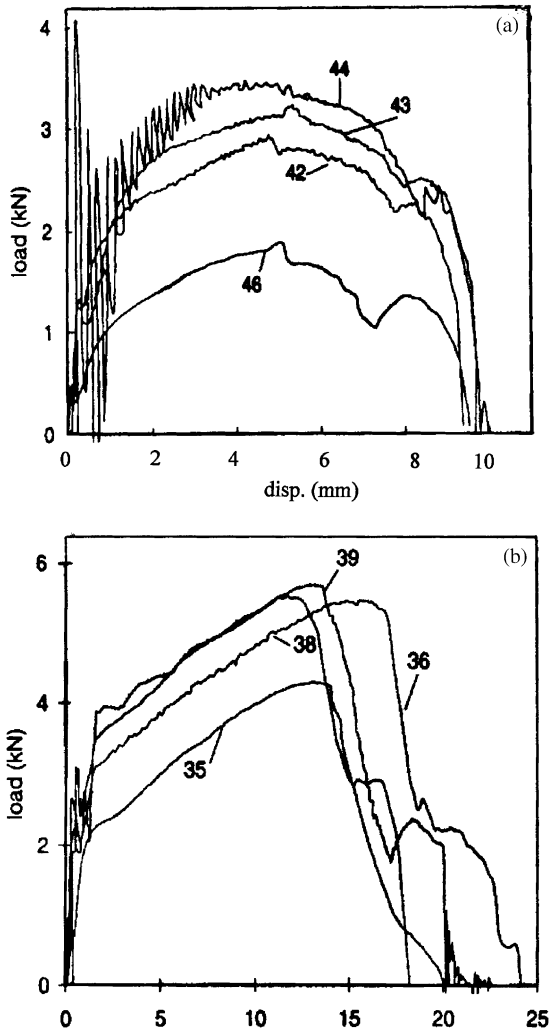

Fig. 28. Load–displacement curves for (a) 3 mm bolted joint: specimen 46 under pull velocity 0.02 mm/s, 42 under 5.2 mm/s, 43 under 50.5 mm/s, and 44 under 500 mm/s; (b) 5 mm bolted joint 35 under 0.02 mm/s, 36 under 3.04 mm/s; 38 under 25.3 mm/s and 39 under 250 mm/s [416].

where σ is the stress, t is time, and ε_c is the creep strain. For a time increment, the stress was held constant and the increment of creep strain accumulated was calculated.

6.2. Riveted joints

The dynamic failure of structural joints is of great concern to automotive and aerospace industries. Many parts of aircraft structure are joined by bolts and rivets and are subject to spectrum fatigue loading [421]. The effect of rivet pitch upon the fatigue strength of single-row riveted joints was studied by Seliger [422]. It was found that the fatigue strength per rivet increases

with increasing rivet pitch. One of major problems of aircraft aging is the effect of fretting contact stresses on crack nucleation in riveted lap joints and pinned joints [423–426]. Langrand et al. [427] considered structural integrity issues in modelling riveted joints for numerical analysis of airframe crashworthiness. The FE modelling included structural embrittlement due to the riveting process, mechanical strength characterization, and simplified modelling of bonding.

Experimental studies by Terada [428–430], Terada and Okada [431,432], and Furuta [433] discussed the influence of fastener type, fastener row, squeezing force, load value, and corrosion on the fatigue performance of riveted lap joints. Their experimental results suggested that fatigue behavior of a fuselage structure could be estimated by evaluating the largest principal stress under complex stress conditions. One of the surprising findings was that overloads were effective to extend the fatigue life of the constant amplitude tests of single lap joint. However, underloads (or compression load) resulted in considerable out-of-plane deformation. The difference between corrosion fatigue and fatigue of corroded joints could be substantial in view of the relation between tightness and load transmission.

The creep behavior of an aircraft structure due to aerodynamic heating may result in excessive deformation and creep rupture during the design lifetime of riveted joints [434,435]. It was reported that the creep of a joint could be considerably greater than the tensile creep of an unriveted sheet. Furthermore, the correlation between the creep of a joint and the tensile creep of an unriveted sheet was questionable [434], but the correlation was found to exist later [435]. Simple methods were described to estimate the time to rupture, mode of rupture, and deformation of structural joints in creep under constant load and temperature conditions. The temperature distribution pattern in a heated structural joint of a given geometry was found to change considerably due to the joint interface. The degree of such change depends on the value of interface thermal conductivity. Barzelay and Holloway [436,437] found that any change in temperature distribution results in a different deformation pattern. Wright and Johnson [438] studied the effect of thermal aging on the bolt bearing behavior of highly loaded composite joints.

Fretting in riveted joints arises from microslip associated with small-scale oscillatory motion of nominally clamped structural members. Farris et al. [425] and Wang et al. [439] indicated that fretting is the main mechanism for creating multiple site damage at fastener holes. Multiple site damage in riveted lap joints was reported by Silva et al. [440]. Beuth and Hutchinson [441], Müller [442] and Piascik and Willard [443] conducted experimental investigations to characterize multi-site damage in fuselage structures and indicated that fretting is the cause for crack nucleation in lap joints. Harish et al. [444] and Harish and Farris [426] used FEA to determine the effects of various parameters such as the magnitude of normal and tangential forces transferred, interface friction and rivet patterns on local contact stresses and crack nucleation life. Fig. 29 shows a comparison of contact stresses estimated by FEM and Mindlin theory for a load transfer ratio (LTR) of 0.4. LTR is defined as the ratio of the load carried by the rivet to the total applied load. The contact normal pressure, p, shear traction on the rivet interface, q, and tangential stress around the fastener hole on the skin, σ_h, are non-dimensional with respect to the remote applied stress σ_0. Fig. 30 shows the life to failure for a lap joint with different values of the squeeze force used during the riveting process. The total life to failure was measured by the number of load cycles at 10 Hz with stress ratio $\sigma_{min}/\sigma_{max} = 0.01$. It was reported that the failure initiated along the 90° direction, i.e., normal to the applied load along the in-plane.

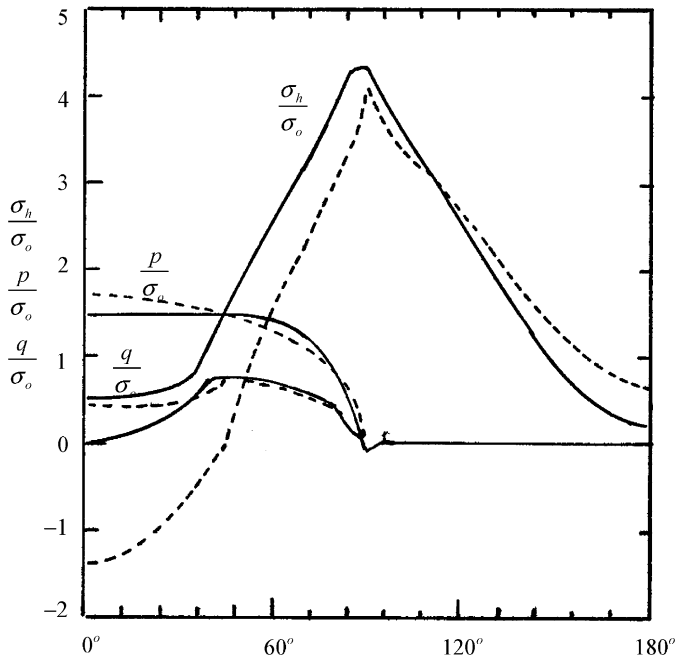

Fig. 29. Comparison of contact stresses for load transfer ratio of 0.4 and friction coefficient $\mu = 0.5$: —, FEM; - - -, Mindlin theory with added effect of bulk stress [426].

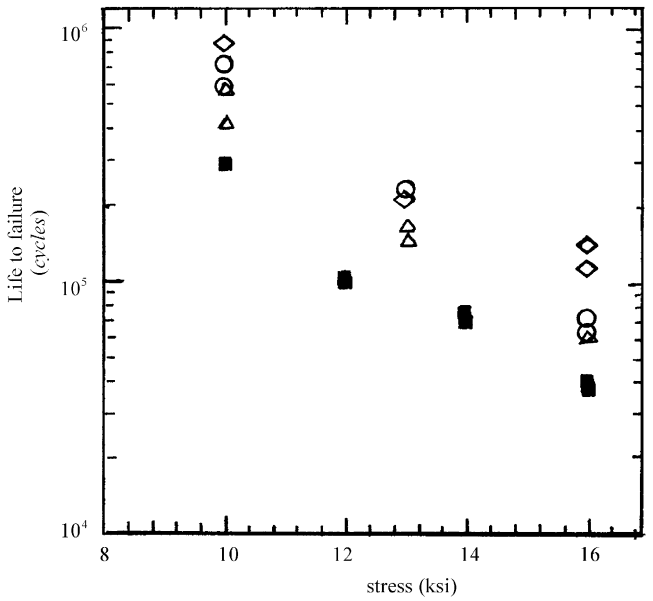

Fig. 30. Life to failure for lap-joint for different values of squeeze force F: ■, $F = 2500$ lb, △, $F = 3500$ lb; ○, $F = 4250$ lb; ◇, $F = 5000$ lb [426].

6.3. Composite joints

Failure and fatigue of composite joints depends on the type of the joint. For example, adhesive bonded joints exhibit high stress concentration near the ends of the joint. Such stress concentration in the adhesive layer results in high stresses in the adjacent plies of the adherend laminates. Accordingly, failure may be initiated in these plies. An effective way of reducing the local high stresses in the plies is to interleave the plies of the adherend laminates so that adhesion takes place in many layers. It has been agreed that the allowable loads on a joint are those at which micromechanical damage first occur. This type of damage will eventually lead to macromechanical damage. Dickson et al. [445] developed a comprehensive linear analysis for bonded joints in composite structures. Schulz et al. [446,447] considered the tension-mode fracture model in studying bolted joints in laminated composites.

Bonded joints have been used in aerospace applications for highly loaded structures, but generally are not used in primary load paths because of the variability in the ultimate strength and the difficulty of non-destructively evaluating their strength. Seven modes of micromechanical damage at bonded joints were discussed in detail by Agarwal and Broutman [13]. Maximum stress criteria and the fracture mechanics criteria, which deal with failure by crack initiation and propagation, are commonly used in composite structures to predict the location for damage initiation. Crack propagation is unstable when it causes the total energy to decrease or remain constant. There are three basic modes of crack loading and extension: (1) crack opening mode (Mode I), (2) shear mode (Mode II), and (3) anti-plane strain or tearing mode (Mode III). More complex stress states lead to mixed mode crack extension. Chiang and Rowlands [448] developed a FE analysis to analyze the mixed-mode fracture of bolted composite joints. The bearing failure of bolted composite joints was experimentally characterized by Wang et al. [449]. Forte et al. [450] examined the influence of adhesive reinforcement on the Mode I fracture toughness of a double cantilever beam specimen. They developed a plane strain axisymmetric damage model to determine the energy release rates for mid-plane cracking in aluminum bonded specimens with varying amounts of adhesive reinforcement. They found that the fracture behavior became less brittle upon the addition of fibers in the bond-line. Gilchrist and Smith [451,452] reported some results pertaining to the development of fatigue cracks in t-peel joints.

The long-term behavior of composite-to-composite joints in severe environments is a difficult problem currently under research in the composite structure community. Creep is one of the main characteristics of composite joints. Su and Mackie [453] developed a two-dimensional creep analysis of adhesive joints. A series of experimental and analytical studies were conducted [454–458] to predict the progressive failure in an adhesively bonded composite-to-composite double-lap shear specimen. Other studies [459–462] estimated the fracture load and the fracture parameters for adhesive joints. For unidirectional adherends, Roy and Donaldson [456] experimentally observed that the crack front profile appeared to be uniform across the width of the specimen, indicating that the free edge fields along the sides of the specimen do not significantly influence the crack front.

FEM and boundary element method have been used to determine the stress and strength of composite joints (see, e.g., Refs. [346,463–471]). These studies have focused primarily on the physics of the problem but have not formally addressed the observed variability in the mechanical properties of composite joints. Richardson et al. [472], and Bogdanovich and Kizhakkethara [454]

carried out three-dimensional FEA for double-lap shear joints with unidirectional outer adherends and an aluminum middle adherend and found that the side edges of the specimen had little effect on the stress field. Later, Bogdanovich and Yushanov [473] conducted a 3-D progressive failure analysis utilizing the strain energy release to predict various scenarios of cohesive, adhesive or interlaminar crack propagation in bonded composite joints. In a series of studies, Iarve [474–476] developed 3-D stress analyses of composite fasteners. Edlund and Larbring [477] and Edlund [478] determined the damage behavior of adhesive joints using geometrically non-linear models.

Fatigue damage of composite bolted joints has been phenomenologically characterized for different structures [404,479–488]. Other studies included deterministic analyses and predictions of fatigue of bolted joints [489–494]. Ko et al. [495] considered the influence of material non-linearity on fatigue behavior of composite bolted joints. The influence of uncertainty and geometric variabilities were studied through probabilistic approaches by Chamis et al. [496], Minnetyan et al. [497], and Tong [498]. The evolution of pull-through failure of composite laminates was studied experimentally and analytically by Banbury and Kelly [488], and Banbury et al. [494]. The fracture mechanics of double cantilever adhesive joints was analyzed in Refs. [499,500]. The case of composite-to-metal lap joints was reported by Reedy and Guess [501].

Cooper and Turvey [502] studied the effects of joint geometry and bolt torque on the performance of single bolt joints in **pultruded** glass reinforced plates (GRP). Turvey [503] presented an assessment of research activities on single-bolt tension joints in structural grade pultruded (GRP) and reported some experimental results. Details were given of 54 tests on single-bolt joints in which the angles between the pultrusion and tension axes (the off-axis angle) and the joint geometry were varied. Ultimate strength, initial stiffness, initial bolt slip and bolt displacement at failure data were presented as functions of the joints' principal geometric ratios. The reported joint failure modes showed that for off-axis angles $\geqslant 30^\circ$, bearing failure (a relatively benign failure mode) did not occur. Instead, tension mode failure predominated and cracks tended to propagate diagonally across the width of the joint.

Saunders [504] and Galea and Saunders [505] studied the generation of fatigue damage around fastener holes in thick bolted joints. Galea et al. [506] presented a non-destructive evaluation of composite-to-metal joints. Ramkumar and Tossavainen [507] studied the dependence of the load ratio $R = \sigma_{min}/\sigma_{max}$ on the fatigue life of AS1/3501-6 graphite/epoxy joints. For tension–tension loading, $R = 0$, the failure mechanism was partial or total shear-out. At 85% of the quasi-static failure stress run-out was observed. The quasi-static strength was slightly higher in compression than in tension. For tension-compression loading, $R = -1$, the failure mode was hole elongation. Xiong [508] developed a complex variational approach for the failure prediction of composite joints involving multiple fasteners. Destuynder et al. [509], Park and Alturi [510], and Persson and Eriksson [511] studied the fatigue of multiple-row bolted joints in lap joints and carbon/epoxy laminates. The joint's failure strength and failure mode were predicted using the results of the joint stress analysis along with the point stress failure criterion originally proposed by Whitney and Nuismer [512]. Ryan and Monaghan [513] used FEM to study the effect of panel material, laminate stacking stiffness and rivet forming load on the stress distribution with both the fiber metal laminate (FML) and the 2024-T3 riveted joints subjected to external loads. It was found that if the rivets were installed in the same manner as in a monolithic aluminum panel, localized delamination was predicted to occur in the FML panels during rivet forming. Allix [514] analyzed

the damage of delamination around a hole. Li et al. [406] observed combined failure modes (bearing/pull-out, bearing/cleavage) in riveted joints made from CFRP. Other failure modes, such as bending-induced cross-section failure and rivet cap penetration failure, were identified in tension tests.

Schön and Nyman [515] and Starikov and Schön [516] investigated the spectrum fatigue life and the local fatigue behavior of CFRP bolted joints. They observed that fatigue degradation of the fastener system involved washer failure, reduction in bolt pre-stress, and fatigue damage at bolt holes. Bolt movement was found to increase measurably during fatigue testing. Changes in the bolt behavior were reported to occur very early in the fatigue life of bolted joints and reflected rapid changes in the damage state of the fastener system and the adjacent composite.

7. Concluding remarks and recommendations

Mechanical joints and fasteners are essential elements in joining structural components in mechanical systems. The dynamic characteristics and reliability of built-up structures depend to a great extent on the dynamic properties of the joint. However, it is not possible to guarantee that all joints are subject to the same load conditions and there is a degree of uncertainty in the preload in each joint. In addition, there is also relaxation in the preload due to environmental conditions once the system is placed in service. The literature has focused on estimating the energy dissipation in bolted joints associated with microslip and macroslip regimes. The problems of joint uncertainties and relaxation have been studied to determine the random eigenvalues and damping in the joints using fuzzy sets, stochastic FEM, Monte Carlo simulation, and special co-ordinate transformations. The identification of linear and non-linear joint properties, such as damping, stiffness and inertia, has occupied a substantial amount of research activity. Design considerations and fatigue and failure modes in metallic and composite joints also have received extensive attention. Based on the white paper by Dohner [2] and the work reviewed in this article, the following are recommended future research avenues:

- There is a need for additional sinusoidal and random excitation tests to measure the evolution of the dynamic characteristics of joints. These studies should focus on variability in mechanical properties of joints to facilitate rigorous modal validation. They should be conducted for various values of preload, and different excitation conditions. The test duration should be long enough to exhibit qualitative variations of the dynamic characteristics of the joint model. Owing to joint relaxation associated with non-linear prying loads, response statistical parameters will be both non-Gaussian and non-stationary. They should be estimated for specified intervals of time.
- The influence of joint preload uncertainty on natural frequency and damping ratio should be experimentally measured. It is important to conduct sensitivity analysis to identify the critical regions of joint conditions that result in significant changes in the system dynamic behavior.
- There is a need to develop analytical models of structural elements with joint uncertainty represented by both fuzzy and random parameters in the differential equations of the systems. Furthermore, the connection between the types of uncertainty in the properties of joints and the chosen uncertainty model (e.g., fuzzy or random) must be more explicit. This will allow

researchers to properly employ measured data to evaluate these models and will also help experimentalists to design laboratory specimens and sensor installations to better support validation studies. The sensitivity of the dynamic characteristic of structural systems to variations of joint parameters is very important to their safety and integrity. The models should take into account such non-linear sources as prying loading, friction forces, and relaxation effects.

- It is important to study the influence of bolted joint uncertainties and relaxation on the first passage problem. This should be conducted analytically, numerically, and experimentally for simple one-dimensional models to aid in the generation of physical intuition.
- Stochastic models of bonded joints are needed to support quality-control efforts that are directed towards substantially decreasing the observed variability in the strength of bonded joints. Models that incorporate many potential sources of variability will help to guide test designers and manufacturing specialists in choosing the most effective parameters for improving the robustness of bonded joints.

Acknowledgements

The first author was supported in this effort by a contract from the Air Vehicles Directorate of the Air Force Research Laboratory, Wright-Patterson Air Force Base, Ohio. The second author gratefully acknowledges the Air Force Office of Scientific Research for sponsoring this work through Laboratory Task 02VA03COR (Dr. Dean Mook, Program Manager).

Appendix A. Common terminology

The purpose of this appendix is to provide the common terminology used in discussing bolts and bolted joints.

Basic bolt geometry and dimensions (see Fig. 31)

L_c total length of fastener, including head
L_t total length of threads on fastener
L_B unthreaded length $= L - L_t$
L_G grip length

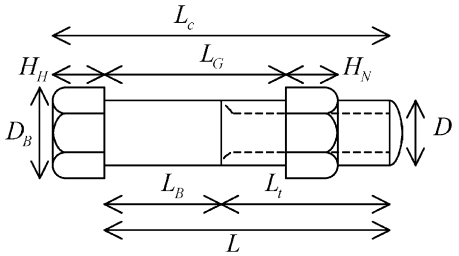

Fig. 31. Bolt–nut geometry and dimensions.

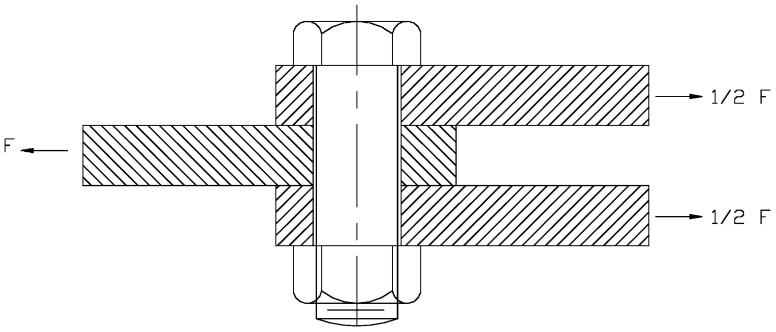

Fig. 32. Slip resistant joint in shear.

D nominal diameter
D_B diameter of bolt head or washer (diameter of contact with joint members)
D_H diameter of bolt hole (not shown)
H_H bolt head height
H_N nut length

Faying surfaces: Surfaces subjected to friction developed between the joint surfaces in a shear joint.

Prying load: Usually it is assumed that the resultant external load in bolted joints under tension load is acted at some point along the axis of the bolt. In reality, the tensile load is applied off to one side of the bolt and thus is called a prying load. Such load can drastically increase the amount of tensile and bending stress produced in the bolt. Fig. 20 shows a schematic diagram in which the tension loads on the joint are offset from the axis of the bolts.

Slip-resistant (*or friction-type*) *joint*: Joints in which friction is responsible for shear resistance, see Fig. 32.

Stress area (A_s) of standard thread is estimated based on the mean pitch and root diameters.

References

[1] M.M. Frocht, H.N. Hill, Stress-concentration factors around a central circular hole in a plate loaded through a pin in the hole, *ASME Journal of Applied Mechanics* 7 (1940) A4–A9.
[2] J.L. Dohner, White paper: on the development of methodologies for constructing predictive models of structures with joints and interfaces, Sandia National Laboratories SAND2001-0003P, 2001.
[3] R.A. Ibrahim, Structural dynamics with parameter uncertainties, *American Society of Mechanical Engineers, Applied Mechanics Reviews* 40 (1987) 309–328.
[4] G.I. Schuëller, State-of-the-art report on computational stochastic mechanics, *Probabilistic Engineering Mechanics* 12 (1997) 199–321.
[5] C.S. Manohar, R.A. Ibrahim, Progress in structural dynamics with stochastic parameter variations: 1987–98, *American Society of Mechanical Engineers, Applied Mechanics Reviews* 52 (1999) 177–197.
[6] J.W. Fisher, J.H.A. Struik, *Guide to Design Criteria for Bolted and Riveted Joints*, Wiley, New York, 1974.
[7] J.H. Bickford, The bolting technology council and the search for more accurate preload, *ASME Pressure Vessels and Piping Conference on Advances in Bolted Joint Technology*, PVP-Vol. 158, 1989, pp. 1–6.

[8] J.H. Bickford, J.H., *An Introduction to the Design and Behavior of Bolted Joints*, 2nd Edition, Marcel Dekker Inc., New York, 1990.
[9] J.H. Bickford, S. Nassar, *Handbook of Bolts and Bolted Joints*, Marcel Dekker, New York, 1998.
[10] J.S. Mitchell, *Large Industrial Threaded Fasteners*, High-gate Publications Beverley Limited, Beverly, 1993.
[11] R.O. Parmley (Ed.), *Standard Handbook of Fastening and Joining*, McGraw-Hill, New York, 1997.
[12] J.A. Speck, *Mechanical Fastening, Joining, and Assembly*, Marcel Dekker Inc., New York, 1997.
[13] B.D. Agarwal, L.J. Broutman, *Analysis and Performance of Fiber Composites*, Wiley, New York, 1990.
[14] E.E. Ungar, Energy dissipation at structural joints: mechanisms and magnitudes, Technical Documentary Report No. FDL-TDR-64-98, Air Force Flight Dynamics Lab, Wright-Patterson Air Force Base, OH, 1964.
[15] E.E. Unger, The status of engineering knowledge concerning the damping of built-up structures, *Journal of Sound and Vibration* 26 (1973) 141–154.
[16] J. Tajima, Effects of relaxation and creep on the slip load of the high strength bolted joints, Structural Design Office, Japanese National Railways, Tokyo, 1964.
[17] E. Chesson Jr. W.H. Munse, Studies of the behavior of high-strength bolts and bolted joints, Bulletin 469, University of Illinois, Experimental Station, 1964.
[18] M. Groper, V. Bausic, G. d'Albon, Measuring and control method for the prestressing force and its variation in time of high tensile bolts, Studii si Cercetari, Seria Const Metalice (7), INCRC, Bucuresti, Romania, 1966.
[19] P.D. Herrington, M. Sabbaghian, Factors affecting the friction coefficients between metallic washers and composite surfaces, *Composites* 22 (1991) 418–424.
[20] P.D. Herrington, M. Sabbaghian, Effect of radial clearance between bolt and washer on the bearing strength of composite bolted joints, *Journal of Composite Material* 26 (1992) 1826–1843.
[21] S.W.E. Earles, Theoretical estimation of the frictional energy dissipation in a simple lap joint, *Journal of Mechanical Engineering Science* 8 (1966) 207–214.
[22] M. Masuko, Y. Ito, K. Yoshida, Theoretical analysis of a damping ratio of a jointed cantilever beam, *Bulletin of Japanese Society of Mechanical Engineering* 16 (1973).
[23] M. Masuko, Y. Ito, T. Koizumi, Horizontal stiffness and microslip on a bolted joint subjected to repeated tangential static loads, *Bulletin of Japanese Society of Mechanical Engineering* 17 (1974).
[24] N. Nishiwaki, M. Masuko, Y. Ito, I. Okumura, A study on damping capacity of a jointed cantilever beam, *Bulletin of Japanese Society of Mechanical Engineering* 21 (1978).
[25] R.S. Richardson, H. Nolte, Energy dissipation in rotary structural joints, *Journal of Sound and Vibration* 54 (1977) 577–588.
[26] L. Jezequel, Structural damping by slip in joints, *American Society of Mechanical Engineers, Journal of Vibration, Acoustics Stress, Reliability, and Design* 105 (1983) 497–504.
[27] K.K. Padmanabhan, A.S.R. Murty, Damping in structural joints subjected to tangential loads, *Institute of mechanical Engineering Proceedings* 205 (1991) 121–130.
[28] T.J. Hertz, E.F. Crawley, Damping in space structure joints, *AIAA Dynamic Specialty Conference*, Palm Springs, CA, 17–18 May 1984, AIAA Paper 84-1039-CP, 1984.
[29] T.J. Hertz, E.F. Crawley, Displacement dependent friction in space structure joints, *American Institute of Aeronautics and Astronautics Journal* 24 (1985) 1998–2000.
[30] A.A. Ferri, Investigation of damping from nonlinear sleeve joints of large space structures, *Proceedings of the ASME 11th Biennial Conference of Mechanical Vibration and Noise*, DE-Vol. 5, Boston, MA, 1987, pp. 187–195.
[31] A.A. Ferri, Modeling and analysis of nonlinear sleeve joints of large space structures, *Journal of Spacecraft and Rockets* 25 (1988) 354–360.
[32] A.A. Ferri, Damping and vibration of beams with various types of frictional support conditions, *Proceedings of the AIAA/ASME/ASCE/AHS/ASC 30th Structures, Structural Dynamics, and Material Conference*, Washington, DC, 1989, pp. 782–787.
[33] A.A. Ferri, A.C. Bindmann, Damping and vibration of beams with various types of frictional support conditions, *American Society of Mechanical Engineers, Journal of Vibration and Acoustics* 114 (1992) 289–296.
[34] S.L. Folkman, F.J. Redd, Gravity effects on damping of a space structure with pinned joints, *Journal of Guidance and Control Dynamics* 13 (1990) 228–233.

[35] S.L. Folkman, E.A. Roswell, G.D. Ferney, Influence of pinned joints on damping and dynamic behavior of a truss, *Journal of Guidance and Control Dynamics* 18 (1995) 1398–1403.
[36] C.F. Beards, Damping in structural joints, *The Shock and Vibration Digest* 14 (1982) 9–11.
[37] C.F. Beards, The damping of structural vibration by controlled interface slip in joints, *American Society of Mechanical Engineers, Journal of Vibration, Acoustics, Stress analysis, Reliability, and Design* 105 (1983) 369–373.
[38] C.F. Beards, Damping in structural joints, *The Shock and Vibration Digest* 17 (1985) 17–20.
[39] C.F. Beards, Damping in structural joints, *The Shock and Vibration Digest* 21 (1989) 3–5.
[40] C.F. Beards, Damping in structural joints, *The Shock and Vibration Digest* 24 (1992) 3–7.
[41] R.Y. Lee, Assessment of Linear and Nonlinear Joint Effects on Space Truss Booms, M.S. Thesis, Department of Aeronautics and Astronautics, Massachusetts Institute of Technology, Cambridge, MA, June 1985.
[42] J. Prucz, A.D. Reddy, L.W. Rehfield, R.W. Trudell, Experimental characterization of passively damped joints for space structures, *Journal of Spacecraft and Rockets* 23 (1986) 568–575.
[43] J. Prucz, Analysis of design tradeoffs for passively damped structural joints, *Journal of Spacecraft and Rockets* 23 (1986) 576–584.
[44] M.L. Bowden, Dynamics of Space Structures with Nonlinear Joints, Sc.D. Thesis, Department of Aeronautics and Astronautics, Massachusetts Institute of Technology, Cambridge, MA, May 1988.
[45] M.L. Bowden, J. Dugundji, Joint damping and nonlinearity in dynamics of space structures, *American Institute of Aeronautics and Astronautics Journal* 28 (1990) 740–749.
[46] M. Groper, J. Hemmye, The dissipation of energy in high strength friction grip bolted joints, *Proceedings of SESA Spring Conference*, Cleveland, OH, 1983.
[47] M. Groper, J. Hemmye, Partial slip damping in high strength friction grip bolted joints, *Proceedings of the Fourth International Conference of Mathematical Modeling*, Pergamon Press, New York, 1983.
[48] M. Groper, Microslip and macroslip in bolted joints, *Experimental Mechanics* 25 (1985) 172–174.
[49] L. Gaul, R. Nitsche, R., The role of friction in mechanical joints, *American Society of Mechanical Engineers, Applied Mechanics Reviews* 54 (2001) 93–106.
[50] Y.S. Shin, K.S. Kim, J.C. Iverson, Analytical and experimental investigations of the damping characteristics of bolted and welded structural connections for plates and shells, part 1: a literature survey on friction damping in joints, NPS-69-86-011, Naval Postgraduate School, 1986.
[51] R.A. Ibrahim, Friction-induced vibration, chatter, squeal, and chaos, Part I: mechanics of contact and friction, *American Society of Mechanical Engineers, Applied Mechanics Reviews* 47 (1994) 209–226.
[52] R.A. Ibrahim, Friction-induced vibration, chatter, squeal, and chaos, part II: dynamics and modeling, *American Society of Mechanical Engineers, Applied Mechanics Reviews* 47 (1994) 227–253.
[53] C. Andrew, J.A. Cockburn, A.E. Waring, Metal surfaces in contact under normal forces: some dynamic stiffness and damping characteristics, *Proceedings of the Institute of Mechanical Engineering* 182 Part 3K, 1968, pp. 92–100.
[54] P.F. Robers, G. Boothroyd, Damping at metallic interfaces subjected to oscillating tangential load, ASME Paper 74-WA/Prod 9, 1974.
[55] S. Vitelleschi, L.C. Schmidt, Damping in friction-grip bolted joints, *American Society of Civil Engineers, Journal of Structure Division* 103 (1977) 1447–1460.
[56] C. Dekoninch, Deformation properties of metallic contact surfaces of joints under the influence of dynamic tangential loads, *International Journal of Machine Tool Design and Research* 12 (1972) 193–199.
[57] B.R. Hanks, D.G. Stephens, Mechanisms and scaling of damping in a practical structural joint, *Shock and Vibration Bulletin* 36 (1967) 1–8.
[58] C.B. Brown, Factors affecting the damping in a lap joint, *American Society of Civil Engineers, Journal of Structures Division* 96 (1968) 1197–1217.
[59] F.C. Nelson, D.F. Sullivan, Damping in joints of built-up structures, *Environmental Technology* 76, *22nd Annual Meeting*, Institute of Environmental Science, 1976.
[60] C.F. Beards, J.L. Williams, The damping of structural vibration by rotating slip in joints, *Journal of Sound and Vibration* 53 (1977) 333–340.
[61] C.F. Beards, I.M.A. Imam, The damping of plate vibration by interfacial slip between layers, *International Journal of Machine Tool Design and Research* 18 (1978) 131–137.

[62] C.F. Beards, Woodwat, The control of frame vibration by friction damping in joints, *American Society of Mechanical Engineers, Journal of Vibration, Acoustics, Stress Analysis, Reliability, and Design* 107 (1985) 27–32.
[63] E.H. Dowell, 1986, Damping in beams and plates due to slipping at the support boundaries, *Journal of Sound and Vibration* 105 (1986) 243–253.
[64] D.M. Tang, E.H. Dowell, Damping in beams and plates due to slipping at the support boundaries, part 2: numerical and experimental study, *Journal of Sound and Vibration* 108 (1986) 509–522.
[65] D.M. Tang, E.H. Dowell, Random response of beams and plates with slipping at support boundaries, *American Institute of Aeronautics and Astronautics Journal* 24 (1986) 1354–1361.
[66] Y.S. Shin, J.C. Iverson, K.S. Kim, Experimental studies on damping characteristics of bolted joints for plates and shells, *American Society of Mechanical Engineers, Journal of Pressure Vessel Technology* 113 (1991) 402–408.
[67] D.J. Segalman, Observations on simulation of joint friction, CDROM-Proc 1999 *ASME Design Engineering Technical Conference*, DETC99/VIB-8188, 1-7, Las Vegas, NV, 1999.
[68] D.J. Segalman, An Initial Overview of Iwan Modeling for Mechanical Joints, Technical Report, Sandia National Laboratories, SAND2001-0811, 2001.
[69] W.D. Iwan, On a class of models for the yielding behavior of continuous composite systems, *American Society of Mechanical Engineers, Journal of Applied Mechanics* 89 (1967) 612–617.
[70] J. Esteban, F. Lalande, Z. Chaudhry, C.A. Rogers, Theoretical modeling of wave propagation and energy dissipation in joints, *Proceedings of the 37th AIAA/ASME/ASCE/AHS/ASCE Structures, Structural Dynamics, and Material Conference*, Salt Lake City, 1996.
[71] J. Esteban, C.A. Rogers, Energy dissipation through joints: theory and experiments, *Computers and Structures* 75 (2000) 347–359.
[72] J.F. Wilson, E.G. Callis, The dynamics of loosely jointed structures, *International Journal of Non-linear Mechanics* 39 (2004) 503–514.
[73] S. Song, et al., Contact area of bolted joint interface: analytical, finite element modeling and experimental study, *ASME Winter Annual Meeting* EEP 3, 1992, pp. 73–81.
[74] S. Song, et al., Experimental study and modeling of thermal contact resistance across bolted joints, *Journal of Thermophysics and Heat Transfer* 8 (1994) 159–163.
[75] H. Rothert, et al., Non-linear three-dimensional finite element contact analysis of bolted connections in steel frames, *International Journal of Numerical Methods in Engineering* 34 (1992) 303–318.
[76] K. Iyer, Peak contact pressure, cyclic stress amplitudes, contact semi-width and slip amplitude: relative effects on fretting fatigue life, *International Journal of Fatigue* 23 (2001) 193–206.
[77] K. Iyer, Solutions for contact in pinned connections, *International Journal of Solids and Structures* 38 (2001) 9133–9148.
[78] T.L. Paez, L.J. Branstetter, D.L. Gregory, 1985, Modal randomness induced by boundary conditions, Society of Automotive Engineering Technical Paper 851930, 1985.
[79] T. Watanabe, Forced vibration of continuous system with non-linear boundary conditions, *American Society of Mechanical Engineers, Journal of Mechanical Design* 11 (1978) 487–491.
[80] W.K. Lee, M.H. Yeo, Two-mode interaction of a beam with a non-linear boundary condition, *American Society of Mechanical Engineers, Journal of Vibration and Acoustics* 121 (1999) 84–88.
[81] T. Fukuoka, Finite element simulation of tightening process of bolted joint with a tensioner, *American Society of Mechanical Engineers, Journal of Pressure Vessel Technology* 114 (1992) 433–438.
[82] T. Fukuoka, Analysis of the tightening process of bolted joint with a tensioner using spring elements, *American Society of Mechanical Engineers, Journal of Pressure Vessel Technology* 116 (1994) 443–448.
[83] T. Fukuoka, Analysis of the tightening process of bolted joint with a tensioner: effects of interface stiffness, *ASME Proceedings of Reliability, Stress Analysis, and Failure Prevention Issues*, DE-Vol. 110, 2000, pp. 119–125.
[84] F. Wang, S. Chen, A method to determine the boundary condition of the finite element model of a slender beam using measured modal parameters, *American Society of Mechanical Engineers, Journal of Vibration and Acoustics* 118 (1996) 474–478.
[85] U. Lee, J. Kim, Determination of non-ideal beam boundary conditions: a spectral element approach, *American Institute of Aeronautics and Astronautics Journal* 38 (2000) 309–316.
[86] L.A. Zadeh, Fuzzy sets, *Information Control* 8 (1965) 338–353.

[87] M. Hanss, S. Oexl, L. Gaul, Simulation and analysis of structural joint models with uncertainties, *Proceedings of the International Conference on Structural Dynamics Modeling—Test, Analysis, Correlation and Validation*, Madeira Island, Portugal, 2002, pp. 165–174.
[88] M. Hanss, S. Oexl, L. Gaul, Identification of a bolted-joint model with fuzzy parameters loaded normal to the contact interface, *Mechanical Research Communication* 29 (2002).
[89] M. Hanss, K. Willner, A fuzzy arithmetical approach to the solution of finite element problems with uncertain parameters, *Mechanical Research Communication* 29 (2000) 257–272.
[90] M. Hanss, The transformation method for the simulation and analysis of systems with uncertain parameters, *Fuzzy Sets and Systems* 90 (2002) 277–289.
[91] G. Alefeld, J. Herzberger, *Introduction to Interval Computation*, Academic Press, New York, 1983.
[92] A. Kaufmann, M.M. Gupta, *Introduction to Fuzzy Arithmetic: Theory and Applications*, Van Nostrand Reinhold Co., New York, 1985.
[93] G.J. Klir, T.A. Folger, *Fuzzy Sets, Uncertainty, and Information*, Prentice-Hall, Englewood Cliffs, NJ, 1988.
[94] M. Hanss, A nearly strict fuzzy arithmetic for solving problems with uncertainties, *Proceedings of the 19th International Conference of North American Fuzzy Information Processing Society*, Atlanta, 2000, pp. 439–443.
[95] L. Chen, S.S. Rao, Fuzzy finite-element approach for the vibration analysis of imprecisely-defined systems, *Finite Elements in Analysis and Design* 27 (1997) 69–83.
[96] M. Shinozuka, F. Yamazaki, Stochastic finite element analysis: an introduction, in: S.T. Ariaratnam, G.I. Schueller, I. Elishakoff (Eds.), *Stochastic Structural Dynamics*, Elsevier, London, 1988, pp. 241–291 (Chapter 14).
[97] R. Ghanem, J.R. Red-Horse, Modal properties of a space-frame with localized system uncertainties, Proceedings of the Eighth *ASCE Specialty Conference on Probabilistic Mechanics and Structural Reliability*, PMC2000-269, 2000, pp. 1–6.
[98] S. Valliappan, T. Pham, Fuzzy finite element analysis of a foundation on an elastic soil medium, *International Journal of Numerical Analysis Methods and Geomechanics* 17 (1993) 771–789.
[99] S. Valliappan, T. Pham, Elasto-plastic finite element analysis with fuzzy parameters, *International Journal of Numerical Analysis Methods and Geomechanics* 34 (1995) 531–548.
[100] S.S. Rao, J.P. Sawyer, Fuzzy finite element approach for the analysis of imprecisely defined systems, *American Institute of Aeronautics and Astronautics Journal* 33 (1995) 2364–2370.
[101] M. Hanss, K. Willner, S. Guidati, On applying fuzzy arithmetic to finite element problems, *Proceedings of the 17th International Conference of North American Fuzzy Information Processing Society*—NAFIPAS'98, Pensacola Beach, FL, 1998, pp. 365–369.
[102] M. Hanss, K. Willner, On using fuzzy arithmetic to solve problems with uncertain model parameters, *Proceedings of Euromechanics* 405 Colloquium, Valenciennes, France, 1999, pp. 85–92.
[103] S. McWilliam, Anti-optimization of uncertain structures using interval analysis, *Computers and Structures* 79 (2001) 421–430.
[104] T.M. Wasfy, A.K. Noor, Finite element analysis of flexible multibody systems with fuzzy parameters, *Computational Methods in Applied Mechanical Engineering* 160 (1998) 223–243.
[105] T.M. Wasfy, A.K. Noor, Application of fuzzy sets to transient analysis of space structures, *Finite Elements in Analysis and Design* 29 (1998) 153–171.
[106] H. Shimizu, C. Hiroaki, Automatic FE mesh generation method for surface models, *Nippon Kikai Gakkai Ronbunshu* (Japan), Part A 59 (565) (1993) 2204–2211.
[107] B. Lallemand, A. Cherki, P. Level, Fuzzy modal finite element analysis of structures with imprecise material properties, *Journal of Sound and Vibration* 220 (1999) 353–364.
[108] G. Plessis, B. Lallemand, T. Tison, P. Level, Fuzzy modal parameters, *Journal of Sound and Vibration* 233 (2000) 797–812.
[109] A. Cherki, T. Son, T.M. Guerra, P. Level, On evaluating structures sensitivities to prescribed displacements uncertainties using fuzzy numbers, *Engineering Computations* (1997) 529–541.
[110] A. Cherki, G. Plessis, B. Lallemand, T. Tison, P. Level, Fuzzy behavior of mechanical systems with uncertain boundary conditions, *Computational Methods in Applied Mechanical Engineering* 189 (2000) 863–873.
[111] K. Handa, K. Andersson, Application of finite element methods in the statistical analysis of structures, *Proceedings of the Third International Conference of Structural Safety and Reliability*, 1981, pp. 409–417.

[112] J.H. Wang, C.M. Liou, Identification parameters of structural joints by use of noise-contaminated FRFs, *Journal of Sound and Vibration* 142 (1990) 261–277.
[113] Z. Yue, W. Guangyuan, S. Fen, The general theory for response analysis of fuzzy stochastic dynamic systems, *Fuzzy Sets and Systems* 83 (1996) 369–405.
[114] G. Cristea, Fuzzy dynamic analysis of single degree of freedom nonlinear systems, *Computers and Structures* 63 (1997) 1101–1111.
[115] K. Fansen, Y. Junui, Fuzzy dynamic response analysis of machine tool structure, *International Journal of Machine Tools Manufacturing* 39 (1999) 1993–2002.
[116] N.J. Lindsley, P.S. Beran, C.L. Pettit, Effects of uncertainty on nonlinear plate response in supersonic flow, *Ninth AIAA Symposium of Multidisciplinary Analysis and Optimization*, Atlanta, GA, Paper 2002-5600, 2002.
[117] N.J. Lindsley, P.S. Beran, C.L. Pettit, Effects of uncertainty on nonlinear plate aeroelastic response, *43rd AIAA/ASME/ASCE/AHS/ASCE Structures, Structural Dynamics, and Material Conference*, Paper No. AIAA 2002-1271, 2002.
[118] W. Eccles, Bolted joint design, *Engineering Design* 10 (1984) 10–14.
[119] R.R. Schmitt, W.J. Horn, Viscoelastic relaxation in bolted thermoplastic composite joints, *Proceedings of SAMPE Symposium and Exhibits*, Vol. 35, 1990, pp. 1336–1347.
[120] W.J. Horn, R.R. Schmitt, Relaxation in bolted thermoplastic composite joints, *AIAA/ASME/ASCE/AHS/ASCE Structures, Structural Dynamics, and Material Conference*, Part 1, 1993, pp. 485–494.
[121] Bolt Science, 1999–02, Vibration loosening of bolts and threaded fasteners, www.boltscience.com/pages/vibloose.
[122] V.H. Yost, Random Vibration and Torque Tests of Fasteners Secured with Cable, Room Temperature Vulcanized (RTV) Rubber, and Closed Cell Foam to Support the Launch of STS-82, National Aeronautics and Space Administration NASA Technical Memorandum 108539, 1997.
[123] A. Daadbin, Y.M. Chow, Theoretical models to study thread loosening, *Mechanics and Machine Theory* 27 (1992) 69–74.
[124] G.H. Junker, New criteria for self-loosening of fasteners under vibrations, Society of Automotive Engineering SAE Paper 690055, 1969, pp. 314–335.
[125] T. Sakai, The friction coefficient of fasteners, *Bulletin of Japanese Society of Mechanical Engineering* 21 (1978) 333–340.
[126] T. Sakai, T., Bolt loosening mechanisms, first report: bolts of transversely loaded joints, and second report: center bolts of twisted joints, *Bulletin of Japanese Society of Mechanical Engineering* 21 (1978) 1385–1394.
[127] T. Sakai, Investigation of bolt loosening mechanisms, third report: bolts tightened over their yield point, *Bulletin of Japanese Society of Mechanical Engineering* 22 (1979) 412–419.
[128] A. Yamamoto, S. Kasei, A solution for self-loosening mechanism of threaded fasteners under transverse vibration, *Bulletin of Japanese Society of Precession Engineering* 18 (1984) 261–266.
[129] O. Vinogradov, X. Huang, On a high frequency mechanism of self-loosening of fasteners, *Proceedings of the 12th ASME Conference of Mechanical Vibration and Noise*, Montreal, Quebec, 1989, pp. 137–145.
[130] D.P. Hess, Vibration- and shock-induced loosening, in: *Handbook of Bolts and Bolted Joints*, Mercer Dekker, New York, 1998 (Chapter 460).
[131] R.I. Zadoks, X. Yu, A preliminary study of self-loosening in bolted connections, *ASME Proceedings of the 14th Conference of Mechanical Vibration and Noise*, 1993, pp. 79–88.
[132] R.I. Zadoks, X. Yu, An investigation of the self-loosening behavior of bolts under transverse vibration, *Journal of Sound and Vibration* 208 (1997) 189–209.
[133] J.N. Goodier, R.J. Sweeney, Loosening by vibration of threaded fastenings, *Mechanical Engineering* 67 (1945) 794–800.
[134] S. Harnchoowong, Loosening of Threaded Fastenings by Vibration, Ph.D. Dissertation, University of Wisconsin-Madison, 1985.
[135] S.K. Clark, J.J. Cook, Vibratory loosening of bolts, Society of Automotive Engineering Paper No. 660432, 1966, pp. 1–10.
[136] S.C. Gambrell, Why bolts loosen? *Machine Design* 40 (1968) 163–167.
[137] R.J. Finkelston, How much shake can bolted joints take? *Machine Design* 44 (1972) 122–125.

[138] R.A. Walker, *The Factors Which Influence the Vibration Resistance of Fasteners*, Standard Pressed Steel Co., Jenkintown, PA, 1973.
[139] J.J. Kerley, *Dynamic and Static Testing of Kaynar Spiralock Microdot Nuts*, National Aeronautics and Space Administration (NASA), Goddard Space Flight Center, Engineering Services Division, Greenbelt, MA, 1984.
[140] J.J. Kerley, *An Application of Retroduction to Analyzing and Testing the Backing off of Nuts and Bolts During Dynamic Loading*, National Aeronautics and Space Administration (NASA), Technical Memorandum 4001, Goddard Space Flight Center, Greenbelt, MA, 1987.
[141] G.E. Ramey, R.C. Jenkins, Experimental analysis of thread movement in bolted connections due to vibrations, Final Report NAS8-39131, Marshall Space Flight Center, AL, 1995.
[142] D.P. Hess, K. Davis, Threaded components under axial harmonic vibration, part 1: experiments, *American Society of Mechanical Engineers, Journal of Vibration and Acoustics* 118 (1996) 417–422.
[143] D.P. Hess, Threaded components under axial harmonic vibration, part 2: kinematic analysis, *American Society of Mechanical Engineers, Journal of Vibration and Acoustics* 118 (1996) 423–429.
[144] M. Leonavicius, A. Krenevicius, Shakedown and failure of the threaded joints under low cyclic loading, *Journal of Construction Steel Research* 46 (1998) 452–453.
[145] A.K. Graham, D.P. Hess, H.M. Stephens, *Screw Loosening in an In Vitro Mid Fibular Osteotomy Model Under Dynamic Loading Conditions*, Foot and Ankle Institute, American Orthopedic Foot and Ankle Society, 2000, pp. 849–851.
[146] D.P. Hess, S.V. Sudhirkashyap, Dynamic analysis of threaded fasteners subjected to axial vibration, *Journal of Sound and Vibration* 193 (1996) 1079–1090.
[147] D.P. Hess, S.V. Sudhirkashyap, Dynamic loosening and tightening of a single-bolt assembly, *American Society of Mechanical Engineers, Journal of Vibration and Acoustics* 119 (1997) 311–316.
[148] S. Basava, D.P. Hess, Bolted joint clamping force vibration due to axial vibration, *Journal of Sound and Vibration* 210 (1998) 255–265.
[149] N.G. Pai, D.P. Hess, Experimental study of loosening of threaded fasteners due to dynamic shear loads, *Journal of Sound and Vibration* 253 (2002) 585–602.
[150] N.G. Pai, D.P. Hess, Three-dimensional finite element analysis of threaded fastener loosening due to dynamic shear load, *Engineering Failure Analysis* 9 (2002) 384–402.
[151] S. Kasai, M. Ishimura, N. Ohashi, On self-loosening of threaded joints in the case of absence of macroscopic bearing-surface sliding, *Bulletin of Japanese Society of Precision Engineering* 23 (1989) 31–36.
[152] Y. Jiang, B. Huang, H. Zhao, C.W. Lee, A study of early stage self-loosening of bolted joints, *ASME IMEC 2001 Threaded and Riveted Connections*, *Design Issues*, *Reliability*, *Stress Analysis*, *and Failure Prevention*, DE-Vol. 114, 2001, pp. 1–10.
[153] K. Koga, Loosening by repeated impact of threaded fastenings, *Bulletin of Japanese Society of Mechanical Engineering* 13 (1970) 140–149.
[154] K. Koga, H. Isono, Study on self-loosening of bolted joints taking account of characteristics of impulsive friction, *Bulletin Japanese Society of Mechanical Engineering* 29 (1986) 1004–1012.
[155] S. Kasai, H. Matsuoka, Consideration of thread loosening by transverse impacts, *American Society of Mechanical Engineers, Pressure Vessels and Piping Division PVP* 367 (1998) 117–123.
[156] S. Qiao, V.N. Pilipchuk, R.A. Ibrahim, Modeling and simulation of elastic structures with parameter uncertainties and relaxation of joints, *American Society of Mechanical Engineers, Journal of Vibration and Acoustics* 123 (2000) 45–52.
[157] M. Shinozuka, C.J. Astill, Random eigenvalue problems in structural analysis, *American Institute of Aeronautics and Astronautics Journal* 10 (1972) 456–462.
[158] J.M. Klosner, S.F. Haber, P. Voltz, Response of non-linear systems with parameter uncertainties, *International Journal of Non-linear Mechanics* 27 (1992) 547–563.
[159] R.A. Ibrahim, D.M. Beloiu, C.L. Pettit, Influence of boundary conditions relaxation on panel flutter, in press, *IUTAM Symposium on Chaotic Dynamics and Control Systems and Processes in Mechanics*, Rome, Italy, June, 2003, in press.
[160] R.A. Ibrahim, P.O. Orono, S.R. Madaboosi, Stochastic flutter of a panel subjected to random in-plane forces part 1: Two mode interaction, *American Institute of Aeronautics and Astronautics Journal* 28 (1990) 694–702.

[161] Y. Ito, M. Masuko, Study on the horizontal bending stiffness of a bolted joint, *Bulletin of Japanese Society of Mechanical Engineering* 14 (1971) 889–976.
[162] Y. Ito, A contribution to the effective range of the preload on a bolted joint, *Proceedings of the 14th International Machine Tool Design and Research Conference*, 1974, pp. 503–507.
[163] T.R. Kim, X.M. Wu, K.F. Eman, Identification of the joint parameters for a taper joint, *American Society of Mechanical Engineers, Journal of Engineering for Industry* 111 (1989) 282–287.
[164] R. Ikegami, S.M. Church, D.A. Keinholz, B.L. Fowler, Experimental characterization of deployable trusses and joints, *Workshop on Structure Control and Interaction Flexible Structures*, Marshall Space Flight Center, Huntsville, AL, 1986.
[165] J.M. Chapman, F.H. Shaw, W.C. Russell, Dynamics of trusses having nonlinear joints, *Workshop on Structure Control of Flexible Structures*, Marshall Space Flight Center, Huntsville, AL, 1986.
[166] K.L. O'Donnell, E.F. Crawley, Identification of nonlinear parameters in space structure joints using the force-state mapping technique, Space Systems Laboratory, Massachusetts Institute of Technology, Cambridge, Report 16-85, 1985.
[167] E.F. Crawley, K.J. O'Donnell, Force-state mapping identification of nonlinear joints, *American Institute of Aeronautics and Astronautics Journal* 25 (1987) 1003–1010.
[168] J.D. Collins, G.C. Hart, T.K. Hasselman, B. Kennedy, B., Statistical identification of structures, *American Institute of Aeronautics and Astronautics Journal* 12 (1974) 185–190.
[169] M.I. Friswell, J.E. Penny, Updating model parameters from frequency domain data via reduced order models, *Mechanical Systems and Signal Processing* 4 (1990) 377–391.
[170] W.J. Visser, M. Imregun, A technique to update finite element models using frequency response data, *Proceedings of the Ninth International Modal Analysis Conference*, 1991, pp. 462–468.
[171] M. Yoshimure, Measurement of dynamic rigidity and damping property of simplified joint models and simulation by computer, *Annals CIRP* 25 (1977) 193–198.
[172] M. Yoshimure, Computer design improvement of machine tool structure incorporation joint dynamics data, *Annals CIRP* 28 (1980) 241–246.
[173] M.R. Good, D.J. Marioce, Using experimental modal analysis to characterize automobile body joints and improve finite element analysis, *Proceedings of the Seventh International Modal Analysis Conference*, Las Vegas, NV, 1989, pp. 106–110.
[174] A.S. Nobari, D.A. Robb, D.J. Ewins, A new modal-based method for structural dynamic model updating and joint identification, *Proceedings of the 10th International Modal Analysis Conference*, Vol. 1, San Diego, 1992, pp. 741–750.
[175] T. Inamura, T. Sata, Stiffness and damping properties of the elements of a machine tool structure, *Annals of the CIRP 28* (1979) 235–239.
[176] J.X. Yuan, X.M. Wu, Identification of the joint structural parameters of machine tool by DDS and FEM, *American Society of Mechanical Engineers, Journal of Engineering for Industry* 107 (1985) 64–69.
[177] J.S. Tsai, Y.F. Chou, The identification of dynamic characteristics of a single bolt joint, *Journal of Sound and Vibration* 125 (1988) 487–502.
[178] J.H. Wang, P. Sas, A new method for identifying parameters of mechanical joints, *American Society of Mechanical Engineers, Journal of Applied Mechanics* 57 (1990) 337–342.
[179] Y. Ren, C.F. Beards, Identification of joint properties using FRF data, *Florence Modal Analysis Conference*, Italy, 1991, pp. 663–669.
[180] J.E. Mottershead, R. Stanway, Identification of structural vibration parameters by using a frequency domain filter, *Journal of Sound and Vibration* 109 (1986) 495–506.
[181] S.W. Hong, C.W. Lee, Identification of linearized joint structural parameters by combined use of measured and computed frequency responses, *Mechanical Systems and Signal Processing* 5 (1991) 267–277.
[182] J.H. Wang, C.M. Liou, Experimental identification of mechanical joint parameters, *Journal of Sound and Vibration* 143 (1991) 28–36.
[183] K.T. Yang, Y.S. Park, Joint structural parameter identification using a subset of frequency response function measurement, *Mechanical Systems and Signal Processing* 7 (1993) 509–530.

[184] J.R.F. Arruda, J.M.C. Santos, Model adjusting of structures with mechanical joints using modal synthesis, *Proceedings of the Seventh International Modal Analysis Conference*, Las Vegas, NV, 1989, pp. 850–856.
[185] J.R.F. Arruda, J.M.C. Santos, Mechanical joint parameter estimation using frequency response functions and component mode synthesis, *Mechanical Systems and Signal Processing* 7 (1993) 493–508.
[186] J.H. Wang, C.M. Liou, Experimental substructure synthesis with special consideration of joint effect, *International Journal of Analytical and Experimental Modal Analysis* 5 (1989) 1012.
[187] H.Y. Hwang, Identification techniques of structure connection parameters using frequency response functions, *Journal of Sound and Vibration* 212 (1998) 469–479.
[188] Y. Ren, C.F. Beards, Identification of 'effective' linear joints using coupling and joint identification techniques, *American Society of Mechanical Engineers, Journal of Vibration and Acoustics* 120 (1998) 331–338.
[189] U. Pabst, P. Hagedorn, Identification of boundary conditions as a part of model correction, *Journal of Sound and Vibration* 182 (1995) 565–575.
[190] J.E. Mottershead, M.I. Friswell, G.H.T. Ng, J.A. Brandon, Geometric parameters of finite element model updating of joints and constraints, *Mechanical Systems and Signal Processing* 10 (1996) 171–182.
[191] J.E. Mottershead, W.X. Shao, Correction of joint stiffnesses and constraints for finite element models in structural dynamics, *American Society of Mechanical Engineers, Journal of Applied Mechanics* 60 (1993) 117–122.
[192] W.L. Li, A new method for structural model updating and joint stiffness identification, *Mechanical Systems and Signal Processing* 16 (2002) 155–167.
[193] H. Ahmadian, J.E. Mottershead, M.I. Fiswell, Joint modeling for finite element model updating, *Proceedings of the 14th International Modal Analysis Conference*, Vol. 1, Dearborn, MI, 1996, pp. 591–596.
[194] U. Edlund, Mechanical Analysis of Adhesive Joints: Models and Computational Methods, Ph.D. Thesis, Linköping Institute of Technology, Sweden, 1992.
[195] J. Bonini, et al., Numerical modeling of contact for low velocity impact damage in composite laminates in: M.H. Aliabadi, et al. (Eds.), *Contact Mechanics*, CMP, 1993, pp. 453–461.
[196] M.R. Bahaari, A.N. Sherbourne 1994, Computer modeling of an extended end-plate bolted connection, *Computers and Structures* 52 (1994) 879–893.
[197] M. Burdekin, N. Back, A. Cowley, Analysis of the local deformations in machine joints, *Journal of Mechanical Engineering Science* 21 (1979) 25–32.
[198] M. Burdekin, N. Back, A. Cowley, A., Experimental study of normal and shear characteristics of mechanical surfaces in contact, *Journal of Mechanical Engineering Science* 20 (1978) 129–132.
[199] A.A. Huckelbridge, C. Lawrence, Identification of structural interface characteristics using component mode synthesis, *ASME Journal of Vibration, Acoustics, Stress, and Reliability Design* 111 (1989) 140–147.
[200] A.A. Huckelbridge, C. Lawrence, Characterization of structural connection using free and forced response test data, *ASME 12th Biennial Conference of Mechanical Vibration and Noise*, Montreal, Quebec, 1989.
[201] Y. Ren, C.F. Beards, On the importance of weighting on FRF joint identification, *Proceedings of the 11th International Modal Analysis Conference*, FL, 1993, pp. 1606–1611.
[202] Y. Ren, C.F. Beards, 1993b, On the nature of FRF joint identification techniques, *Proceedings of the 11th International Modal Analysis Conference*, FL, 1993, pp. 473–478.
[203] Y. Ren, C.F. Beards, An iterative FRF joint identification technique, *Proceedings of the 11th International Modal Analysis Conference*, FL, 1993, pp. 1133–1139.
[204] R.E.D. Bishop, The analysis and synthesis of vibrating systems, *Journal of the Royal Aeronautical Society* 58 (1954) 703–719.
[205] Y. Ren, C.F. Beards, A new multi-step two coordinate coupling technique and its application for detecting linearly-dependent coordinates, *Proceedings of the 11th International Modal Analysis Conference*, FL, 1993, pp. 872–876.
[206] Y. Ren, C.F. Beards, A new receptance-based perturbative multi-harmonic balance method for the calculation of the steady-state response of nonlinear systems, *Journal of Sound and Vibration* 172 (1994) 593–604.
[207] M. Imregun, D.A. Robb, D.J. Ewins, 1987, Structural modification and coupling dynamic analysis using measured FRF data, *Proceedings of the Fifth International Modal Analysis Conference*, London, 1987, pp. 1136–1141.

[208] M.J. Ratcliffe, N.A.J. Lieven, A generic element-based method for joint identification, *Mechanical Systems and Signal Processing* 14 (2000) 3–28.
[209] F.C. Moon, G.X. Li, Experimental study of chaotic vibration in a pin-jointed space truss structure, *American Institute of Aeronautics and Astronautics Journal* 28 (1990) 915–921.
[210] H.J. Klepp, 1994, The existence and uniqueness of solutions for the pendulum with friction, *Journal of Sound and Vibration* 175 (1994) 138–143.
[211] H.J. Klepp, The existence and uniqueness of solutions for a single-degree-of-freedom system with two friction-affected sliding joints, *Journal of Sound and Vibration* 185 (1995) 364–371.
[212] H.J. Klepp, Trial-and-error procedure for single-degree-of-freedom systems with friction-affected sliding joints, *Journal of Sound and Vibration* 191 (1996) 598–605.
[213] M.L. Tinker, Nonlinearities due to joint friction and clearance in a structural dynamic test fixture, in: A.A. Ferri, G.T. Flower, S.C. Sinha (Eds.), *ASME Proceedings of the Symposium on Elasto-Impact and Friction in Dynamic Systems*, DE-Vol. 90, 1996, pp. 35–46.
[214] K.C. Ho, K.T. Chau, 1997, An infinite plane loaded by a rivet of a different material, *International Journal of Solids and Structures* 34 (1997) 2477–2496.
[215] C.P. Chasten, et al., Prying and shear in end-plate connection design, *American Society of Civil Engineers, Journal of Structure Engineering* 118 (1992) 77–89.
[216] S. Groves, et al., Evaluation of shear joints for composite material, *Journal of Composite Material* 26 (1992) 1134–1150.
[217] N. Gebbeken, et al., Numerical analysis of endplate connections, *Journal of Construction Steel Research* 30 (1994) 177–196.
[218] S.F. Masri, T.K. Caughey, A nonparametric identification technique for nonlinear dynamic problems, *American Society of Mechanical Engineers, Journal of Applied Mechanics* 46 (1979) 433–447.
[219] S.F. Masri, H. Sassi, T.K. Caughey, Nonparametric identification of nearly arbitrary nonlinear systems, *American Society of Mechanical Engineers, Journal of Applied Mechanics* 49 (1982) 619–628.
[220] S.F. Masri, R.K. Miller, A.F. Saud, T.K. Caughey, Identification of nonlinear vibrating structures, part I: Formulation, *American Society of Mechanical Engineers, Journal of Applied Mechanics* 54 (1987) 918–922.
[221] S.F. Masri, R.K. Miller, A.F. Saud, T.K. Caughey, Identification of nonlinear vibrating structures, part II: Application, *American Society of Mechanical Engineers, Journal of Applied Mechanics* 54 (1987) 923–929.
[222] M.A. Al-Hadid, J.R. Wright, 1989, Developments in the force-state mapping technique for nonlinear systems and the extension to the location of nonlinear elements in a lumped-parameter system, *Mechanical Systems and Signal Processing* 3 (1989) 269–290.
[223] M.L. Soni, B.N. Agrawal, Damping synthesis for flexible space structures using combined experimental and analytical models, AIAA Paper 85-0779, April 1985.
[224] E.F. Crawley, A.C. Aubert, Identification of nonlinear structural elements by force-state mapping, *American Institute of Aeronautics and Astronautics Journal* 24 (1986) 155–162.
[225] W.J. Kim, Y.S. Park, Nonlinear joint parameter identification by applying the force-state mapping technique in the frequency domain, *Mechanical Systems and Signal Processing* 8 (1994) 519–529.
[226] S.S. Lee, Y.S. Park, Position of nonlinear elements and identification of their type by a local nonparametric method, *Mechanical Systems and Signal Processing* 5 (1991) 403–420.
[227] H.S. Tzou, Nonlinear joint dynamics and controls of jointed flexible structures with active and viscoelastic joint actuators, *Journal of Sound and Vibration* 143 (1990) 407–422.
[228] D.P. Hess, N.J. Wagh, 1992, Chaotic vibrations and friction at mechanical joints, in: R.A. Ibrahim, A. Soom (Eds.), *Proceedings of the ASME Symposium on Friction-Induced Vibration*, Chatter, Squeal and Chaos, DE-Vol-49, 1992, pp. 149–156.
[229] A.A. Ferri, B. Heck, Analytical investigation of damping enhancement using active and passive structural joints, *Journal of Guidance and Control Dynamics* 15 (1992) 1258–1264.
[230] L. Gaul, J. Lenz, D. Sachau, Active damping of space structures by contact pressure control in joints, *Mechanical Structures and Machines* 26 (1998) 81–100.
[231] L. Gaul, R. Nitsche, Friction control for vibration suppression, *Mechanical Systems and Signal Processing* 14 (2000) 139–150.

[232] T.M. Cameron, J.H. Griffin, An alternating frequency/time domain method for calculating the steady-state response of nonlinear dynamic systems, *American Society of Mechanical Engineers, Journal of Applied Mechanics* 56 (1989) 149–154.
[233] Y. Ren, T.M. Lim, M.K. Lim, Identification of properties of nonlinear joints using dynamic test data, *American Society of Mechanical Engineers, Journal of Vibration and Acoustics* 120 (1998) 324–330.
[234] X. Ma, L. Bergman, A. Vakakis, Identification of bolted joints through laser vibrometry, *Journal of Sound and Vibration* 246 (2001) 441–460.
[235] L. Gaul, S. Bohlen, Identification of nonlinear structural joint models and implementation in discretized structure models, *ASME Proceedings of the 11th Conference of Mechanical Vibration and Noise*, DE-Vol. 5, 1987a, pp. 213–219.
[236] L. Gaul, S. Bohlen, Vibration of structures coupled by nonlinear transfer behavior of joints; a combined computational and experimental approach, *Proceedings of the Fifth International Modal Analysis Conference*, London, 1987b, pp. 86–91.
[237] L. Gaul, U. Nackenhorst, K. Willner, J. Lenz, Nonlinear vibration damping of structures with bolted joints, *Proceedings of the 12th International Modal Analysis Conference*, 1994, pp. 875–881.
[238] J. Lenz, L. Gaul, The influence of microslip on the dynamic behavior of bolted joints, *Proceedings of the 13th International Modal Analysis Conference*, Nashville, TE, 1995.
[239] L. Gaul, J. Lenz, Nonlinear dynamics of structures assembled by bolted joints, *Acta Mechanica* 125 (1997) 169–181.
[240] S.W. Jones, P.A. Kirby, D.A. Nethercot, The analysis of frame with semi-rigid connections—a state-of-the-art report, *Journal of Construction Steel Research* 3 (1983) 2–13.
[241] W.M. Wilson, H.F. Moore, Test to determine the rigidity of riveted joints in steel structures, Bulletin 104, Urbana Illinois, Engineering Experiment Station, 1917.
[242] B. Sourochnikoff, Wind stresses in semi-rigid connections of steel framework, *American Society of Civil Engineers, Transactions* 115 (1950) 382–393.
[243] G.R. Monforton, T.S. Wu, Matrix analysis of semi-rigidly connected steel frames, *American Society of Civil Engineers, Journal of Structure Division* 90 (1963) 13–42.
[244] C.H. Yu, N.E. Shanmugam, Stability of frames with semi-rigid joints, *Computers and Structures* 23 (1986) 639–648.
[245] M.J. Frye, G.A. Morris, Analysis of flexible connected steel frames, *Canadian Journal of Civil Engineering* 2 (1975) 280–291.
[246] K.M. Ang, G.A. Morris, Analysis of three-dimensional frame with flexible beam-column connection, *Canadian Journal of Civil Engineering* 11 (1984) 241–254.
[247] B.S. Dhillon, S. Abdel-Majid, Interactive analysis and design of flexibility connected frames, *Computers and Structures* 36 (1990) 189–202.
[248] W.F. Chen, Y. Goto, J.Y.R. Liew, *Stability Design of Semi-rigid Frames*, Wiley, New York, 1996.
[249] R. Bjorhovde, A. Colson, J. Brozzetti, Classification system for beam-to-column connections, *American Society of Civil Engineers, Journal of Structure Division* 116 (1990) 3059–3076.
[250] E.M. Lui, W.F. Chen, Analysis and behavior of flexibly-jointed frames, *Engineering Structures* 8 (1986) 107–118.
[251] R. Cunningham, Some aspects of semi-rigid connections in structural steel work, *Structure Engineering* 68 (1990) 88–92.
[252] S.L. Chan, G.W.M. Ho, Nonlinear vibration analysis of steel frames with semi-rigid connections, *International Journal of Numerical Methods* 28 (1991) 2635–2650.
[253] W.F. Chen, E.M. Lui, *Stability Design of Steel Frames*, CRC Press, Boca Raton, FL, 1991.
[254] K.M. Romstad, C.V. Subramanian, Analysis of frames with partial connection rigidity, *American Society of Civil Engineers, Journal of Structures Division* 96 (1970) 2283–2300.
[255] C.W. Wong, W.H, Mak, J.M. Ko, System and parametric identification of flexible connections in steel framed structures, *Engineering Structures* 17 (1995) 581–595.
[256] F.C. Rodrigues, A.C. Saldanha, M.S. Pfeil, Nonlinear analysis of steel plane frames with semi-rigid connections, *Journal of Construction Steel Research* 46 (1998) 94–97.

[257] P.D. Moncarz, K.H. Gerstle, Steel frames with nonlinear connections, *American Society of Civil Engineers, Journal of Structure Division* 107 (1981) 1427–1441.
[258] K.S. Sivakumaran, Seismic response of multi-story steel buildings with flexible connects, *Engineering Structures* 10 (1988) 239–248.
[259] F.G.A. Al-Bermani, S. Kitiponchai, Elasto-plastic nonlinear analysis of flexibly jointed space frame, *American Society of Civil Engineers, Journal of Structural Engineering* 118 (1992) 108–127.
[260] F.G.A. Al-Bermani, B. Li, K. Zhu, S. Kitiponchai, Cyclic and seismic response of flexibility jointed frames, *Engineering Structures* 16 (1994) 249–255.
[261] K.C. Tsai, S. Wu, E.P. Popov, Cyclic performance of steel beam-column moment joints, *Engineering Structures* 17 (1995) 596–602.
[262] S.L. Chan, P.P.J. Chui, *Nonlinear Static and Cyclic Steel Frames with Semi-Rigid Connections*, Elsevier, London, 2000.
[263] W.F. Chen, E.M. Lui, Analysis and behavior of flexibly-jointed frames, *Engineering Structures* 8 (1986) 107–118.
[264] W.F. Chen, E.M. Lui, Effects of joint flexibility on the behavior of steel frames, *Computers and Structures* 26 (1987) 719–732.
[265] P. Pui, T. Chui, L.C. Siu, Vibration and deflection characteristics of semi-rigid jointed frames, *Engineering Structures* 19 (1997) 1001–1010.
[266] J.Y. Liew, W.F. Richard, D.W. Chen, Limit states design of semi-rigid frames using advanced analysis, Part 1: connection modeling and classification, *Journal of Construction Steel Research* 26 (1993) 1–27.
[267] J.Y. Liew, W.F. Richard, D.W. Chen, Limit states design of semi-rigid frames using advanced analysis, Part 2: analysis and design, *Journal of Construction Steel Research* 26 (1993) 29–57.
[268] M. Sekulovic, R. Salatic, Nonlinear analysis of frames with flexible connections, *Computers and Structures* 79 (2001) 1097–1107.
[269] R.T. Leon, Semi-rigid composite construction, *Composite Construction Steel and Concrete* 15 (1990) 585–597.
[270] R.T. Leon, Composite semi-rigid construction, *Engineering Journal* 31 (1994) 57–66.
[271] R.T. Leon, J.J. Hoffman, T. Staeger, Partially restrained composite connections, *Steel Design Guide Series* 8, AISC, Chicago, IL, 1996.
[272] T.Q. Li, B.S. Choo, D.A. Nethercot, Determination of rotation capacity requirements for steel and composite beams, *Journal of Construction Steel Research* 32 (1995) 303–332.
[273] T.Q. Li, D.A. Nethercot, B.S. Choo, Behavior of flush end-plate composite connections with unbalanced moment and variable shear/moment ratios—II: prediction of moment capacity, *Journal of Construction Steel Research* 38 (1996) 165–198.
[274] D.A. Nethercot, T.Q. Li, B.S. Choo, Required rotations and moment redistribution of composite and continuous, *Journal of Construction Steel Research* 35 (1995) 121–163.
[275] T.Q. Li, D.A. Nethercot, B.S. Choo, Behavior of flush end-plate composite connections with unbalanced moment and variable shear/moment ratios—I: experimental behavior, *Journal of Construction Steel Research* 38 (1996) 125–164.
[276] T.Q. Li, D.B. Moore, D.A. Nethercot, B.S. Choo, The experimental behavior of a full-scale, semi-rigidly connected composite frame: detailed appraisal, *Journal of Construction Steel Research* 38 (1996) 193–220.
[277] D.A. Nethercot, Semi-rigid joint action and the design of non-sway composite frames, *Engineering Structures* 17 (1995) 554–567.
[278] A. Haldar, Y. Zhou, Reliability of geometrically nonlinear PR frames, *American Society of Civil Engineers, Journal of Engineering Mechanics* 118 (1992) 2148–2155.
[279] Y. Goto, W.F. Chen, On the computer-based design analysis for the flexibility of jointed frames, *Journal of Construction Steel Research* 8 (1987) 203–231.
[280] E.M. Lui, W.F. Chen, Steel frame analysis with flexible joints, *Journal of Construction Steel Research* 8 (1987) 893–913.
[281] G.W.M. Ho, S.L. Chan, Semi-bifurcation analysis of flexibly connected steel frames, *American Society of Civil Engineers, Journal of Structure Engineering* 117 (1991) 2299–2319.
[282] G.W.M. Ho, S.L. Chan, An accurate and efficient method for large deflection analysis of frames with semi-rigid connections, *Journal of Construction and Steel Research* 26 (1993) 171–191.

[283] L. Xu, D.E. Grierson, Computer automated design of semi-rigid steel frameworks, *American Society of Civil Engineers, Journal of Structure Engineering* 119 (1993) 1740–1760.
[284] B.S. Dhillon, J.W. O'Malley, 1999, Interactive design of semi-rigid steel frames, *American Society of Civil Engineers, Journal of Structure Engineering* 125 (1999) 556–564.
[285] I. Yaghmai, D.A. Frohrib, A sensitive analysis of the effects of interconnection joint size, flexibility, and inertia on the natural frequencies of Timoshenko frames, *Journal of Sound and Vibration* 75 (1981) 329–346.
[286] J.H. Oh, Y.G. Kim, D.G. Lee, Optimum bolted joints for hybrid composite materials, *Composite Structures* 38 (1997) 329–341.
[287] S. Lionberger, W. Weaver, Dynamic response of frames with non-rigid connections, *American Society of Civil Engineers, Journal of Engineering Mechanics Division* 95 (1969) 95–114.
[288] S. Kawashima, T. Fujimoto, Vibration analysis of frames with semi-rigid connections, *Computers and Structures* 1 (1984) 85–92.
[289] S.L. Chan, Vibration and modal analysis of steel frames with semi-rigid connections, *Engineering Structures* 16 (1994) 25–31.
[290] R. Masika, L. Dunai, Behavior of bolted end-plate portal frame joints, *Journal of Construction Steel Research* 32 (1995) 207–225.
[291] L.E. Suarez, M.P. Singh, E.E. Matheu, Seismic response of structural frameworks with flexible connects, *Computers and Structures* 58 (1996) 27–41.
[292] E.M. Lui, A. Lopes, Dynamic analysis and response of semirigid frames, *Engineering Structures* 19 (1997) 644–654.
[293] S.Y. Hsu, A. Fafitis, 1992, Seismic analysis design of frames with viscoelastic connections, *American Society of Civil Engineers, Journal of Structure Division* 118 (1992) 2459–2474.
[294] Y.L. Xu, W.S. Zhang, Modal analysis and seismic response of steel frames with connection dampers, *Engineering Structures* 23 (2001) 385–396.
[295] G. Shi, S.N. Atluri, Static and dynamic analysis of space frames with nonlinear flexible connections, *International Journal of Numerical Methods in Engineering* 28 (1989) 2635–2650.
[296] L. Gao, A. Haldar, Nonlinear seismic analysis of space structures with partially restrained connections, *Microcomputers in Civil Engineering* 10 (1995) 27–37.
[297] A. Reyes-Salzar, A. Haldar, Non-linear seismic response of steel structures with semi-rigid and composite connections, *Journal of Construction Steel Research* 51 (1999) 37–59.
[298] P.M. Frank, *Introduction to System Sensitivity Theory*, Academic Press, New York, 1978.
[299] R.L. Fox, M.P. Kapoor, Rates of change of eigenvalues and eigenvectors, *American Institute of Aeronautics and Astronautics Journal* 6 (1968) 2426–2429.
[300] L.A. Kiefling, Comment on 'The eigenvalue problem for structural systems with statistical properties', *American Institute of Aeronautics and Astronautics Journal* 8 (1970) 1371–1372.
[301] A.G. Nalecz, J. Wicher, 1988, Design sensitivity analysis of mechanical systems in frequency domain, *Journal of Sound and Vibration* 120 (1988) 517.
[302] R.S. Sharp, P.C. Brooks, Sensitivities on frequency response function of linear dynamic systems to variations in design parameter values, *Journal of Sound and Vibration* 126 (1988) 167.
[303] L.C. Rogers, Derivatives of eigenvalues and eigenvectors, *American Institute of Aeronautics and Astronautics Journal* 8 (1970) 943–944.
[304] R.H. Plaut, K. Huseyin, Derivatives of eigenvalues and eigenvectors in non-self-adjoint systems, *American Institute of Aeronautics and Astronautics Journal* 11 (1973) 250–251.
[305] C.S. Rudisill, Derivatives of eigenvalues and eigenvectors for a general matrix, *American Institute of Aeronautics and Astronautics Journal* 12 (1974) 721–722.
[306] C.C. Baniotopolos, K.M. Abdalla, Sensitivity analysis results on the separation problem of bolted steel column-to-column connections, *International Journal of Solids and Structures* 32 (1995) 251–265.
[307] L. Socha, The sensitivity analysis of stochastic nonlinear dynamical systems, *Journal of Sound and Vibration* 110 (1986) 271–296.
[308] G. Juhn, G.D. Manolis, Stochastic sensitivity and uncertainty of secondary systems in base-isolated structures, *Journal of Sound and Vibration* 159 (1992) 207.

[309] T.D. Hien, M. Klieber, Stochastic design sensitivity in structural dynamics, *International Journal of Numerical Methods in Engineering* 32 (1991) 1247–1265.
[310] C.D. Huang, T.T. Soong, Stochastic sensitivity analysis of nonlinear primary-secondary structural systems, *Engineering Structures* 16 (1994) 91–96.
[311] C.D. Huang, L. Socha, T.T. Soong, Stochastic sensitivity analysis of nonlinear primary-secondary structural systems, *Engineering Structures* 15 (1993) 135–142.
[312] A. Der Kiureghian, J.B. Ke, The stochastic finite element method in structural reliability, *Probabilistic Engineering Mechanics* 3 (1988) 83–91.
[313] S. Mahadevan, A. Haldar, Efficient algorithm for stochastic structural optimization, *American Society of Civil Engineers, Journal of Structure Division* 115 (1989) 1579–1598.
[314] P. Cacciola, P. Colajanni, G. Muscolino, Stochastic sensitivity of steel frames with connection dampers by modal analysis, *Proceedings of the 20th International Modal Analysis Conference*, Vol. 1, 2002, pp. 127–133.
[315] S. Benfratello, S. Caddemi, G. Muscolino, Gaussian and non-Gaussian stochastic sensitivity analysis of discrete structural systems, *Computers and Structures* 78 (2000) 425–434.
[316] G. Muscolino, Dynamically modified linear structures: Deterministic and stochastic response, *American Society of Civil Engineers, Journal of Engineering Mechanics Division* 122 (1996) 1044–1051.
[317] R.A. Ibrahim, *Parametric Random Vibration*, John Wiley, New York, 1985.
[318] C. Petersen, Tragfähigkeit imperfektionsbehafteter geschraubter Ringflansch-verbindungen, *Stahlbau* 59 (1990) 97–104.
[319] H. Schmidt, Th.A. Winterstetter, M. Kramer, Nonlinear elastic behavior of imperfect, eccentrically tensioned L-flange ring joints with pre-stressed bolts as basis for fatigue design, CD ROM, *Proceedings of European Conference on Computational Mechanics*, Munich, Germany, 1999.
[320] C. Bucher, M. Ebert, Load carrying behavior of pre-stressed bolted steel flanges considering random geometrical imperfections, *Proceedings of the Eighth ASCE Specialty Conference on Probabilistic Mechanics and Structural Reliability*, PMC2000-185, 2000.
[321] T. Sawa, T. Morohoshi, A. Shimizu, An analysis of circular bolted flanged joints on solid round bars subjected to external bending moments, *ASME Proceedings of Reliability Stress Analysis and Failure Prevention Issues*, DE-Vol. 110, 2000, pp. 109–118.
[322] H. Zhao, Analysis of the load distribution in a bolt-nut connector, *Computers and Structures* 53 (1994) 1465–1472.
[323] A. Taniguchi, M. Tsutsumi, Y. Ito, A treatment of a contact surface in structural analyses (part 1, an expression for contact stiffness and some numerical results by using its expression), *Transactions of the Japanese Society of Mechanical Engineering* 49 (1983) 1282–1288.
[324] I.R. Grosse, L.D. Mitchell, Nonlinear axial stiffness characteristics of axisymmetric bolted joints, *American Society of Mechanical Engineers, Journal of Mechanical Design* 112 (1990) 442–449.
[325] J. Wileman, M. Choudry, I. Green, Computation of member stiffness in bolted connections, *American Society of Mechanical Engineers, Journal of Mechanical Design* 113 (1991) 432–437.
[326] A. Chaaban, M. Jutras, Static analysis of buttress threads using the finite element method, *American Society of Mechanical Engineers, Journal of Pressure Vessel Technology* 114 (1992) 209–212.
[327] A. Chaaban, U. Muzzo, On the design of threaded-end closures for high pressure vessels, *American Society of Mechanical Engineers, Pressure Vessel Piping Conference*, Denver, PVP263, 1993, pp. 59–65.
[328] T.F. Lenhoff, K.I. Ko, M.L. McKay, Member stiffness and contact pressure distribution of bolted joints, *American Society of Mechanical Engineers, Journal of Mechanical Design* 116 (1994) 550–557.
[329] T.F. Lenhoff, W.E. Wistehuff, Nonlinear effects on the stiffness of bolted joints, *American Society of Mechanical Engineers, Journal of Pressure Vessel Technology* 118 (1994) 48–53.
[330] T.F. Lenhoff, B.A. Bunyard, Effects of bolt threads on the stiffness of bolted joints, *American Society of Mechanical Engineers, Journal of Pressure Vessel Technology* 123 (2001) 161–165.
[331] R.L. Norton, *Machine Design: An Integrated Approach*, Prentice-Hall, Englewood Cliffs, NJ, 1996.
[332] M.B. Karamis, B. Selcuk, Analysis of the friction behavior of bolted joints, *Wear* 166 (1993) 73–83.
[333] E. Niisato, A. Fujii, T. Nakaho, M. Tsuboi, 1997, Effect of surface roughness on fastening performance of bolted joints, *Journal of Society of Automotive Engineering Review* 18 (1997) 200–212.

[334] E. Dragoni, Effect of thread pitch and frictional coefficient on the stress concentration in metric nut-bolt connections, *American Society of Mechanical Engineers, Journal of offshore Mechanics and Arctic Engineering* 116 (1994) 21–27.
[335] T.A. Duffey, Optimal bolt preload for dynamic loading, *International Journal of Mechanical Sciences* 35 (1993) 257–265.
[336] E. Esmailzadeh, M. Chorashi, Optimal design of pre-loaded joints under dynamic loadings, *Proceedings of the Eighth International Conference on Pressure Vessel Technology*, Vol. 2, 1996, pp. 7–13.
[337] E. Esmailzadeh, M. Chorashi, A.R. Ohadi, Analysis of pre-loaded bolted joints under exponential decaying pressure, *ASME Journal of Pressure Vessel Technology* 118 (1996) 393–398.
[338] Y. Dong, D.P. Hess, Optimum placement of bolts in structures based on dynamic shear, *Journal of Sound and Vibration* 217 (1998) 396–404.
[339] Y. Dong, D.P. Hess, Accelerated vibration life tests of thread-locking adhesive, *Journal of Aircraft* 35 (1998) 816–820.
[340] I.A. Rashquinha D.P. Hess, Modeling nonlinear dynamics of bolted assemblies, *Applied Mathematics and Modeling* 21 (1997) 801–810.
[341] F.M. Leon, N.G. Pai, D.P. Hess, The effect of thread dimensional conformance on yield and tensile strength, *Engineering Failure Analysis* 8 (2001) 49–56.
[342] Y. Dong, D.P. Hess, The effect of dimensional conformance on vibration-induced loosening, *American Society of Mechanical Engineers, Journal of Vibration and Acoustics* 121 (1999) 209–213.
[343] B. Lincoln, K.J. Gomes, J.F. Braden, *Mechanical Fastening of Plastics*, Marcel Dekker, Inc., New York, 1984.
[344] G. Verchery (Ed.), *Mechanical Behavior of Adhesive Joints*, Pluralis, 1987.
[345] J.R. Vinson, Mechanical fastening of polymer composites, *Polymer Engineering Science* 29 (1989) 1332–1339.
[346] D.Y. Hwang, Finite Element Analysis of High Pressure Bolted Flange Connections, Ph.D. Thesis, Auburn University, 1992.
[347] N. Rastogi, B.P. Deepak, S.R. Soni, Stress analysis codes for bonded joints in composite structures, *Proceedings of the AIAA/ASME/ASCE/AHS/ASCE Structures, Structural Dynamics, and Material Conference*, Vol. 4, 1997, pp. 2772–2782.
[348] N. Rastogi, M. Xie, S.R. Soni, Strength prediction codes for bolted joints in composite structures, *Proceedings of the AIAA/ASME/ASCE/AHS/ASCE Structures, Structural Dynamics, and Material Conference*, Vol. 2, 1997, pp. 1088–1098.
[349] N. Rastogi, S.R. Soni, A. Nagar, A combined analytical and experimental study of design parameters in composite bonded joints, *Proceedings of the 39th AIAA/ASME/ASCE/AHS/ASCE Structures, Structural Dynamics, and Material Conference*, Part 2, 1998, pp. 1567–1577.
[350] M.K. Apalak, R. Davies, 1993, Analysis and design of adhesively bonded corner joints, *International Journal of Adhesion and Adhesives* 13 (1993) 219–235.
[351] R.J. Lee, J.C. McCarthy, An overview of the composite-to-metal jointing project, *Advances in Joint Plastics and Composites*, Bradford, 1991, pp. 61–70.
[352] A.O. Ogunjimi, et al., Thermal stress analysis of conductive adhesive joints, *Proceedings of the 14th Japanese International Electronic Manufacturing Technical Symposium*, Kanazawa, IEEE, 1993, pp. 349–353.
[353] L.E. Bailey, J.C. Roberts, D.L. Jones, Optimal design parameters for thermal and mechanical performance of a metal/composite joint, *Proceedings of American Society of Composites*, 1995, pp. 428–437.
[354] L.E. Bailey, J.C. Roberts, D.L. Jones, Selection of critical thermal/structural design parameters for a metal/composite joint in a composite electronics enclosure, *Journal of Thermoplastic Composite Materials* 10 (1997) 362–380.
[355] J.H. Hermann, R.E. Martin, D.G. Mandic, 1999, Thermoelastic stress analysis of a pultruded composite double lap joint, *Proceedings of the SPIE—International Society of Optical Engineering* 3585 (1999) 68–70.
[356] J.T. Wang, A. Banbury, D.W. Kelly, Evaluation of approaches for determining design allowable for bolted joints in laminated composites, *Composite Structures* 41 (1998) 167–176.
[357] R.D. Adams, V. Mallick, Method for the stress analysis of lap joints, *Journal of Adhesion* 38 (1992) 199–217.
[358] E. Madenci, L. Ileri, Analytical determination of contact stresses in mechanically fastened composite laminates with finite boundaries, *International Journal of Solids and Structures* 30 (1993) 2469–2484.

[359] K. Nono, et al., Stress analysis of asymmetric single lap joints, *Japanese Society of Mechanical Engineering, Series A* 59 (1993) 646–653.
[360] T. Sawa, et al., Elasto-plastic finite element analysis of single-lap adhesive joints subjected to tensile shear loads, *Transactions of the Japanese Society of Mechanical Engineering, Series A* 59 (1993) 1881–1887.
[361] C. Yang, Stress-Strain Analysis of Adhesive-Bonded Composite Single-Lap Joints under Various Loadings, Ph.D. Thesis, Louisiana State University, 1993.
[362] O.H. Griffin Jr., M.W. Hyer, D. Cohen, M.J. Shuart, S.R. Yalamanchili, C.B. Prasad, Analysis of multi-fastener composite joints, *Journal of Spacecraft and Rockets* 31 (1994) 278–284.
[363] M. Hildebrand, Nonlinear analysis and optimization of adhesively bonded single lap joints between fiber-reinforced plastics and metals, *International Journal of Adhesion and Adhesives* 14 (1994) 261–267.
[364] J.L. Oakeshott, F.L. Matthews, Determination of fastener load distribution in double lap composite joints, *American Society of Mechanical Engineers, Petroleum Division* PD-64(2) (1994) 243–251.
[365] Z. MeiYing, Y. Ling, W. XiaoPeng, Load distribution in composite multi-fastener joints, *Computers and Structures* 60 (1996) 337–342.
[366] E. Madenci, L. Ileri, J.H. Starnes Jr., Analysis of pin-loaded holes in composite laminates under combined bearing-bypass and shear loading, *International Journal of Solids and Structures* 32 (1995) 2053–2062.
[367] E. Madenci, S. Shkarayev, B. Sergeev, D.W. Oplinger, P. Shyprykevich, Analysis of composite laminates with multiple fasteners, *International Journal of Solids and Structures* 35 (1998) 1793–1811.
[368] M. Elsley, et al., Analysis of highly loaded bonded joints for thin skins, *Proceedings of the Fifth Australian Aeronautical Conference*, Melbourne, 1993, pp. 96–100.
[369] N.S. Prasad, et al., Stress distribution in interference joints, *Computers and Structures* 51 (1994) 535–540.
[370] Z. Prabhakaran, Z. Razzaq, S. Devara, Load and resistance factor design (LRFD) approach for bolted joints in pultruded composites, *Composites Part B: Engineering* 27 (1995) 351–360.
[371] H. Hamada, K. Haruna, Z. Maekawa, Effects of stacking sequences on mechanically fastened joint strength in quasi-isotropic carbon-epoxy laminates, *Journal of Composite Technology and Research* 17 (1995) 249–259.
[372] H. Hamada, Z. Maekawa, K. Haruna, Strength prediction of mechanically fastened quasi-isotropic carbon/epoxy joints, *Journal of Composite Material* 30 (1996) 1596–1612.
[373] T. Ireman, Three-dimensional stress analysis of bolted single-lap composite joints, *Composite Structures* 43 (1998) 195–216.
[374] P.F. Packman, H.J. Hietala, K.C. Schulz, Experimental and statistical analysis of some fastener anomalies on the bolted joint strength of graphite/epoxy laminates, *Proceedings of SAMPE Symposium and Exhibition*, Vol. 38, 1993, pp. 66–80.
[375] K.C. Schulz, H.J. Hietala, P.F. Packman, A statistical approach to the analysis of ultimate strengths of bolted joints in laminated composites, *Composites Science and Technology* 56 (1996) 505–517.
[376] W.H. Lin, M.H.R. Jen, Strength of bolted and bonded single-lapped composite joints in tension, *Journal of Composite Materials* 33 (1999) 640–666.
[377] R.M. Jones, *Mechanics of Composite Materials*, Hemisphere Publishing, New York, 1975.
[378] L.J. Hart-Smith, Mechanically fastened joints for advanced composites, *Phenomenological Considerations and Simple Analysis*, McDonnel Douglas Corporation DO6748A, 1978.
[379] A.O. Ankara, P.G. Dara, Optimization of composite bolted joint design, *Proceedings of Computer Aided Design in Composite Material Technology*, CADCOMP Computational Mechanics Publication 347, 1994.
[380] A.O. Ankara, P.G. Dara, Computer modeling of mechanical joints in advanced composites, *Proceedings of the ASME Petroleum Division* PD64, 1994, pp. 175–180.
[381] W.S. Arnold, I.H. Marshal, J. Wood, Optimum design considerations for mechanically fastened composite joints, *Composite Structures* 16 (1990) 85–101.
[382] T. Ireman, T. Nyman, K. Hellborn, On design methods for bolted joints in composite aircraft structures, *Composite Structures* 25 (1993) 567–578.
[383] B.D. Snyder, J.G. Burns, V.B. Venkayya, Composite bolted joints analysis programs, *Journal of Composites Technology Research* 12 (1990) 41–51.
[384] J.S. Shih, Experimental–Numerical Analysis of Bolted Joints in Finite Composites with and without Inserts, Ph.D. Thesis, University of Wisconsin-Madison, 1992.

[385] B. Skalerud, Yield surface formulations for eccentrically loaded planar bolted or welded connects, *Computers and Structures* 48 (1992) 811–818.
[386] N. Gattesco, Strength and local deformability of wood beneath bolted connectors, *American Society of Civil Engineers, Journal of Structure Engineering* 124 (1998) 195–202.
[387] D.M. Running, J.B. Ligon, I. Miskioglu, Fastener design for transversely loaded composite plates, *Journal of Composite Materials* 33 (1999) 928–940.
[388] C.N. Rosner, S.H. Rizkalla, Bolted connections for fiber-reinforced composite structural members: Experimental program, *American Society of Civil Engineers, Journal of Materials in Civil Engineering* 7 (1995) 223–231.
[389] C.N. Rosner, S.H. Rizkalla, Bolted connections for fiber-reinforced composite structural members: Analytical model and design recommendations, *American Society of Civil Engineers, Journal of Materials in Civil Engineering* 7 (1995) 232–238.
[390] L. Yang, L.Y. Ye, Study of the behavior of a composite multi-bolt joint, *Computers and Structures* 34 (1990) 493–497.
[391] X. Wan, L. Yang, Effect of joint parameters, patterns and interference on the bolt loading in composite multi-bolt joints, *International Conference of Composite Structures*, 1991, p. 519.
[392] M.U. Rahman, R.E. Rowlands, Finite element analysis of multiple-bolted joints in orthotropic plates, *Computers and Structures* 46 (1993) 859–867.
[393] I. Eriksson, J. Backlund, P. Moller, 1995, Design of multiple-row bolted composite joints under general in-plane loading, *Composite Engineering* 5 (1995) 1051–1068.
[394] B. Sergeev, E. Madenci, D.R. Ambur, Influence of bolt spacing and degree of laminate anisotropy in single-lap joints, *NATO Advances Study Institute: Mechanics of Composite Material Structures*, Troia, Portugal, 3, 1998, pp. 167–193.
[395] S. Chutima, A.P. Blackie, Effect of pitch distance, row spacing, end distance and bolt diameter on multi-fastened composite joints, *Composites, Part A: Applied Science and Manufacturing* 27 (1996) 105–110.
[396] P.P. Camanho, F.L. Matthews, Stress analysis and strength prediction of mechanically fastened joints in FRP: A review, *Composites, Part A: Applied Science and Manufacturing* 28A (1997) 529–547.
[397] S. Sotiropoulos, H.V.S. GangaRao, R. Lopez-Anido, Evaluation of FRP composites bolted and adhesive joints, *Proceedings of Material Engineering Conference*, Vol. 1, 1996, pp. 233–242.
[398] P.P. Camanho, S. Bowron, F.L. Matthews, Failure mechanisms in bolted CFRP, *Journal of Reinforced Plastics and Composites* 17 (1998) 205–233.
[399] P.P. Camanho, F.L. Matthews, Delamination onset prediction in mechanically fastened joints in composite laminates, *Journal of Composite Materials* 33 (1999) 906–927.
[400] W.C. Wang, Y.M. Sheu, Stress analysis of bolted joints in CFRP laminates by half-fringe birefringent-coating technique, *Composite Structures* 34 (1996) 91–100.
[401] N.K. Hassan, C.N. Rosner, S.H. Rizkalla, Bolted connections for GFRP laminated structural members, *Proceedings of Material Engineering Conference*, Vol. 804, 1994, pp. 1018–1025.
[402] N.K. Hassan, M.A. Mohamedien, S.H. Rizkalla, Rational model for multibolted connections for GFRP members, *Journal of Composite Construction* 1 (1997) 71–78.
[403] N.K. Hassan, M.A. Mohamedien, S.H. Rizkalla, Multibolted joints for GFRP structural members, *Journal of Composite Construction* 1 (1997) 3–9.
[404] N. Andreasson, C.P. Mackinlay, C. Soutis, Experimental and numerical failure analysis of bolted joints in CFRP woven laminates, *Aeronautical Journal* 102 (1998) 445–450.
[405] J.M. Menendez, J.A. Guemes, 1999, Strain measurements inside thick CFRP laminates at the vicinity of bolted joints *Proceedings of SPIE—International Society of Optical Engineering* 3670 (1999) 184–194.
[406] Q.M. Li, R.A.W. Mines, R.S. Birch, Static and dynamic behavior of composite riveted joints in tension, *International Journal of Mechanical Science* 43 (2001) 1591–1610.
[407] W.J. Horn, Influence of clamp-up force on the strength of bolted composite joints, *American Institute of Aeronautics and Astronautics Journal* 32 (1994) 665–667.
[408] C.L. Hung, Response of Mechanically Fastened Composite Joints under Multiple Bypass Loads, Ph.D. Thesis, Stanford University, 1994.

[409] C.L. Hung, Y. Yan, F.K. Chang, Strength envelope of bolted composite joints under multi-axial bypass loads, *AIAA/ASME/ASCE/AHS/ASCE Structures, Structural Dynamics, and Material Conference*, 1994, pp. 2298–2307.
[410] C.L. Hung, F.K. Chang, Bearing failure of bolted composite joints. Part II: model and verification, *Journal of Composite Materials* 30 (1996) 1359–1400.
[411] C.L. Hung, F.K. Chang, Strength envelope of bolted composite joints under bypass loads, *Journal of Composite Materials* 30 (1996) 1402–1435.
[412] Y. Yan, W.D. Wen, F.K. Chang, P. Shyprykevich, Experimental study on clamping effects on the tensile strength of composite plates with a bolt-filled hole, *Composites—Part A: Applied Science and Manufacturing* 30 (1999) 1215–1229.
[413] M.A. Erki, et al., Design of glass-fiber reinforced plastic bolted connections, *Microcomposite in Civil Engineering* 8 (1993) 367–376.
[414] P. Lazzarin, V. Milani, M. Quaresimin, Scatter bands summarizing the fatigue strength of aluminum alloy bolted joints, *International Journal of Fatigue* 19 (1997) 401–407.
[415] B. Atzori, P. Lazzarin, M. Quaresimin, A re-analysis on fatigue data of aluminum alloy bolted joints, *International Journal of Fatigue* 19 (1997) 579–588.
[416] R.S. Birch, M. Alves, Dynamic failure of structural joint systems, *Thin-Walled Structures* 36 (2000) 137–154.
[417] J. Bolton, Design consideration for high temperature bolting, in: *Performance of Bolting Materials in High Temperature Plant Applications*, The Institute of Materials, London, UK, 1995, pp. 1–14.
[418] M.B.H. Mantelli, M.M. Yovanovich, Compact analytical model for overall thermal resistance of bolted joints, *International Journal of Heat Mass Transfer* 41 (1998) 1255–1266.
[419] T. Fukuoka, Q. Xu, K. Yoshida, Numerical analysis of the mechanical behaviors of bolted joint under thermal load *ASME Proceedings of Reliability, Stress Analysis, and Failure Prevention Issues*, DE-Vol. 110, 2000, pp. 127–132.
[420] F.V. Ellis, D.R. Sielski, R. Viswanathan, An improved analytical method for life prediction of bolting, *American Society of Mechanical Engineers, Journal of Pressure Vessel Technology* 123 (2001) 70–74.
[421] J. Schive, The Fatigue Strength of Riveted Joints and Lugs, National Advisory Committee for Aeronautics NACA TM 1395, 1956.
[422] V. Seliger, Effect of Rivet Pitch Upon the Fatigue Strength of Single-Row Riveted Joints of 0.025 to 0.025-inch 24S-T ALCLAD, National Advisory Committee for Aeronautics NACA TN 900, 1943.
[423] K. Iyer, G.T. Hahn, P.C. Bastias, C.A. Rubin, Analysis and fretting in pinned connections, *Wear* 181 (1995) 524–530.
[424] K. Iyer, C.A. Rubin, G.T. Hahn, Three-dimensional analysis of single rivet-row lap joints—part I: elastic response, Recent Advances in Solids and Structures, *ASME Pressure Vessels and Piping* PVP-Vol. 398, 1999, pp. 23–40.
[425] T.N. Farris, A.F. Grandt Jr., G. Harish, H.L. Wang, Analysis of widespread fatigue damage in structural joints, *Proceedings of the 41st International SAMPE Symposium and Exhibition*, 1996, pp. 65–79.
[426] G. Harish, T.N. Farris, Effect of fretting contact stress on crack nucleation in riveted lap joints, *Proceedings of the 39th AIAA/ASME/ASCE/AHS/ASCE Structures, Structural Dynamics, and Material Conference*, Part 1, 1998, pp. 383–391.
[427] B. Langrand, E. Deletombe, E. Markiewics, P. Drazetic, Riveted joint modeling for numerical analysis of airframe crashworthiness, *Finite Elements in Analysis and Design* 38 (2001) 21–44.
[428] H. Terada, A study on fundamental damage tolerant testing methods, durability of metal aircraft structures, *Proceedings of the International Workshop on Structural Integrity of Aging Airplanes*, Atlanta, 1992, pp. 472–482.
[429] H. Terada, A proposal on damage tolerant testing for structure integrity of aging aircraft—learning from Jal accident in 1985, *Fracture Mechanics*, Vol. 25, ASTM STP 1220, 1995, pp. 557–574.
[430] H. Terada, Structural fatigue and joint degradation, *International Journal of Fatigue* 23 (2001) S21–S30.
[431] H. Terada, T. Okada, Problems of mechanics in structural integrity of aging aircraft safety, *Proceedings of the International Workshop on Technical Elements for Aviation Safety*, Tokyo, 1999, pp. 150–157.
[432] H. Terada, T. Okada, Fatigue test of fuselage scale model under simulated service loading, *NAL Research Progress*, 2000, pp. 44–45.

[433] S. Furuta, H. Terada, H. Sashikuma, Fatigue strength of fuselage joint structure under ambient and corrosive environment, *Proceedings of the 19th Symposium of ICAF*, Vol. 1, 1997, pp. 231–249.
[434] L. Mordfin, Creep and creep-rupture characteristics of some riveted and spot-welded lap joints of aircraft materials, National Advisory Committee for Aeronautics NACA TN 3412, 1955.
[435] L. Mordfin, A.C. Legate, Creep behavior of structural joints of aircraft materials under constant loads and temperatures, National Advisory Committee for Aeronautics NACA TN 3842, 1957.
[436] M.E. Barzelay, G.F. Holloway, Effect of an interface on transient temperature distribution in composite aircraft joints, National Advisory Committee for Aeronautics NACA TN 3824, 1957.
[437] M.E. Barzelay, G.F. Holloway, Interface of thermal conductance of twenty-seven riveted aircraft joints, National Advisory Committee for Aeronautics NACA TN 3991, 1957.
[438] R.J. Wright, W.S. Johnson, Effect of thermal aging on the bolt bearing behavior of highly loaded composite joints, *Proceedings of the American Society of Composites* 709 (1996) 1076–1085.
[439] Y.J. Chiang, R.E. Rowlands, Finite element analysis of mixed-mode fracture of bolted composite joints, *Journal of Composite Technological Research* 13 (1991) 227–235.
[440] L.F.M. Silva, J.P.M. Goncalves, F.M.F. Olveira, P.M.S.T. de Castro, Multiple-site damage in riveted lap-joints: experimental simulation and finite element prediction, *International Journal of Fatigue* 22 (2000) 319–338.
[441] J.L. Beuth, J.W. Hutchinson, Fracture analysis of multi-site cracking in fuselage lap joints, *Computational Mechanics* 13 (1994) 315–331.
[442] R.P.G. Müller, An Experimental and Analytical Investigation on the Fatigue Behavior of Fuselage Lap Joints, Ph.D. Thesis, Delft University of Technology, The Netherlands, 1995.
[443] R. Piascik, S. Willard, Characterization of multi-site damage in fuselage structure, *Proceedings of the First Joint DoD/FAA/NASA Conference on Aging Aircraft*, Ogden, UT, 1997.
[444] G. Harish, M.P. Szolwinski, T.N. Farris, Finite element modeling of rivet installation and riveted joints for prediction of fretting crack nucleation, *Proceedings of the First Joint DoD/FAA/NASA Conference on Aging Aircraft*, Ogden, Utah, 1997.
[445] J.N. Dickson, T.M. Hsu, J.M. McKinney, *Development of an Understanding of the Fatigue Phenomena of Bonded and Bolted Joints in Advanced Filamentary Composite Materials*, AFFDL-TR-72-64, Vols. I & II, Air Force Flight Dynamics Laboratory, Wright-Patterson Air Force Base, OH, 1972.
[446] K.C. Schulz, H.J. Hietala, P.F. Packman, Statistical analysis of bushing, sleeve, and oversize hole effects on the bolted joint strength of graphite/epoxy laminates, *American Society for Testing Materials, Journal of Composites Technology and Research* 17 (1995) 17–32.
[447] K.C. Schulz, P.E. Packman, J.R. Eisenmann, Tension-mode fracture model for bolted joints in laminated composites, *Journal of Composite Materials* 29 (1995) 37–58.
[448] Y.J. Chiang, R.E. Rowlands, Finite element analysis of mixed-mode fracture of bolted composite joints, *Journal of Composite Technological Research* 13 (1991) 227–235.
[449] H.S. Wang, C.L. Hung, F.K. Chang, Bearing failure of bolted composite joints. Part I: experimental characterization, *Journal of Composite Materials* 30 (1996) 1284–1313.
[450] M.S. Forte, J.M. Whitney, N.J. Pagano, 1998, Influence of adhesive reinforcement on the mode I fracture toughness of a bonded joint, *Proceedings of the 39th AIAA/ASME/ASCE/AHS/ASCE Structures, Structural Dynamics, and Materials Conference*, Part II, pp. 1605–1615.
[451] M.D. Gilchrist, R.A. Smith, Development of cohesive fatigue cracks in t-peel joints, *International Journal of Adhesion and Adhesives* 13 (1993) 53–57.
[452] M.D. Gilchrist, R.A. Smith, Fatigue growth of cohesive defects in t-peel joints, *Journal of Adhesion* 42 (1993) 179–190.
[453] N. Su, R.I. Mackie, Two-dimensional creep analysis of structural adhesive joints, *International Journal of Adhesion and Adhesives* 13 (1993) 33–40.
[454] A.E. Bogdanovich, I. Kizhakkethara, Three-dimensional finite element analysis of adhesively bonded plates, *Proceedings of the 38th AIAA/ASME/ASCE/AHS/ASC Structures, Structural Dynamics, and Materials Conference*, April 7–10, Kissimmee, FL, 1997, pp. 1984–1993.
[455] S.L. Donaldson, A.K. Roy, Experimental studies on composite bonded joints, *Proceedings of the 11th International Conference of Composite Material* (ICCM-11), Australia, 14–18 July, 1997.

[456] A.K. Roy, S.L. Donaldson, Experimental investigation of crack-front profile in bonded composite materials, *Proceedings of ASME WAM IMECE*, Dallas, 1997.
[457] A.K. Roy, S.L. Donaldson, G.A. Schoeppner, Bonded joints of unidirectional and cross-ply laminates: an experimental study, *Proceedings of the 38th AIAA/ASME/ASCE/AHS/ASCE Structures, Structural Dynamics, and Materials Conference*, Kissimmee, FL, 1997.
[458] G.A. Schoeppner, A.K. Roy, S.L. Donaldson, Damage progression in bonded composite double-lap joints, *AIAA/ASME/ASCE/AHS/ASCE Structures, Structural Dynamics, and Materials Conference*, Part 2, 1998, pp. 1594–1604.
[459] C.L. Chow, T.J. Lu, Analysis of failure properties and strength of structural adhesive joints with damage mechanics, *International Journal of Damage Mechanics* 1 (1992) 404–434.
[460] F.C. Edde, Fatigue des Joints Colles Structuraux, Ph.D. Thesis, Ecole Polytech, Canada, 1992.
[461] F.C. Edde, Y. Verreman, On the fracture parameters in a clamped cracked lap shear adhesive joint, *International Journal of Adhesion and Adhesives* 12 (1992) 43–48.
[462] G. Fernlund, et al., Fracture load predictions for adhesive joints, *Computer Science and Technology* 51 (1994) 587–600.
[463] A.P. Assanelli, E.N. Dvorkin, Finite element models of OCTG threaded connections, *Computers and Structures* 46 (1993) 725–734.
[464] L. Dorn, N. Salem, FEM calculations of plastic–metal adhesive joints: a way of describing the state of stressing in the adhesion zone as a function of the time, *Adhesion* 37 (1993) 34–38.
[465] H.I. Epstein, F.S. Gulia, Finite element studies of bolt stagger effects in tension members, *Computers and Structures* 48 (1993) 1153–1156.
[466] A.M. Hoor, et al., Developments in finite element analysis of single bolted timber joints, in: S. Valiappan (Ed.), *Composite Mechanics: Concrete Composites*, Balkema, Rotterdam, 1993, pp. 745–750.
[467] C.C. Lin, C.H. Lin, Stress and strength analysis of composite joints using direct boundary element method, *Composite Structures* 25 (1993) 209–215.
[468] C.C. Lin, Y.S. Lin, A finite element model of single-lap adhesive joints, *International Journal of Solids and Structures* 30 (1993) 1679–1692.
[469] D.Y. Hwang, J.M. Stallings, Finite element analysis of bolted flange connections, *Computers and Structures* 51 (1994) 521–533.
[470] N.K. Hassan, M.A. Mohamedien, S.H. Rizkalla, Finite element analysis of bolted connections for PFRP composites, *Composites Part B: Engineering* 27 (1996) 339–349.
[471] A.R. Kallmeyer, R.I. Stephens, Finite element model for predicting time-dependent deformations and damage accumulation in laminated composite bolted joints, *Journal of Composite Materials* 33 (1999) 794–826.
[472] G. Richardson, et al., A comparison of two- and three-dimensional finite element analyses of adhesive joints, *International Journal of Adhesion and Adhesives* 13 (1993) 193–200.
[473] A.E. Bogdanovich, S.P. Yushanov, 3-D Progressive failure analysis of bonded composite joints, *Proceedings of the 39th AIAA/ASME/ASCE/AHS/ASCE Structures, Structural Dynamics, and Materials Conference*, Part II, 1998, pp. 1616–1626.
[474] E.V. Iarve, Three-dimensional stress analysis in laminated composites with fasteners based on the B-spline approximation, *Composites—Part A: Applied Science and Manufacturing* 28 (1997) 559–571.
[475] E.V. Iarve, Three-dimensional singular stresses in open hole and rigid fastener composites, *American Society of Mechanical Engineers, Materials Division, MD* 84 (1998) 255–257.
[476] E.V. Iarve, Three-dimensional stress analysis of fastener hole composites, *American Society of Mechanical Engineers, Materials Division MD* 69 (1998) 345–355.
[477] U. Edlund, A. Larbring, A geometrically nonlinear model of the adhesive joint problem and its numerical treatment, *Computational Methods in Applied Mechanical Engineering* 96 (1992) 329–350.
[478] U. Edlund, Surface adhesive joint description with coupled elastic-plastic damage behavior and numerical applications, *Computational Methods in Applied Mechanical Engineering* 115 (1994) 253–276.
[479] D.W. Wilson, Y. Tsujimoto, On Phenomenological Failure Criteria for Composite Bolted Joint Analysis, *Composites Science and Technology* 26 (1986) 283–305.

[480] R.E. Little, P.K. Mallick, Fatigue of bolted joints in SMC-R18 sheet molding compound composites, *Journal of Composite Technical Research* 12 (1990) 155–163.
[481] R.E. Little, P.K. Mallick, Fatigue of bolted joints between e-glass/epoxy composite and steel, *Proceedings of American Society of Composites*, 1993, pp. 409–418.
[482] D. Liu, B.Z. Ying, W.G. Gua, Selection and measure of the bearing fatigue damage parameter in CFRP laminate bolted joints, *International Conference of Composite Structures*, 1991, p. 531.
[483] D. Liu, W.G. Gau, K.D. Zhang, B.Z. Ying, Empirical damage evaluation of graphite/epoxy laminate bolt joint in fatigue, *Theoretical Applied Fracture Mechanics* 19 (1993) 145–150.
[484] C.L. Rao, Deformation and Failure of Adhesively Bonded Elastomeric Lap Joints, D.Sc. Thesis, Massachusetts Institute of Technology, 1992.
[485] P.D. Herrington, M. Sabbaghian, Fatigue failure of composite bolted joints, *Journal of Composite Material* 27 (1993) 491–512.
[486] W.H. Chen, S.S. Lee, Numerical and experimental failure analysis of composite laminates with bolted joints under bending loads, *Journal of Composite Materials* 29 (1995) 15–36.
[487] A. Lanciotte, L. Lazzeri, M. Raggi, Fatigue behavior of mechanically fastened joints in composite materials, *Composite Structures* 33 (1995) 87–94.
[488] A. Banbury, D.W. Kelly, Study of fastener pull-through failure of composite laminates: Part 1, experimental, *Composite Structures* 45 (1999) 241–254.
[489] R.A. Jurf, J.R. Vinson, Failure analysis of bolted joints in composite laminates, ASTM Special Technical Publication 1059, 1990, p. 165.
[490] R. Yuuki, et al., Evaluation of fracture and strength of metal/ceramic bonded joints based on interfacial fracture mechanics, *Transaction of the Japanese Society of Mechanical, Series A* 60 (1994) 37–45.
[491] W.H. Chen, S.S. Lee, J.T. Yeh, Three-dimensional contact stress analysis of a composite laminate with bolted joints, *Composite Structures* 30 (1995) 287–297.
[492] H.J. Lin, C.C. Tsai, Failure analysis of bolted connections of composites with drilled and molded-in hole, *Composite Structures* 30 (1995) 159–168.
[493] H.A. Whitworth, Fatigue evaluation of composite bolted and bonded joints, *SAMPE Journal of Advanced Materials* 30 (1998) 25–31.
[494] A. Banbury, A.D.W. Kelly, L.K. Jain, Study of fastener pull-through failure of composite laminates: Part 2, Failure prediction, *Composite Structures* 45 (1999) 255–270.
[495] H.Y. Ko, B.M. Kwak, S. Im, Contact stress and failure analysis on bolted joints in composite plates by considering material nonlinearity, *International Conference of Computer Aided Design in Composite Material Technology*, Computational Mechanics Publication, 1996, pp. 31–40.
[496] C.C. Chamis, S.N. Singhal, L. Minnetyan, Probabilistic simulation of progressive fracture in bolted joint composite laminates, National Aeronautics and Space Administration Tech Memo 107, 1996.
[497] L. Minnetyan, C.C. Chamis, P.K. Gotis, Damage progression in bolted composites, *Journal of Thermoplastic Composite Materials* 11 (1998) 231–248.
[498] L. Tong, Bearing failure of composite bolted joints with non-uniform bolt-to-washer clearance, *Composites: Part A* 31 (2000) 609–615.
[499] P.R. Borgmeier, K.L. DeVries, Fracture mechanics analysis of the effects of tapering adherends on the strength of adhesive lap joints, *Journal of Adhesion Science and Technology* 7 (1993) 967–986.
[500] P.R. Borgmeier, A Fracture Mechanics Analysis of Double Cantilever Beam Adhesive Joints: Effects of Adhesive and Adherends Thickness, Ph.D. Thesis, The University of Utah, 1994.
[501] E.D. Reedy, T.R. Guess, Composite-to-metal tubular lap joints: strength and fatigue resistance, *International Journal of Fracture* 63 (1993) 351–367.
[502] C. Cooper, G.J. Turvey, Effects of joint geometry and bolt torque on the structural performance of single bolt tension joints in pultruded GRP sheet material, *Composite Structures* 32 (1995) 217–226.
[503] G.J. Turvey, Single-bolt tension joint tests on pultruded GRP plate—effects of tension direction relative to pultrusion direction, *Composite Structures* 42 (1998) 341–351.
[504] D.S. Saunders, The development of fatigue damage around fastener holes in thick graphite/epoxy composite laminates, *Composites* 24 (1993) 309–321.

[505] S.C. Galea, D.S. Saunders, Effects of hot/wet environments on the fatigue behavior of composite-to metal mechanically fastened joints, *Proceedings of the International Conference of Advanced Composite Materials*, *Mine*, *Metallurgy*, *and Material Society* (TMS), 1993, pp. 525–531.
[506] S.C. Galea, L. Mirabella, W.K. Chiu, *Non-destructive Evaluation of Composite-to-metal Mechanically Fastened Joints*, National Conference Publications, Institute of Engineering, Australia 1(93), Part 6, 1993, pp. 87–93.
[507] R.L. Ramkumar, E.W. Tossavainen, Strength and life time of bolted laminates, in: *Fatigue in Mechanically Fastened Composite and Metallic Joints*, ASTM STP 927, 1986, pp. 251–273.
[508] Y. Xiong, Analytical method for failure prediction of multi-fastener composite joints, *International Journal of Solids and Structures* 33 (1996) 4395–4409.
[509] P. Destuynder, et al., Some theoretical aspects in computational analysis of adhesive lap joints, *International Journal of Numerical Methods in Engineering* 35 (1992) 1237–1262.
[510] J.H. Park, S.N. Atluri, Fatigue growth of multiple-cracks near a row of fastener-holes in a fuselage lap-joint, *Computational Mechanics* 13 (1993) 189–203.
[511] E. Persson, I. Eriksson, Fatigue of multiple-row bolted joints in carbon/epoxy laminates: ranking of factors affecting strength and fatigue life, *Journal of Fatigue* 21 (1999) 337–353.
[512] J.M. Whitney, R.J. Nuismer, Stress fracture criteria for laminated composites containing stress concentrations, *Journal of Composite Materials* 8 (1974) 253–265.
[513] L. Ryna, J. Monaghan, Failure mechanism of riveted joint in fiber metal laminates, *Journal of Material Processing and Technology* 103 (2000) 36–43.
[514] O. Allix, Damage analysis of delamination around a hole, in: P. Ladevez (Ed.) *New Advances in Composite Structure Mechanics*, Elsevier, Amsterdam, 1992, pp. 411–421.
[515] J. Schön, T. Nyman, Spectrum fatigue of composite bolted joints, *International Journal of Fatigue* 24 (2002) 273–279.
[516] R. Starikov, J. Schön, Local fatigue behavior of CFRP bolted joints, *Composite Science and Technology* 62 (2002) 243–253.